Analysis of Regulatory Mechanisms on RNA Interference by Molecular Chaperone Hsp90 and Protein Phosphorylation in Yeast

by

Yang Wang

A thesis submitted in partial fulfillment of the requirements for the degree of

Doctor of Philosophy

Department of Cell Biology
University of Alberta

ABSTRACT

RNA interference (RNAi) is a conserved mechanism that eukaryotes employ small RNAs to regulate gene expression at transcriptional and post-transcriptional levels in a sequence-specific manner. However, current understanding on the regulatory mechanisms of RNAi via its core components is quite limited.

In the RNAi-deficient budding yeast *Saccharomyces cerevisiae* (*S. cerevisiae*), I demonstrated that the integration of genes encoding *Saccharomyces castellii* (*S. castellii*) Dicer and *S. castellii* or human Argonaute restored RNAi-mediated reporter gene silencing. Conversely, the introduction of genes encoding human Dicer and human (or *S. castellii*) Argonaute, with or without Dicer co-factor TAR RNA-binding protein 2 (TRBP2), was unable to reconstitute RNAi. My studies also showed that *S. castellii* Dicer does not detectably interact with either Argonaute protein, whereas human Dicer associates with human but not *S. castellii* Argonaute independently of TRBP2. Moreover, deletion of several genes proteins with one or more double-stranded RNA binding domains (dsRBDs) did not noticeably affect RNAi-mediated reporter gene silencing in *S. cerevisiae*. I hypothesized Dicer proteins in budding yeast do not require dsRBP cofactor(s) to stabilize dsRNA substrates as their counterparts in mammals. My study also revealed that the restored RNAi pathways in *S. cerevisiae* are dependent on the ATPase activity of the molecular chaperone Hsp90. One explanation is that Hsp90 facilitates a conformational change of Argonaute, which is required for the loading of small RNA duplexes.

In the fission yeast *Schizosaccharomyces pombe* (*S. pombe*), I identified a number of kinases that are required for heterochromatin assembly at centromeres, a process that depends on the

RNAi-mediated silencing of pericentromeric transcripts. Further research is needed to find out which kinase(s) catalyze the phosphorylation reaction targeting core RNAi components. Argonaute protein in the deletion strains of three kinase, Gsk3, Byr1, and Dsk1, strongly associated with Poly (A) binding protein (PABP) and non-selectively bound more RNAs. Moreover, the kinase Pka1 was found to be essential for the biogenesis and/or stability of Chp1, a binding partner of Argonaute and an essential component of RNA-induced transcriptional silencing complex (RITS).

My results indicate that RNAi is subject to intricate and extensive regulation by the molecular chaperone Hsp90 and protein phosphorylation through RNAi core components.

ACKNOWLEDGEMENT

The journey of my Ph.D. study has been challenging but rewarding. This work would not have been possible without the encouragement and support from many people. I would like to take this opportunity to express my sincere gratitude.

To my co-supervisors, Dr. Tom Hobman and Dr. Paul LaPointe, I will forever be indebted to you. Thank you for accepting me as a transfer student when I had an unfortunate start of my graduate study. Thank you for all the guidance, patience, support, and trust. What you did for me is way beyond a supervisor's responsibility. You are not only brilliant, vigorous, and deeply devoted scientists, but also kind, gentle, and compassionate people. Although I have chosen an alternative career path, you are the role models that I will strive to emulate in whatever future endeavours I decide to pursue.

To my current and previous lab mates: Baochan, Heather, Katie, Anna, and Rebecca in LaPointe lab; and Jungsook, Justin, and Joaquin in Hobman lab. Thank you all for your technical support, inspiring discussion, and friendship. I will always remember those delicious birthday cakes and creative Christmas door decorations. Eileen, thank you for ordering reagents and digging through the lab stocks to find plasmids for me. Zack, thank you for all the talks we had about science, career, and life.

I would like to express my gratitude to Dr. Richard Rachubinski for sitting in my supervisory committee for four years, and to Dr. Andrew Simmonds for stepping up to assume the vacant role. I appreciate your advice and suggestions on my research project. I would also like to thank Dr. Andrew MacMillan and Dr. Gordon Chua for serving as external examiners.

I thank all the faculty members, fellow graduate students, and supporting staffs in the Department of Cell Biology. There is no shortage of great people with brilliant ideas in this well-organized and close-knit community. I only wish I had opportunities to get to know more people at a personal level.

To Henry and Lisa, you opened your home to me and treated me like your own child. To Xinyu, Lianhua, Yifan, Xiaoyan, Haitao, and all my friends for the laughter and food we shared. You guys made this city a home away from my home.

Dear mom and dad, thank you for giving me life and encouraging me to follow my dreams. You are always there, love and care for me. To grandpa, I know you are looking down from the heaven and smile at me if I look up. I miss you so much.

To Fang, you are my best friend and the better half of me. Your love and companion kept me strong in those darkest moments. I don’t have to pretend to be anyone or anything in front of you. In my eyes, you are everything. Isabel, my only sunshine and dear little angel, holding you in my arms for the first time was the most beautiful moment in my life. Thank you for coming into my life and giving me joy.

TABLE OF CONTENTS

LIST OF TABLES

LIST OF FIGURES

LIST OF NOMENCLATURE AND ABBREVIATIONS

2-DE	two-dimensional gel electrophoresis
3'UTR	3' untranslated region
17-AAG	17-N-allylamino-17-demethoxygeldanamycin
Aha1	activator of heat shock 90kDa protein ATPase homolog 1
AMP	adenosine 5'-monophosphate
ATP	Adenosine triphosphate
bp	base pair
BSA	bovine serum albumin
Cdc37	cell division cycle protein 37
cDNA	complementary deoxyribonucleic acid
C. elegans	*Caenorhabditis elegans*
Chp1	Chromodomain-containing protein 1
Clr4	calcitonin-like receptor 4
CLRC	Clr4-Rik1-Cul4 complex
CMP	cytidine 5'-monophosphate
cnt	central core region of centromere
Cyp40	cyclophilin 40
DGCR8	DiGeorge syndrome critical region 8
DMSO	dimethyl sulfoxide
DNA	deoxyribonucleic acid
dsRNA	double-stranded RNA

dsRBD	double-stranded RNA binding domain
DTT	dithiothreitol
eIF4E	eukaryotic translation-initiation factor 4E
EGFR	epidermal growth factor receptor
EMM	Edinburgh minimal medium
endo-siRNA	endogenous siRNA
GA	geldanamycin
GFP	green fluorescent protein
G. intestinalis	*Giardia intestinalis*
GMP	guanosine 5'-monophosphate
GW repeats	glycine-tryptophan repeats
H3K9me	histone H3 lysine 9 methylation
HA	hemagglutinin
hAgo2	human Argonaute 2
Hop	Hsc70 and Hsp90 organizing protein
HSP	heat shock protein
Hsp90	Heat shock protein 90
HU	hydroxyurea
IEF	isoelectric focusing
imr	innermost DNA repeats
IP	immunoprecipitation
kDa	kilodalton

Loqs1	Loquacious 1
M	moles per litre
MAPK	mitogen-activated protein kinase
MS	mass spectrometry
miRNA	microRNA
mitron	miRNA intron
mRNA	messenger RNA
natNT2	nourseothricin
NVP-AUY922	5-(2,4-Dihydroxy-5-isopropyl-phenyl)-N-ethyl-4-[4-(morpholinomethyl)phenyl]isoxazole-3-carboxamide
nt	nucleotide
otr	outermost DNA repeats
PABP	poly (A)-binding protein
PACT	Protein Activator of PKR
PARylation	Poly-ADP-ribosylation
PAZ domain	Piwi/Argonaute/Zwille domain
P-body (or PB)	processing body
PEG	polyethylene glycol
piRNA	Piwi-interacting RNA
PPIase	peptidylprolyl isomerase
pre-miRNA	precursors miRNA
pri-miRNA	primary miRNA

PTGS	post-transcriptional gene silencing
PTM	post-translational modification
PTP1B	protein tyrosine phosphatase 1B
qRT-PCR	quantitative reverse transcription PCR
RD	radicicol
Rdp1	RNA-dependent RNA polymerase 1
RDRC	RNA-directed RNA polymerase complex
RISC	RNA-induced silencing complex
RITS	RNA-induced transcriptional silencing complex
RNAi	RNA interference
RNase III	ribonuclease III
RNP	ribonucleoprotein
ROX	5-carboxy-X-rhodamine
S. castellii	*Saccharomyces castellii*
S. cerevisiae	*Saccharomyces cerevisiae*
S. pombe	*Schizosaccharomyces pombe*
SDS-PAGE	sodium dodecyl sulfate-polyacrylamide gel electrophoresis
SG	stress granule
shRNA	short hairpin RNA
siRNA	small interfering RNA
snoRNA	small nucleolar RNA
ssRNA	single-stranded RNA

Tas3	tyrosine auxotrophy suppressor 3
TBZ	thiabendazole
TEMED	N,N,N’,N’-tetramethylenediamine
TGS	transcriptional gene silencing
TPR	tetratricopeptide repeat
TRBP2	TAR RNA-binding protein 2
U	enzymatic unit
UMP	uridine 5'-monophosphate
UTR	untranslated region
V	volts
v/v	volume per volume
w/v	weight per volume
YE	yeast extract
YES	yeast extract, dextrose, and amino acid supplements

Chapter 1

Introduction

1.1. RNA interference (RNAi)

1.1.1. Overview of RNAi

RNA interference (RNAi) is an evolutionary conserved mechanism present in nearly all eukaryotes. One notable exception is the model organism budding yeast *S. cerevisiae*, although RNAi is present in some other budding yeast species including *Saccharomyces castellii* (*S. castellii*), *Kluyveromyces polysporus* (*K. polysporus*), and *Candida albicans* (*C. albicans*) (Drinnenberg et al. 2009, 2011; Staab et al. 2011; Nakanishi et al. 2012). RNAi-mediated gene silencing is triggered by several categories of small RNAs, including but not limited to small interfering RNAs (siRNAs), microRNAs (miRNAs), and Piwi-interacting RNAs (piRNAs) (Carthew and Sontheimer 2009; Kim et al. 2009; Siomi et al. 2011). RNAi pathways can regulate gene expression at both transcriptional and post-transcriptional levels in a sequence specific manner (Hannon 2002; Volpe et al. 2002), and are predicted to modulate more than half of all genes in mammalian genomes (Yu et al. 2002; McManus et al. 2002).

The canonical RNAi pathways require the type III ribonuclease Dicer to process double-stranded RNA (dsRNA) precursors into mature RNA duplexes in the cytoplasm (Provost et al. 2002; Lee et al. 2003). These RNA duplexes are then loaded onto Argonaute proteins, which form the core of the RNA-induced silencing complex (RISC). After strand separation, the tethered guide strand leads the RISC to complementary messenger RNAs (mRNAs) to trigger either translational repression or mRNA cleavage (Hammond et al. 2000; Meister and Tuschl 2004; Tomari and Zamore 2005).

RNAi pathways are subject to tight regulation that allow eukaryotes to swiftly respond to viral invasion and various stress conditions. Previous publications from our laboratory and others reported

that the heat shock protein 90 (Hsp90) physically interacts with Argonaute proteins in *Drosophila* and mammals, to facilitate the structural rearrangements of Argonaute that are required for RNA duplex loading (Tahbaz et al. 2001; Liu et al. 2004; Pare et al. 2009). Moreover, several independent studies have revealed that human Argonaute 2 (hAgo2) is subject to multiple post-translational modifications including phosphorylation, hydroxylation, and ubiquitination (Zeng et al. 2008; Qi et al. 2008; Rudel et al. 2011). Although extensive progress has been made since the discovery of RNAi pathways two decades ago, much more remains to be discovered, in particular, how RNAi pathways are regulated. Identifying the mechanisms that regulate the structure and function of core RNAi components may lead to a better understanding of the spatial and temporal events that regulate eukaryotic gene expression on a global level.

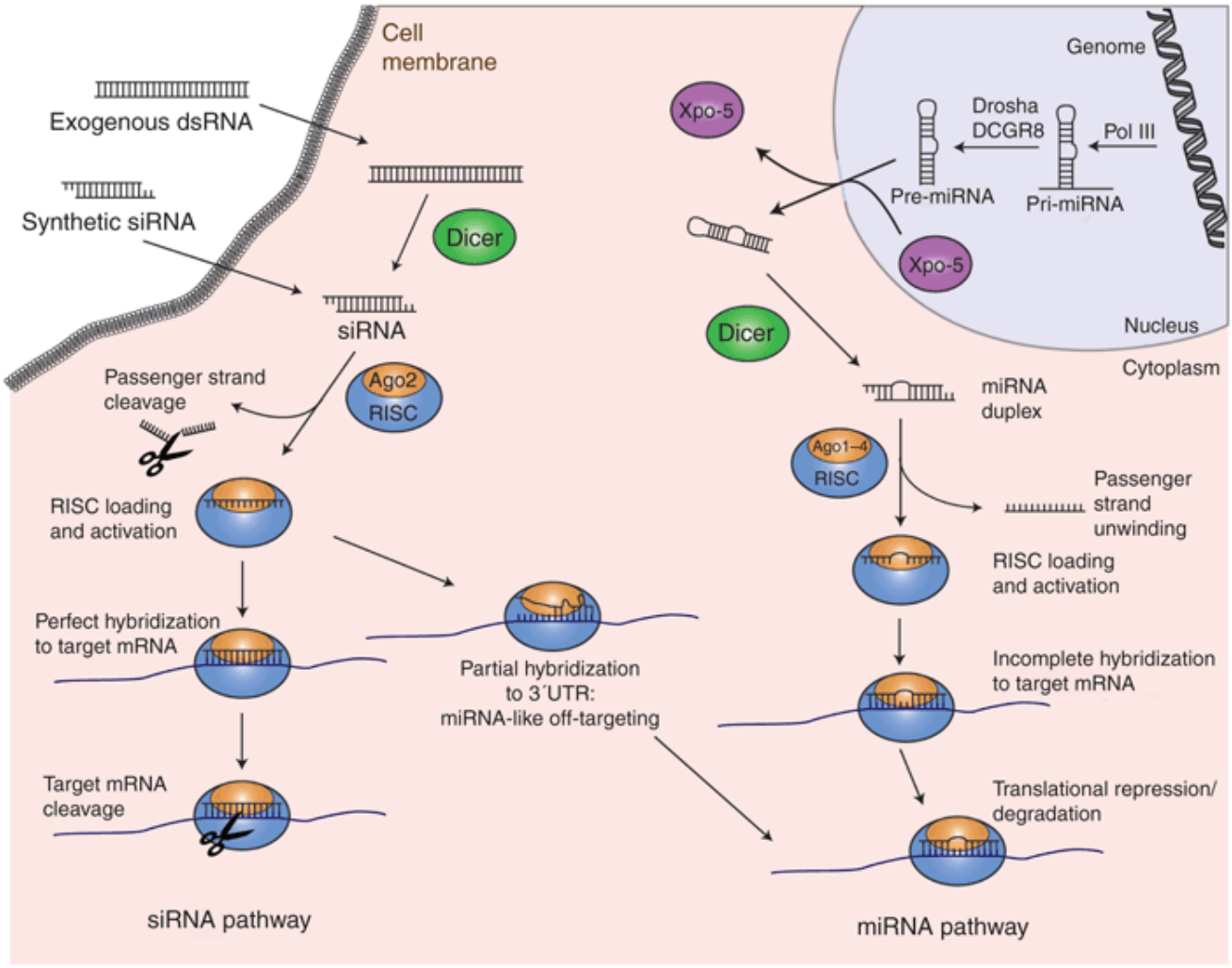

Figure 1.1 siRNA and miRNA pathways in mammals.

siRNA pathway: Exogenous dsRNA precursors are processed by Dicer into mature siRNAs with 2-nt overhangs on the 3′ ends. After the loading of siRNA duplexes onto Argonaute 2, the guide strands are retained while the passenger strands are degraded. The guide strands lead the ribonucleoprotein complexes to complimentary mRNA targets which are then cleaved. If the siRNA is not 100% complementary to the 3' untranslated region (UTR) of a mRNA target, cleavage does not occur.

miRNA pathway: Endogenous miRNA genes are transcribed by RNA polymerase III into long primary miRNAs (pri-miRNAs), which are processed by RNase III Drosha into precursor miRNAs (pre-miRNAs) in the nucleus. Pre-miRNAs are then transported into the cytoplasm and further processed by Dicer. Argonaute proteins loaded with mature miRNA duplexes usually hybridize imperfectly with mRNA targets, which leads to translational repression more often than mRNA cleavage (Kanasty et al. 2012).

1.1.2. Major types of small RNAs that function in RNAi

Small non-coding RNAs that have been characterized in eukaryotes that cause sequence-specific gene regulation include but are not limited to siRNAs, miRNAs, and piRNAs (Khvorova et al. 2003; Sontheimer and Carthew 2005; Khraiwesh et al. 2010). Both miRNAs and siRNAs are derived from dsRNA precursors that are processed by Dicer, and then loaded onto Argonaute proteins. In contrast, piRNAs are usually generated from ssRNA precursors, processed by endoribonuclease Zucchini and other unidentified trimming enzymes. Moreover, piRNAs are mostly found in animal germ line cells where they repress transposons and regulate multigenerational epigenetic inheritance (Parker et al. 2004; Vagin et al. 2006). For the sake of brevity, I have limited the scope to miRNA- and siRNA-mediated gene silencing.

1.1.2.1. Small interfering RNA (siRNA) pathways

1.1.2.1.1. Exogenous siRNA pathways

Andrew Fire and Craig Mello were the first to report that the injection of dsRNAs can potently and specifically inhibit the expression of genes that share perfect sequence complementarity in *C. elegans* (Fire et al. 1998). Since then, this so-called RNA interference (RNAi) mechanism has become widely used in laboratories as a powerful tool to knockdown gene expression.

The majority of siRNA precursors are long, perfectly paired dsRNA substrates from exogenous sources such as viral origin and artificial synthesis (Mello and Conte 2004). The proposed primary function of siRNA is to defend against viral infections (Meister and Tuschl 2004; Mello and Conte 2004). In most situations, the generation of 21-23 nt siRNAs requires only Dicer processing in the cytoplasm (Meister and Tuschl, 2004; Tomari and Zamore, 2005) **(Figure 1.1)**. After mature siRNAs

are loaded onto Argonute proteins, strand separation occurs and only the guide strand is retained (Meister and Tuschl 2004; Tomari and Zamore 2005). Perfect hybridization between the guide strand and mRNA targets usually triggers endonucleolytic cleavage of the mRNA. However, translational repression can also occur if the siRNA seed region (base pairing between nucleotides 2–8) is partially complementary to the 3′ untranslated region (UTR) sequence of mRNA (Lippman and Martienssen 2004).

1.1.2.1.2. Endogenous siRNA (endo-siRNA) pathways

In contrast to the majority of siRNAs originated from exogenous sources described above, a small portion of siRNAs are generated from endogenous repetitive sequences transcribed from centromeres, telomeres, transposons, and mating type loci. These transcripts naturally fold into double-stranded intramolecular hairpins or intermolecular duplexes (Okamura et al. 2008; Ghildiyal et al. 2008; Ender and Meister 2010). Other endogenous siRNA sources include natural antisense transcripts, convergent mRNAs, pseudogene-derived antisense transcripts, and hairpin RNAs (Vazquez et al. 2004; Allen et al. 2005; Golden et al. 2008). Therefore, siRNAs can arise from both exogenous and endogenous sources (Chapman and Carrington 2007; Carthew and Sontheimer 2009).

In addition to the post-transcriptional silencing, siRNAs can also regulate gene expression at the transcriptional level by hybridizing with DNA in the nucleus (Volpe et al. 2002). At least four siRNA pathway-related mechanisms operate in the nucleus: RNAi-mediated heterochromatin assembly, RNA-directed DNA methylation, DNA elimination, and meiotic silencing of unpaired DNA (Matzke and Birchler 2005). Among these, the first two are epigenetic processes that covalently modify lysine in histones and cytosine in DNA, respectively. Although these two mechanisms are usually

interconnected in self-regulating feedback loops in higher eukaryotes, it is unclear whether they represent the outcome of a single pathway or two separate pathways (Lund and Lohuizen 2004). Furthermore, RNAi-mediated regulatory mechanisms in the nucleus may directly affect chromosome structure, function, and behaviour through chromatin modifications.

1.1.2.1.3. Pharmaceutical application of siRNAs

The discovery of sequence-specific gene silencing by the introduction of chemically synthesized small RNAs ignited strong hope that RNAi could be an effective therapeutic approach for the prevention and treatment of many diseases including cancer and human immunodeficiency virus (HIV) infection (de Fougerolles et al. 2007; Whitehead et al. 2009). Preclinical studies confirmed that RNAi could be used to effectively knockdown expression of target genes in various pathological conditions including viral infections including hepatitis B virus and human papillomavirus, and in bone and ovarian cancers (Song et al. 2003; Morrissey et al. 2005; Niu et al. 2006; Halder et al. 2006). One of the biggest challenges in the clinical implementation of RNAi therapeutics is to effectively deliver the small RNAs to target tissues or organs in a non-toxic manner. Currently, there are more than 20 RNAi-based therapeutics in clinical trials, and several of these are phase III trials (Bobbin and Rossi 2016).

1.1.2.2. MicroRNA (miRNA) pathways

1.1.2.2.1. Canonical miRNA pathways

In the canonical miRNA pathways, miRNA genes with their own promoters, or miRNA introns (mitrons) which reside within the host genes, are transcribed into primary miRNAs (pri-miRNAs) by

RNA polymerase II (Li and Rana 2014; Ha and Kim 2014). A typical 1,000 nt single transcript of 5' capped and 3' polyadenylated pri-miRNA usually contains multiple stem-loop modules connected by single-stranded links (Cai et al. 2009; Fabian et al. 2010).

Two consecutive scissions are required to process pri-miRNAs into mature miRNAs that occur in the nucleus and the cytoplasm, respectively (Bartel et al. 2004) **(Figure 1.1)**. First, a nuclear protein complex containing the class 2 RNase III enzyme Drosha catalyzes the cleavage at the neck of the stem loop structure of pri-miRNAs to release ~70 nt hairpin-shaped precursor miRNAs (pre-miRNAs) that bear 2 nt 3' overhangs. Efficient and precise processing of pri-miRNAs into pre-miRNAs depends on interaction between Drosha and its binding partner that contains dsRNA binding domains (dsRBDs) (*e.g.* DiGeorge syndrome critical region 8 (DGCR8) in mammals, Pasha in *Drosophila*, and PASH-1 in *C. elegans*) (Bartel et al. 2004). These pre-miRNAs are then exported out of the nucleus into the cytoplasm through the karyopherin exportin-5. In the cytoplasm, pre-miRNAs undergo the second cleavage by the class 3 RNase III enzyme Dicer near the terminal loops to generate mature miRNA: miRNA* duplexes of approximately ~21 nt in length with 2 nt 3' overhangs at both ends (Li and Rana 2014; Ha and Kim 2014). The duplexes are then loaded onto Argonaute proteins, which act as the catalytic center of the ribonucleoprotein (RNP) complexes. After the miRNA* strand is discarded, the miRNA strand guides the RNP complex to bind and silence complementary mRNA targets. The biogenesis of miRNAs is controlled at multiple steps and can be affected by a variety of stimuli. As of 2014, the miRNA database (http://www.mirbase.org) has catalogued 434 miRNAs in *C. elegans*, 466 miRNAs in *D. melanogaster*, and 2,588 miRNAs in humans (Ha and Kim 2014).

1.1.2.2.2. Non-canonical miRNA pathways

The non-canonical miRNA biogenesis pathways can bypass the cleavage step catalyzed by either Drosha or Dicer protein complex, but not both. The Drosha-independent pathway utilizes mRNA splicing machinery to generate stem-loop modules that resemble pre-miRNAs (Flynt et al. 2010). Small RNAs originating from tRNAs, short hairpin RNAs, or small nucleolar RNAs can also be processed into miRNAs (Babiarz et al. 2008, Chong et al. 2010). Some of these precursors undergo 3' end sequential processing first mediated by RNase Z and then by Dicer (Xie et al. 2013). On the other hand, the biogenesis of some miRNAs is Dicer-independent. For example, mammalian miR-451 matures by direct cleavage via slicer activity of hAgo2 once its hairpin precursor loads onto Argonaute (Pfeffer et al. 2005; Cheloufi et al. 2010; Yang et al. 2012). Although these non-canonical pathways account for generation of less than 1% of currently known miRNAs and are not well conserved, their existence reflects the evolutionary flexibility of miRNA biosynthesis.

1.1.2.3. Comparison of miRNA and siRNA pathways

In summary, miRNAs and siRNAs differ in origins, biogenesis, and silencing outcomes. First, miRNAs originate from endogenous RNA transcripts containing one or more stem-loop structures, whereas siRNAs are primarily derived from perfectly matched exogenous dsRNA substrates. Second, the processing of miRNAs requires two cleavage steps, the first in the nucleus by Drosha and then in the cytoplasm by Dicer. In contrast, generation of siRNA from precursors occurs in the cytoplasm and requires Dicer cleavage only. Third, miRNA-mediated silencing usually leads to the translational repression of multiple mRNA targets; while the perfect hybridization between the siRNA guide strand and complementary mRNA target results in mRNA cleavage. Lastly, miRNA-mediated

post-transcriptional gene silencing is mainly confined to the cytoplasm; while siRNAs generated by RNA-dependent RNA polymerase (RdRP) in the nucleus can also trigger transcriptional silencing of repeat elements at telomeres, centromeres, and mating type loci, process that are required for local heterochromatin assembly (Volpe et al. 2002).

1.1.3. Protein components required for RNAi pathways

1.1.3.1. The RNase III enzyme Dicer

A canonical Dicer contains a DExD/H ATPase helicase domain, a PAZ (Piwi/Argonaute/ Zwille) domain, two RNase III (RIIIDa and RIIIDb) domains in tandem, and up to two dsRNA binding domains (dsRBDs) (Zhang et al. 2004; Qin et al. 2010; Tsutsumi et al. 2011) (**Figure 1.2A**).

PAZ domains, which have only been identified in Dicer and Argonaute proteins so far, bind to the 3' end overhangs of dsRNA molecules (Cerutti et al. 2000; Lingel et al. 2003). The two RNase III domains form an intramolecular pseudo-dimer that creates a catalytic center that allows Dicer molecules to cleave two nearby phosphodiester bonds on opposite strands of RNA duplexes (Song et al. 2003; Zhang et al. 2004). The twisted position of the two RNase III domains leads to a non-parallel scission that generates 2 nt 3' overhangs as a "signature" of Dicer cleavage. The active center of the RNase III domain is comprised of 3-4 acidic amino acid residues and two Mg^{2+} ions coordinated by phosphodiester bonds (Denli et al. 2004; Macrae et al. 2006; Park et al. 2011) (**Figure 1.2B**).

The N-terminal helicase domain was originally implicated in unwinding dsRNA substrates (Zou et al. 2009), however new evidence suggests that the DExD/H and helicase C regions form bi-lobed structures that allow the helicase domain to act as a clamp that orients dsRNA substrates (Tsutsumi

et al. 2011; Lau et al. 2012) (**Figure 1.2B**). During processing of long dsRNA substrates into siRNAs, the helicase domain of Dicer hydrolyzes ATP to translocate the RNA duplex towards the RNase catalytic center to consecutively generate siRNAs (Cenik et al. 2011; Wilson and Doudna 2013). For pre-miRNAs, the helicase domain stabilizes the loop while the PAZ domain anchors the 2 nt 3' overhangs (Welker et al. 2011; Lau et al. 2012).

The dsRBD domain binds to the dsRNA precursors to stabilize the Dicer-RNA interaction. For Dicer proteins that contain zero to two dsRBD domains, co-factors with one or more dsRBDs (*e.g.* TRBP in humans, R2D2 in *Drosophila*) help to stabilize the RNA duplex substrates (Lau et al. 2012). These co-factors also facilitate precise cleavage by correctly positioning the RNase III domains of Dicer.

Structural studies of the molecular architecture of metazoan Dicer proteins have been hampered by their large sizes and complicated structures. Therefore, it has only been possibly to study individual domains rather than the whole enzyme. A structural study of *Giardia intestinalis* Dicer revealed that the PAZ domain is 65 angstroms (Å) away from the RNase catalytic center (MacRae et al. 2006) (**Figure 1.2B**). This distance is consistent with the length of 25-27 nt siRNAs generated by *G. intestinalis* Dicer. It has been proposed that the angle and orientation of the helix extending from the PAZ to RNase III domains determines the length of the RNA duplex products, and thus acts as a "molecular ruler" (MacRae et al. 2006; Jinek and Doudna 2009). A recent electron microscopy study by Lau and colleagues revealed that the "L" shape of human Dicer is comprised of multiple discrete morphological regions (Lau et al. 2012). The two RNase III domains sit in between the helicase and the PAZ domains that anchor the loops and 3' overhangs of small RNA duplexes, respectively.

While the domain architecture of Dicer varies between organisms, the principal RNase "dicing"

mechanism is conserved. The Dicer encoded by the parasite *G. intestinalis* lacks helicase and C-terminal dsRBD domains, whereas the more recently identified non-canonical Dicers in budding yeast contains a single RNase III domain but lacks helicase and PAZ domains (MacRae 2006; Weinberg et al. 2011). This suggests that budding yeast Dicer functions as a homodimer to cleave dsRNA substrates and evidence indicates that the cleavage works via an "inside-out" mechanism. The cleavage starting from the middle of the long dsRNAs, and to generate adjacent 23 nt RNA duplexes (Weinberg et al. 2011) (**Figure 1.2C**). In contrast to the canonical Dicer "molecular ruler" mechanism, the distance between the neighbouring homodimers of yeast Dicer would determine the length of the cleavage products (Weinberg et al. 2011).

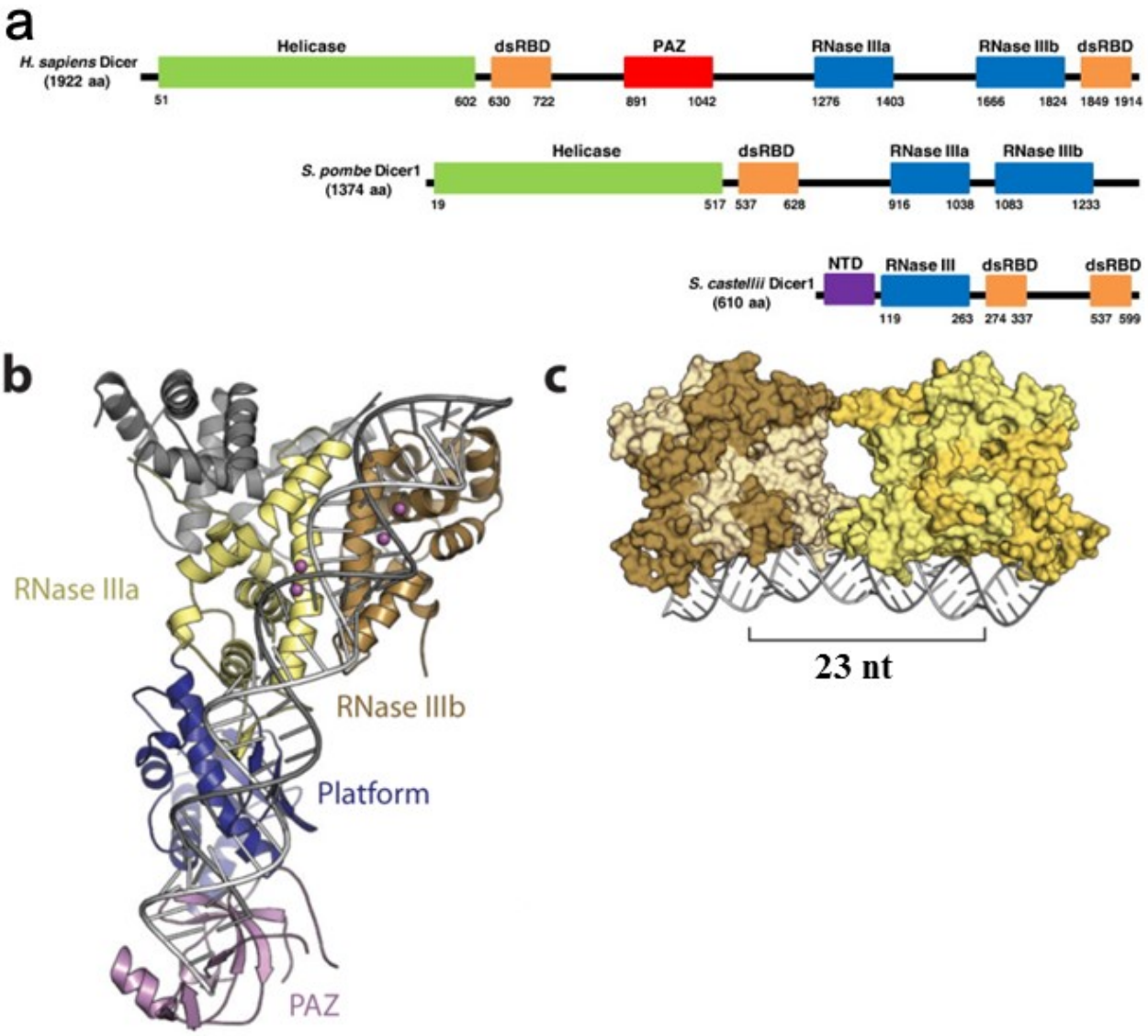

Figure 1.2 Domain architectures of Dicer. **(A)** Domains identified in canonical and non-canonical Dicer proteins. Helicase (light green), dsRNA binding (orange), PAZ (red), and RNase III (blue) domains are depicted in ribbons. **(B)** Canonical Dicer processes RNA duplexes as a "molecular ruler". The 3' prime of a RNA duplex is anchored in the dock of the PAZ domain, and the catalytic triad of RNase III domains (in purple spheres) cleave the dsRNA at the distance of 21-23 nt. **(C)** Non-canonical budding yeast Dicer proteins lack PAZ and helicase domains, which form multiple homodimers to cooperatively generate mature dsRNAs (Figure 1.2B and C from Wilson and Doudna, 2013).

1.1.3.2. Argonaute proteins as the cores of RNA silencing complexes

Argonautes act as the core of both the RNA-induced silencing complex (RISC) in the cytoplasm and RNA-induced transcriptional silencing (RITS) complex in the nucleus (Matranga et al. 2005; Preall et al. 2005; Hutvagner et al. 2008). RITS-based gene silencing is discussed in more detail later in this chapter. Argonaute proteins are found throughout eukaryotes, bacteria, and archaea. The eukaryotic Argonaute superfamily has evolved into two subfamilies with distinct functions, Argonaute and Piwi (Deng and Lin 2002; Farazi et al. 2008; Shabalina and Koonin 2008). Members of the Argonaute subfamily associate with siRNAs and miRNAs to mediate gene silencing in somatic cells, whereas proteins of the Piwi clade are primarily expressed in the germline cells to manage mobile genetic elements such as transposons (Carmell et al. 2007; Gunawardane et al. 2007).

Argonaute family members contain four conserved domains: an N-terminal (N) domain, a Piwi-Argonaute-Zwille (PAZ) domain, a Middle (MID) domain, and a C-terminal PIWI domain (Lingel et al. 2003; Song et al. 2004; Miyoshi et al. 2005; Kim et al. 2007) (**Figure 1.3A**). Crystallographic studies of Argonaute proteins in bacteria, fungi, and human cells revealed a conserved bi-lobed structure, where the N and PAZ domains form one lobe and the MID and PIWI domains form the other (Schirle and MacRae et al. 2012; Schirle et al. 2014).

As mentioned above, the PAZ domain, which recognizes and binds to the 2 nt 3’ overhangs of dsRNAs, are also found in some Dicer proteins (Song et al. 2003; Yan et al. 2003; Ma et al. 2004). The 2 nt 3’ overhangs are characteristic of the cleavage by RNase III enzymes including Drosha and Dicer. The anchoring of a 3’ overhang in a hydrophobic pocket is structurally but not sequence specific (**Figure 1.3B**). The seed region (nucleotides 2-6) of the negatively charged RNA duplex is bound through extensive polar interactions along the positively charged surface of the central basic

track between the two lobes of Argonaute (Chiu and Rana 2003) (**Figure 1.3B**). The binding of the 5'- terminal phosphate of RNA duplexes to the MID domain is nucleotide-dependent. Nuclear magnetic resonance studies showed that the efficiency of small RNA binding to Argonaute proteins is 30 times higher when the 5' terminal residue is AMP and UMP compared to CMP or GMP (Parker et al. 2005; Boland et al. 2010).

The structural study of *Thermus thermophilus* Argonaute shows that the PIWI domain contains an RNase H-like DDX (Asp-Asp-Asp/His) catalytic triad that recruits a pair of Mg^{2+} ions (Wang et al. 2009; Nakanishi et al. 2012). The phosphodiester linkage of mRNA base-paired to guide strand residues 10 and 11 from the 5' end is cleaved to create 5'-monophosphate and 3'-hydroxyl termini (Tomari and Zamore 2005). Exonucleases in the cytoplasm degrade the cleaved fragments to complete the process. The release of cleaved mRNA may require other factors and may be dependent on ATP hydrolysis (Rivas et al. 2005).

To bind mRNA targets, the 3' end of the guide strand releases from the PAZ domain binding pocket when the guide strand-mRNA helix exceeds a single A-form turn (11 nt) (Wang et al. 2008; 2009). Mutagenesis studies revealed that amino acids in the MID domain that recognize the 5' end of the guide strand are important for cleavage of the target mRNA (Tolia and Joshua-Tor, 2007; Wang et al. 2008). In contrast, mutations in the PAZ domain rarely affect the slicing activity of Argonaute proteins. These findings support a two-state model over a fixed-end model. The former contends that correct orientation for mRNA binding and cleavage requires the release of the 3' terminus of the guide strand, whereas the latter stipulates that both 3' and 5' termini of the guide strand stay anchored with the PAZ and PIWI domains throughout mRNA recognition and cleavage steps.

Previous studies in our laboratory identified a 58-aa box in PIWI domain in hAgo2 that is sufficient for Dicer binding (Tahbaz et al. 2004). Further studies are necessary to elucidate the nature of the interaction between Argonaute and Dicer proteins that is vital for RNA loading into RISC.

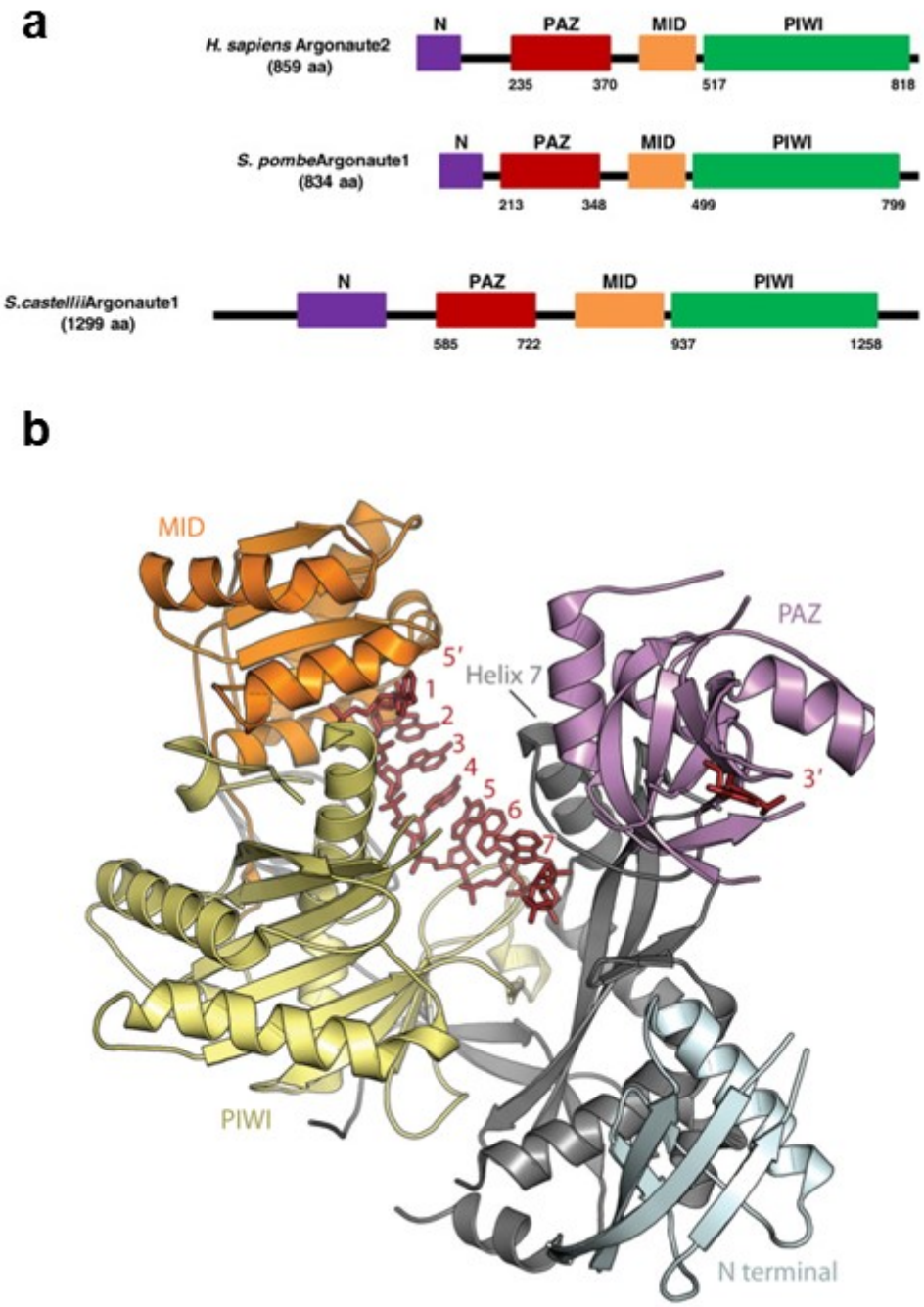

Figure 1.3 Domain architectures of Argonaute. (**A)** Argonaute proteins contain four conserved domains: N (purple), PAZ (red), Middle (orange), and PIWI (green). (**B)** The crystal structure of human Ago2 bound in complex with an RNA guide strand. The seed region (nucleotides 2–6) on the 5' end forms a well-ordered A-form helix and that is recognized by the MID domain, and the 3' end of the dsRNA is anchored into a RNA binding pocket in the PAZ domain. (Figure 1.3B from Wilson and Doudna, 2013)

1.1.3.3. Co-factors required for RNAi

Multiple protein factors may facilitate Dicer cleavage and RISC loading (Doyle and Jantsch 2002). The majority of these proteins are double-stranded RNA binding proteins (dsRBPs), which typically contain a C-terminal dsRBD dedicated to protein-protein interaction rather than dsRNA binding. Other dsRBDs recognize RNA in a structural-based manner rather than based on sequence. It was hypothesized that the dsRBPs are involved in transfer of dsRNA between Dicer and Argonaute by stabilizing the RNA bound protein complexes and facilitating their unwinding as well as retention of the guide strand (Paroo et al. 2009). Two dsRBPs in mammals, TRBP2 and PACT (Protein Activator of PKR) are know to recognize Dicer, homodimerize, and heterodimerize with each other (Laraki et al. 2008). The domain architecture of TRBP2, the best characterized dsRBP, resembles beads on a string (Wang et al. 2009).

The interaction between Argonaute and GW182, a glycine-tryptophan (GW) repeat-enriched protein, is essential for gene silencing induced by miRNAs but not siRNAs (Jakymiw et al. 2005; Ding and Han 2007; Zipprich et al. 2009; Eulalio et al. 2009). Vertebrates contain three GW182 paralogues (*e.g.* TNRC6A, TNRC6B and TNRC6C in humans) and insects have one (*e.g.* GW182 in *Drosophila*), but there are no known GW182 homologues in fungi (Behm-Ansmant et al. 2006).

Mammalian and *C. elegans* GW182 proteins were shown to co-immunoprecipitate with poly (A)-binding proteins (PABP) (Landthaler et al. 2008; Fabian et al. 2009; Tritschler et al. 2010). PABP binds to the poly (A) tail of mRNAs, and forms a closed-loop structure with eukaryotic translation-initiation factor 4E (eIF4E) and 4G (eIF4G) (Svitkin et al. 2001). This structure protects the mRNA from degradation, and facilitates ribosome binding and translation initiation (Svitkin et al. 2001; Kahvejian et al. 2005). The interaction between GW182 and PABP is thought to result in

disassembly of the closed-loop structure of the mRNA (Fabian et al. 2009; Zekri et al. 2009, 2013). In turn, the open conformation of mRNA exposes the 5'-cap and poly (A) tail to deadenylase complexes and mRNA decapping enzymes (Fabian et al. 2009). Consequently, the binding of the major deadenylase complex (*e.g.* CAF1, CCR4 and the NOT complex) mediates the release of PABP from the poly (A) tail (Piao et al. 2010; Huntzinger and Izaurralde 2011; Petit et al. 2012). The mRNA targets of miRNA bound Argonaute-GW182 complex are either translationally repressed and/or are de-capped by DCP1, EDC4 and DDX6 complexes and then rapidly degraded by exonuclease XRN1 (Ikeda et al. 2006; Huntzinger and Izaurralde 2011; Zekri et al. 2013).

1.2. RNAi pathways in eukaryotes

1.2.1. RNAi pathways in *Caenorhabditis elegans*

The single Dicer protein expressed in *C. elegans*, DCR-1, is required for the biogenesis of both miRNAs and siRNAs. Conversely, more than twenty genes encoding Argonaute family proteins have been identified in the genome of *C. elegans* (Hutvágner et al. 2001; Yigit et al. 2006). Whether DCR-1 coordinates with various Argonaute proteins in a cell type and/or cell cycle-dependent manner, or Argonaute proteins have redundant functions has not yet been elucidated (Ambros et al. 2003; Liu et al. 2003).

In the miRNA pathway, mature miRNAs associate with Argonaute proteins, either ALG-1 or ALG-2, to silence the target mRNAs (Lee and Ambros 2001; Zhang et al. 2007). In the siRNA pathway, dsRNA precursors from endogenous, viral or other exogenous sources are processed by DCR-1 in concert with its cofactor RDE-4 (RNAi-defective 4) (Knight et al. 2001; Tabara et al. 2002). Mature siRNAs then either associate with RDE-1 to induce the production of secondary

siRNA by RNA-dependent RNA polymerases ERI-6 and ERI-7, or directly bind to Argonaute proteins ALG-3, ALG-4, and ERGO-1 to initiate mRNA cleavage (Pak and Fire 2007; Sijen et al. 2007; Fischer et al. 2011).

1.2.2. RNAi pathways in *Drosophila melanogaster*

Two Dicer proteins, Dcr1 and Dcr2, orchestrate distinct small RNA-induced silencing pathways in *Drosophila* (Lee et al. 2004). Dcr1 specializes in processing endogenous hairpin RNA precursors into mature miRNAs (Jiang et al. 2005), whereas Dcr2 mediates cleavage of dsRNA substrates into siRNAs (Liu et al. 2006). Dcr1 and Dcr2 associate with different dsRNA-binding proteins, Loquacious 1 (Loqs1) and R2D2, respectively (Lee et al. 2004). The functional interaction between Dcr1 and R2D2 in miRNA biogenesis has been extensively studied (Tomari and Zamore 2005). It is thought that R2D2 functions as a sensor for the thermodynamic stability of the 5' ends of miRNA loading, similar to the role played by TRBP2 in mammalian cells. Depletion of Loq1 but not R2D2 affects Dcr1-catalyzed biogenesis of endo-siRNAs and target silencing (Forstemann et al. 2005; Jiang et al. 2005).

Gawky, a GW182 homologue, is required for miRNA-based silencing, but not siRNA pathways in *Drosophila* (Rehwinkel et al. 2005; Schneider et al. 2006). Loss of the *Drosophila* GW182 changes the pattern of mRNA expression in a similar way as that observed in Ago1-depleted cells (Findley et al. 2003). The N-terminal domain of GW182 interacts directly with the PIWI domain of Ago1 and induces degradation of mRNA transcripts in a manner that requires de-adenylation and a de-capping complex of Dcp1 and Dcp2 (Okamura et al. 2004).

1.2.3. RNAi pathways in mammalians

Four Argonaute subfamily members are encoded by the human genome, of which Argonaute2 (hAgo2) is the only one with endonuclease activity. Accordingly, only hAgo2 can cleave mRNA targets (Liu et al. 2004; Meister et al. 2004). The other three paralogues that lack slicing activity can still induce robust translational repression (Song et al. 2004; Meister et al. 2004). Although RNAi pathways in mammalian cells are more complicated than in lower eukaryotes, as discussed above, it was shown that hAgo2, hDcr, and TRBP2 can form a functional RISC complex *in vitro* (MacRae et al. 2008; Miyoshi et al. 2008).

TRBP2 and another dsRNA binding protein PACT were identified as important co-factors of Dicer protein in mammalian systems (Kok et al. 2007). TRBP2 is a 366 amino acids protein that contains three dsRBDs and two intervening linkers (Duarte et al. 2000). It was reported that TRBP2, in concert with Tat protein, activates HIV-1 gene expression by binding to the RNA regulatory elements between the loops of viral RNA (Gatignol et al. 1991). Electron microscopy studies revealed that TRBP2 functions as a structural bridge to connect Dicer to Argonaute (Lau et al. 2009). One possibility is that TRBP2 facilitates the release of Dicer generated siRNAs or miRNAs and accommodate the RNA duplexes loading onto Argonaute.

1.2.4. RNAi pathways in plants

The processing of plant miRNAs are completed in the nucleus by Dicer-like 1(DCL1) cleavage of the dsRNA precursors. The mature miRNA: miRNA* duplex is then methylated at the 3´ end by HUA Enhancer 1, a conserved S-adenosyl-l-methionine-dependent RNA methyltransferase (Fagard et al. 2000; Vaucheret et al. 2001). This keeps newly generated miRNAs intact by inhibiting

uridylation and subsequent decay. Mature miRNAs are then exported from the nucleus to the cytoplasm by transporter Hasty, a plant homologue of animal Exportin 5 (Klahre et al. 2002; Tang et al. 2003). In the cytoplasm, miRNA duplexes are loaded onto Argonaute 1, which is the major Argonaute isoform for the plant miRNA-mediated gene silencing pathway (Klahre et al. 2002; Tang et al. 2003).

The biogenesis of siRNA in plants can be divided into two major pathways that generate 21 and 24 bp RNA duplexes by distinct sets of protein factors (Zilberman et al. 2003; Zamore 2004). The 21 bp siRNAs are generated by the RNase III enzyme Dicer-like protein 4, which then bind to Argonaute 1 or 2 to exert target recognition and silencing function (Nakazawa et al. 2007). The 24 bp siRNAs are processed by Dicer-like protein 3 after which they associate with Argonaute 4 (Henderson et al. 2006). The 21 bp siRNAs induce the post-transcriptional cleavage of mRNA targets through the endonuclease activity of Argonaute 1 or 2, whereas the 24 bp siRNAs mediate transcriptional silencing through the methylation of the target DNA loci (Xie et al. 2004; Zilberman et al. 2003). This heritable RNAi-mediated DNA methylation epigenetically can regulate gene expression through multiple rounds of cell division (Henderson and Jacobsen 2007). The 21 bp and 24 bp siRNAs can be generated from either exogenous sources of long dsRNA such as those of viral origin, or from endogenous transposable elements (Kasschau et al. 2007).

1.2.5. RNAi is required for heterochromatin assembly in fission yeast

Gene silencing at the transcriptional level has been extensively studied in the fission yeast *S. pombe* (Volpe et al. 2002; Bühler et al. 2006; Moazed 2009). The RNA-induced transcriptional silencing (RITS) complex contains Argonaute 1 (SpAgo1), chromodomain protein Chp1, and the

SpAgo1 binding protein Tas3 which also interacts with Chp1 (Verdel et al. 2004). The RITS complex facilitates transcriptional gene-silencing through heterochromatin assembly at telomeres, centromeres, and mating type loci (Verdel et al. 2004; Ekwall 2004). These heterochromatic regions share repetitive DNA elements (Grewal and Jia 2007). For example, each centromere contains a kinetochore-binding region in the center (*cnt*), which is flanked by the innermost (*imr*) and outermost (*otr*) DNA repeats (Volpe et al. 2002; Blackwell et al. 2004; Yamada et al. 2005). The *otr* region is composed of *dg* and *dh* repeats that are coated with methylated histone H3 (**Figure 1.4A**).

Volpe and colleagues showed that RNAi-mediated pericentromeric silencing is required for heterochromatin assembly at centromeres in *S. pombe* (Volpe et al. 2002). A self-feedback loop orchestrated by RNAi starts from the transcription of *dg* and *dh* repeats in the pericentromeric region by RNA polymerase II during S phase. The RNA-dependent RNA polymerase Rdp1 then converts the nascent single-stranded transcripts into double-stranded RNA duplexes. SpDcr1 recognizes and processes the RNA duplexes into mature siRNAs, and eventually SpAgo1 that is loaded with siRNA duplexes, forms the RITS complex with Chp1 and Tas3 in the nucleus. The RITS complex facilitates histone H3 lysine 9 methylation (H3K9me) catalyzed by chromatin modifying complex CLRC (Clr4-Rik1-Cul4 complex), which subsequently recruits heterochromatin proteins Swi6/HP1 to assemble and spread heterochromatin structure (Motamedi et al. 2004; Moazed 2009) (**Figure 1.4B**)

Rdp1 forms the RNA-directed RNA polymerase complex (RDRC) with Hrr1 (helicase required for RNA-mediated heterochromatin assembly 1) and Cid12 (caffeine-induced death resistant 12) (Motamedi et al. 2004). RDRC physically interacts with the RITS complex in a Clr4 (calcitonin-like receptor 4) dependent manner (Motamedi et al. 2004). The recruitment of RDRC to specific heterochromatin regions allows Rdp1 to use the nascent forward pericentromeric transcript to

generate dsRNA for SpDcr1 cleavage (Colmenares et al. 2007) (**Figure 1.4B**). This suggests that heterochromatin assembly in *S. pombe* is facilitated by interdependency between RNAi machinery and histone methylation.

Interestingly, deletion of SpAgo1 or SpDcr1, but not Rdp1, leads to abnormal phenotypes including cell cycle arrest, mating defects, and abnormal cytokinesis (Carmichael et al. 2004). It was thought that SpAgo1 and SpDcr1 were involved in cell cycle regulation independent of their function in RNAi-mediated heterochromatin assembly since Rdp1 was dispensable for these roles. Further studies showed that SpAgo1 and SpDcr1 genetically interact with Cdc2, a key cell cycle regulator, to prevent hyper-phosphorylation under abiotic and toxic stress (Carmichael et al. 2004, 2006). DNA replication of the centromeric regions occurs in early S phase, simultaneously with pericentromeric transcription at *dg* and *dh* repeats (Chen et al. 2008). Release of RNA polymerase II from the pericentromeric region allows DNA replication to complete, which is followed by the spreading of histone H3K9me modification. It was found that SpAgo1 is a repressor of the S/M cell cycle transition, and thus its deletion allows early entry into M phase without complete DNA replication (Carmichael et al. 2004).

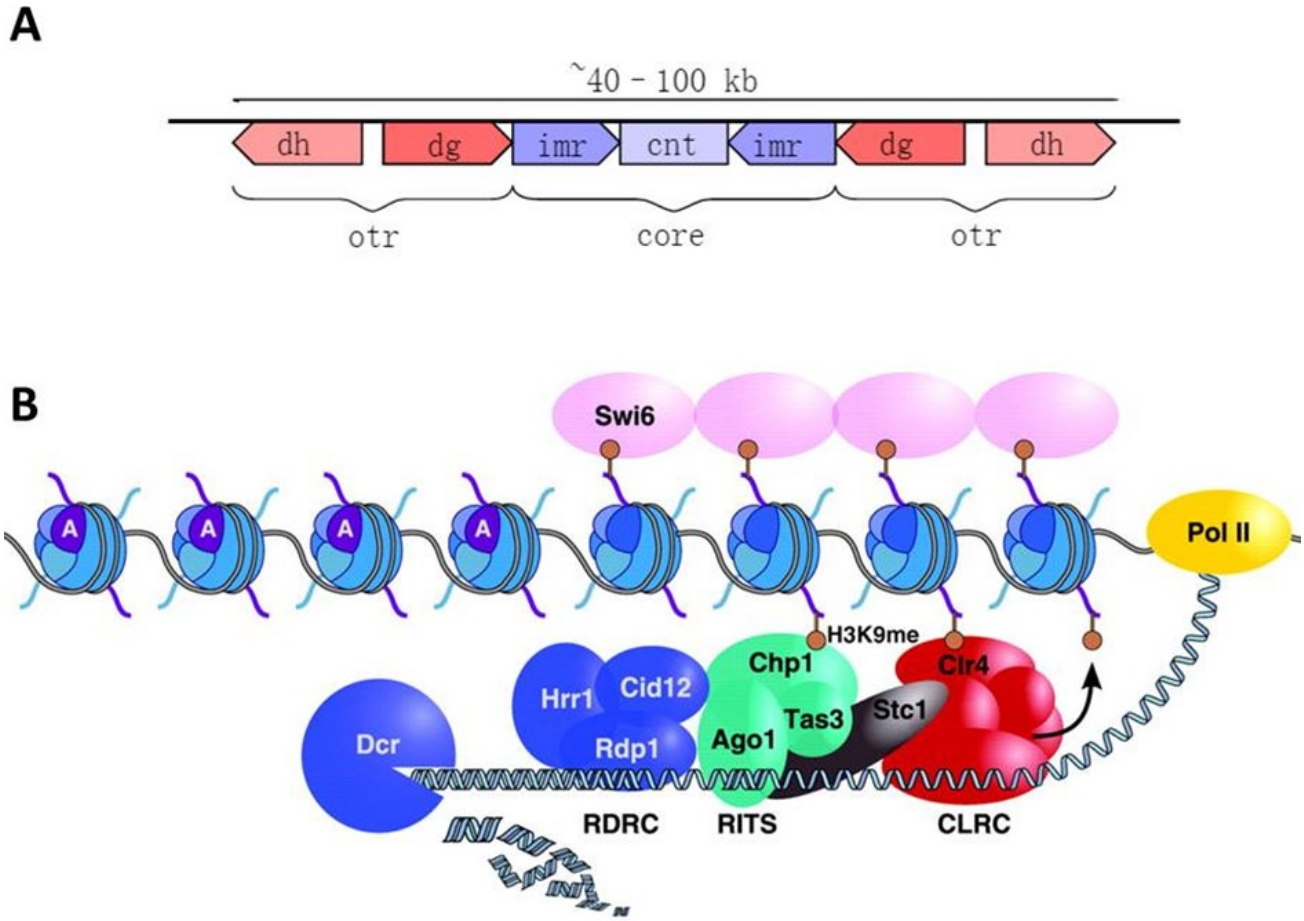

Figure 1.4 RNAi-mediated transcriptional silencing at centromeres in *S. pombe*.
(A) A typical centromeric DNA element in *S. pombe* is comprised of central kinetochore-binding region (cnt), innermost (imr) DNA repeats, and dg/dh repeats in the outermost (otr) regions.
(B) Low level pericentromeric transcription by Pol II still occurs at pericentromeric regions. RNA polymerase binds to the nascent ssRNA transcript and generates dsRNAs by reverse transcription. The RNA duplexes are processed by Dcr1, loaded onto Ago1, and then facilitates CLRC binding. Clr4 methylates pericentromeric H3K9 allows the heterochromatin proteins Swi6/HP1 to assemble and spread the heterochromatic structure. (Figure 1.4A from Sullivan et al., 2001; Figure 1.4B from Grewal and Elgin 2007)

1.2.6. RNAi pathways are conserved in some budding yeast species

The budding yeast *S. cerevisiae* has been widely used as a model organism for genetic and molecular studies of eukaryotic cells. However, it lacks recognizable homologues of Argonaute, Dicer, or RNA-dependent RNA polymerase (Houseley and Tollervey 2008; Harrison et al. 2009; Drinnenberg et al. 2009). RNAi-deficient organisms may evolve novel pathways or depend on parallel mechanisms to compensate for the role of RNAi in gene regulation. RNAi-independent noncoding RNAs with functional roles in gene regulation and protein activity have been identified in *S. cerevisiae* (Houseley and Tollervey 2008; Mercer et al. 2009). These noncoding RNAs physically interact with RNA polymerase II to regulate transcription of *IMD2* and *PSA1* in budding yeast (Kuehner and Brow 2008; Kwapisz et al. 2008). Also, transcription of noncoding RNAs interferes with transcription of mRNAs by affecting the recruitment of transcriptional factors, and thus modifying chromatin structure (Martens et al. 2004). Other noncoding RNAs that interact with polysomes affect protein translation under certain circumstances have been reported in *S. cerevisiae* and *E. coli* (Cheung et al. 2008; Dinger et al. 2008).

It was originally thought that all budding yeast species were RNAi-deficient like *S. cerevisiae* because none of them were found to have canonical Dicer homologues although Argonaute proteins were identified in some species. However, subsequent phylogenetic analysis suggested that *S. cerevisiae* at one time may have had an RNAi apparatus that was subsequently lost during evolution (Shabalina and Koonin 2008). The Argonaute proteins in the budding yeast species *S. castellii*, *C. albicans*, and *K. polysporus* all contain the four conserved domains found in mammalian Argonaute proteins. However, their N-terminal domains contain an additional ~400 amino acid long uncharacterized region (**Figure 1.3A**). The laboratory of David Bartel identified a subset of small

RNAs with 5'- monophosphates and 3'-hydroxyl groups in budding yeast that express Argonaute proteins, but not in *S.cerevisiae* (Drinnenberg et al. 2009). These 21-23 bp long dsRNAs are most enriched with adenine (A) or uracil (U) at the ends, which reminisces siRNAs and miRNAs generated by canonical Dicer cleavage. The majority of these small RNAs share sequence identity/similarly with loci encoding repetitive elements, including long interspersed nuclear element retrotransposons, long terminal repeat retrotransposons (Ty elements), and sub-telomeric repeats (Y' elements). Conversely, the small RNAs that can be detected in *S. cerevisiae* (18-30 bp) appear to be fragments of mRNAs, tRNAs, and rRNAs (Drinnenberg et al. 2009).

The presence of siRNA-like molecules in some budding yeast species indicated that these organisms encode an enzyme with Dicer-like activity. The only previously characterized gene encoding an RNase III in budding yeast is *RNT1*, which processes rRNA and other noncoding RNAs (Elela and Ares 1998; Lamontagne et al. 2001). Interrogation of the genome of budding yeast *S. castellii* revealed that a second RNase III domain-containing gene was present (Drinnenberg et al. 2009). With the anticipation that this newly identified gene encodes a protein with Dicer-like function, it was named Dicer 1 (*DCR1*). Orthologs of *S. castellii* Dcr1 were also found in other Argonaute-containing budding yeast including *C. albicans* and *K. polysporus* but not in *S. cerevisiae* (Drinnenberg et al. 2009).

Unlike canonical Dicer proteins that contain an N-terminal helicase domain, a PAZ domain, two RNase III domains, and one or more dsRBDs, budding yeast Dicer proteins possess a single RNase III domain and two dsRBDs (**Figure 1.2A**). Since the cleavage of dsRNA precursors by Dicer requires the activity of two RNase III domains, it was hypothesized that budding yeast Dicer functions as a homodimer (Drinnenberg et al. 2009). Moreover, four dsRBD domains may obviate

the need for other dsRBD-containing cofactors such as TRBP2 in mammalian systems. This hypothesis is consistent with the finding that a purported homodimer of Rnt1 which would have two dsRBD domains is unable to generate siRNAs.

Silencing of reporter genes driven by the *GAL1* inducible promoter in *S. castellii* is dependent on the expression of both Argonaute and Dicer. Furthermore, RNAi-mediated gene silencing can be reconstituted in *S. cerevisiae* by introducing Argonaute and Dicer from either *S. castellii* (Drinnenberg et al. 2009; Staab et al. 2010). This reconstituted RNAi machinery silences both exogenous reporter genes (*e.g. GFP* and *URA3*) and endogenous retrotransposons. Therefore, *S. cerevisiae* may in fact be able to serve as a powerful model system to study the mechanism and regulation of RNAi pathways. The potential to use this extremely well-characterized organism for which there is a wealth of genetic tools and resources to study RNAi offers exciting possibilities. Part of my PhD studies involved the use of a reconstituted RNAi system in *S. cerevisiae* to investigate how molecular chaperones regulate RNAi activity.

1.3. The Hsp90 molecular chaperone facilitates conformational change of Argonaute

1.3.1. The Hsp90 molecular chaperone

Eukaryotes employ various molecular chaperones to help newly synthesized proteins adopt their native conformations. Many molecular chaperones respond to heat stress and are thus named heat shock proteins (Hsp) (Borkovich et al. 1989p). Hsp90 is one of the most abundant proteins (~2% of total protein) in eukaryotes. It is also highly evolutionarily conserved with ATPase activity that mediates various crucial cellular processes including hormone signalling, cell cycle control, and response to abiotic stress (Sato et al. 2000; Meyer et al. 2004; Taipale et al. 2010). Biochemical and

structural studies revealed that Hsp90 accommodates a selective group of more than 200 proteins called Hsp90 client proteins. Hsp90 activity is required for its client proteins to overcome their energy barrier and fold into a stable and/or functional conformation in an ATP-dependent manner. Since many of these proteins are involved in signal transduction, Hsp90 inhibition has shown promise as a therapeutic strategy to treat diseases including cancer and HIV infection (Blachere et al. 1993; Neckers 2002; Maloney and Workman 2002; Mahalingam et al. 2009). In cancer cells, Hsp90 may be important to keep mutated cancer cells viable by buffering unstable proteins. Moreover, the ability of Hsp90 to buffer unstable proteins that arise through mutation appears to be an important mechanism to increase genetic heterogeneity, which eventually propels the generation of new strains and species with mutation-gained phenotype and function.

Each Hsp90 monomer contains an N-terminal domain with an ATP-binding pocket, a middle domain with binding sites for co-chaperones and client proteins, and a C-terminal dimerization domain followed by a MEEVD motif recognized by various tetratricopeptide repeat (TPR) domain containing co-chaperones (Young et al. 1998; Meyer et al. 2004) (**Figure 1.5A**). In some eukaryotic genomes, inducible and constitutive Hsp90 isoforms coexist to adjust the abundance of this chaperone under various situations. Examples include Hsp90α and Hsp90β in humans and Hsp82p and Hsc82p in *S. cerevisiae* (Borkovich et al. 1989; Hansen et al. 1991; Erkine et al. 1995).

1.3.2. Hsp90 chaperone cycle and client protein maturation

More than twenty co-chaperones regulate Hsp90 function in eukaryotic cells. These Hsp90 co-chaperones stimulate or inhibit the ATPase activity of Hsp90, modulate the interactions of Hsp90 with client proteins and other chaperone systems (Siligardi et al. 2002; Ali et al. 2006; McLaughlin et

al. 2006). The most well characterized co-chaperones include Hop/Sti1p, p23/Sba1p, Cdc37p, Aha1p, Hch1p, and Cyp40/Cpr6p. Among them, Hop (Hsc70 and Hsp90 organizing protein)/Sti1p and Cyp40 (cyclophilin 40)/Cpr6p bind to the MEEVD motif; p23/Sba1p facilitates client protein maturation by stabilizing the closed conformation of Hsp90; Cdc37p (cell division cycle protein 37) inhibits whereas Aha1p (activator of heat shock 90 kDa protein ATPase homolog 1) activates the ATPase activity of Hsp90 (Freeman et al. 2000; Siligardi et al. 2002; Roiniotis et al. 2005; Ali et al. 2006; McLaughlin et al. 2006). Other co-chaperones are involved in physiological processes that affect mitochondrial/chloroplast protein import (Tom70/Toc64), melanoma progression (TTC4), nuclear migration (NudC), and Hsp90/Hsp70-dependent protein degradation (CHIP) (Qbadou et al. 2006; Crevel et al. 2008). Thus, despite a great deal of activity in the area, we still know comparatively little about Hsp90 co-chaperones.

The interaction of Hsp90 with client proteins involves the sequential formation of complexes with three different co-chaperones. At first, the "early complex" Hsp40/70 binds with the client protein to initiate the folding process. Next, the "intermediate complex" is formed after the early complex associates with Hsp90. Hop/Sti1p acts as an adaptor protein between Hsp70 and Hsp90 to facilitate client protein transfer between the two complexes. Finally, the "late complex" which contains a PPIase (peptidylprolyl isomerase) and the co-chaperone p23/Sba1p is formed. Notably, similar complexes can be found in diverse organisms from budding yeast to mammals suggesting that this process is highly conserved (Taipale et al. 2010) (**Figure 1.5B**). A typical ATP-dependent Hsp90 cycle starts when Hop/Sti1p binds to Hsp90 in open conformation thus inhibiting its ATPase activity. Next, a PPIase occupies the other TPR-acceptor binding site, leading to an asymmetric Hsp90 intermediate complex. Hsp90 then adopts a closed conformation that releases Hop/Sti1p

followed by the binding of ATP and p23/Sba1p. Finally, p23/Sba1p, PPIase, and the folded mature client protein are released from Hsp90 after ATP hydrolysis (Sullivan et al. 1997; Chadli et al. 2000; Prodromou et al. 2003; Meyer et al. 2004; Taipale et al. 2010) (**Figure 1.5B**).

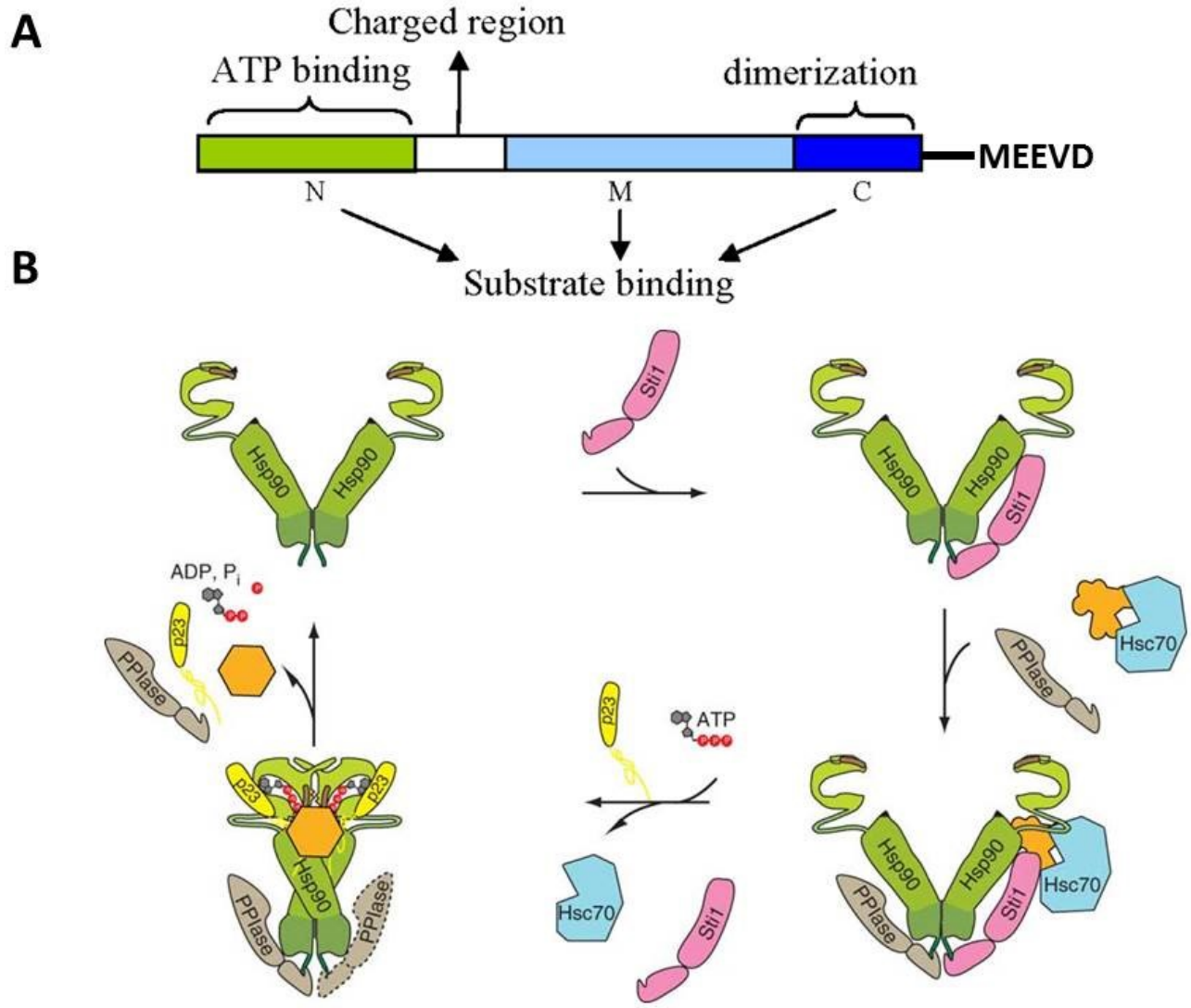

Figure 1.5 Domain architecture of Hsp90 and its ATPase cycle.
(A) Hsp90 contains an N-terminal ATP-binding domain (N, in green), a middle domain (M, in cyan), a C-terminal dimerization domain (C, in blue), and a MEEVD tail sequence. All three domains interact with Hsp90 co-chaperones and client proteins. **(B)** Protein complexes containing immature client protein (yellow irregular shape) and Hsc70 enter the Hsp90 cycle after Sti1/Hop binds to Hsp90 homodimer. Sti1 serves as an adaptor to facilitate client protein transfer between Hsp70 and Hsp90. A PPIase occupies the TPR-acceptor site on the other monomer thereby forming an asymmetric Hsp90 complex. After releasing Hsp70 and Sti1, Hsp90 binds ATP and p23 to transform into a closed conformation. ATP hydrolysis catalyzed by Hsp90 facilitates folding of the client protein into a mature and functional conformation (yellow hexagon). The client protein is then released from Hsp90 with p23 and PPIase (Figure 1.5A from Xu et al. 2012; Figure 1.5B from Li et al. 2011).

1.3.3. Argonaute as a client protein of Hsp90

1.3.3.1. RNAi machinery associated with cytoplasmic granules

Previous studies from our laboratory and other researchers revealed that Argonaute proteins directly interact with Hsp90 chaperone machinery in *Drosophila* and mammalian cells (Tahbaz et al. 2004; Pare et al. 2009; Johnston et al. 2010; Iwasaki et al. 2010; Miyoshi et al. 2010). These data suggested that Argonaute is a client protein of Hsp90. It was also reported that RNAi-mediated silencing complexes associate with two different kinds of cytoplasmic granules: stress granules (SGs) and processing bodies (PBs) (Kedersha et al. 2002; Jakymiw et al. 2005; Liu et al., 2005). SGs are thought to function as mRNA triage centers during cellular stress, within which stalled mRNAs accumulate and are potentially sorted. The stalled mRNAs of essential house-keeping genes are allowed to resume translation whereas mRNAs encoding non-essential gene products are routed to degradation pathways or stored in stress granules for longer periods of times (Anderson and Kedersha 2002; Stohr et al. 2006). Conversely, PBs are specialized for mRNA decay and storage. The characteristic components of PBs include the RNA decapping enzymes Dcp1 and Dcp2, the 5'-3' exonuclease XRN1, RNAi co-factor GW182, and Lsm1-7 heptamer (Sm and Sm-like protein) (Andrei et al. 2005; Wilczynska et al. 2005; Stoecklin et al. 2006). Not all mRNAs in PBs are targeted for degradation as it has been observed that some can exit these structures and resume translation (Yang et al. 2004; Moser et al. 2007). While SGs and PBs are discrete cytoplasmic structures with different morphologies and composition, they are spatially and functionally connected and share common components including XRN1, TTP, and eIF4E (Liu et al. 2005; Leung et al. 2006; Hoyle et al. 2007). The dynamic interactions between them suggest that cytoplasmic compartmentalization is crucial for regulating the fate of mRNA transcripts.

Live cell imaging demonstrated that hAgo2 cycles between the cytoplasm and PBs but not SGs

under normal growth conditions. However, hAgo2 is rapidly recruited to SGs when protein translation is blocked with hippuristanol, a potent inhibitor of eukaryotic initiation factor (eIF) 4A (Pare et al. 2009). Whereas Dicer and TRBP2 are not associated with PBs or SGs, PACT is recruited to SGs during cellular stress (Pare et al. 2009).

1.3.3.2. Hsp90 facilitates structural rearrangements of Argonaute

The inhibition of Hsp90 ATPase activity by geldanamycin reduces the recruitment of hAgo2 to SGs, and impairs RNAi-mediated translational repression and mRNA cleavage (Pare et al. 2009). This suggests that Hsp90 activity is important for hAgo2 subcellular localization and function in gene silencing. Subsequently, it was found that an ATP-dependent conformational change is required for Argonaute proteins to load miRNAs or siRNAs in *Drosophila* (Miyoshi et al. 2010; Iwasaki et al. 2010). Mounting evidence suggests that the loading of RNA duplexes onto Argonaute is ATP-dependent, whereas strand separation occurs in an ATP-independent manner (Miyoshi et al. 2005; Leuschner et al. 2006). Hsc70/Hsp90 chaperone machinery catalyzed ATP hydrolysis is required for a dynamic conformational adjustment to stretch Argonaute proteins so that they can accommodate bulky RNA duplexes. The released tension when Hsp90 transitions from the open to closed form drive the strand separation without the need for ATP hydrolysis (Iwasaki et al. 2010). Immunoprecipitation of FLAG-tagged *Drosophila* Ago1 and Ago2 resulted in co-purification of Hsp90-binding proteins including Hsc70, Hsp83 (a human hsp90 homolog), Hop, and Droj2 (DnaJ-like-2) (Iwasaki et al. 2010). Association of Argonaute proteins with Hsc70/Hsp90 chaperone machinery in mammalian cells was reported even earlier (Tahbaz et al. 2001; Hock et al. 2007).

This is consistent with a scenario in which hAgo2 undergoes Hsp90-dependent conformational

changes to load small RNA duplexes. Moreover, multiple co-chaperones are crucial for this process. Our laboratory reported that p23 and FKBP4 stably associate with hAgo2 before small RNA loading, whereas Cdc37 and Aha1 may be involved in Argonaute maturation (Pare et al. 2013). Aha1 stimulates ATPase activity of Hsp90 that drives the release of mature client proteins. Knockdown of Aha1 reduces the RNAi efficiency; the transient nature of Aha1 interaction with Hsp90-client complex may explain the lack of detectable interaction with hAgo2 (Pare et al. 2013). Together, the published evidence suggests that Hsp90 and a subset of co-chaperones mediate a conformational change in Argonaute proteins that is required to accommodate RNA duplexes. As the Hsp90 system has only been identified as a modulator of RNAi in *Drosophila* and mammalian cells, it will be of interest to determine if this chaperone plays a similar role in distantly related species, such as fission and budding yeasts.

1.4. Post-translational modifications of RNAi core components

1.4.1. Phosphorylation of Argonaute proteins

Mass spectrometry revealed that human Ago2 is phosphorylated on at least seven amino acid residues (Rüdel and Meister 2008; Zeng et al. 2008). Three phosphorylated amino acid residues were located in the PAZ domain (S253, T303, T307), one in the PIWI domain (S798), two in the L2 linker region (S387, Y393), and one in the MID domain (Y529) (Zeng et al. 2008) (**Figure 1.6A**). The majority of these phosphorylation sites are conserved in a wide range of eukaryotes from *Drosophila* to budding and fission yeast (**Table 1.1**). A number of kinases that mediate phosphorylation of hAgo2 have been identified and of significance, changes in the phosphorylation of this protein are linked to the metastatic phenotype (Shen et al. 2013; Horman et al. 2013).

Tyrosine 529 is within the ^{526}-TPVYAEVK-^{533} pocket that binds the 5' phosphates of small RNA duplexes (Rüdel et al. 2011). This amino acid residue is conserved in all identified Argonaute proteins in humans, mouse, *Drosophila*, fission and budding yeast (**Figure 1.6B**). Phosphorylation at this site changes the catalytic activity and substrate binding of hAgo2. Since RNA also contains negatively charged phosphate groups, phosphorylation of Y529 may lead to impaired loading of small RNAs. Structural studies of hAgo2 suggest that Y529 resides deep in a binding pocket that is too narrow for kinases to access. Argonaute proteins do undergo drastic Hsp90-dependent conformational changes to facilitate small RNA duplex loading and it is possible that Y529 could be transiently exposed to kinases at certain stages.

It was presumed that phosphorylation of S798 would have a dramatic effect on Ago2-dependent silencing mRNA targets because it locates within the PIWI domain which possesses RNase H activity. Our laboratory found that a phospho-mimetic substitution of aspartic acid for serine at position 798 (S798D) completely blocks association of hAgo2 with PBs and SGs (Lopez-Orozco et al. 2015). However, the gene silencing activity of hAgo2 was only modestly affected. This suggests that contrary what was widely believed in the RNAi field, localization of hAgo2 to PBs and SGs is not strictly linked to its role in RNAi.

Zeng and colleagues reported that phosphorylation of S387 is required for hAgo2 association to PBs. A study by our laboratory that employed quantitative image analyses, suggests that this is not the case. Phosphorylation of hAgo2 at this residue has been shown to affect its mode of silencing (Pare et al. 2013). Specifically, decreased cleavage-mediated silencing is observed with a concomitant increase in translational repression.

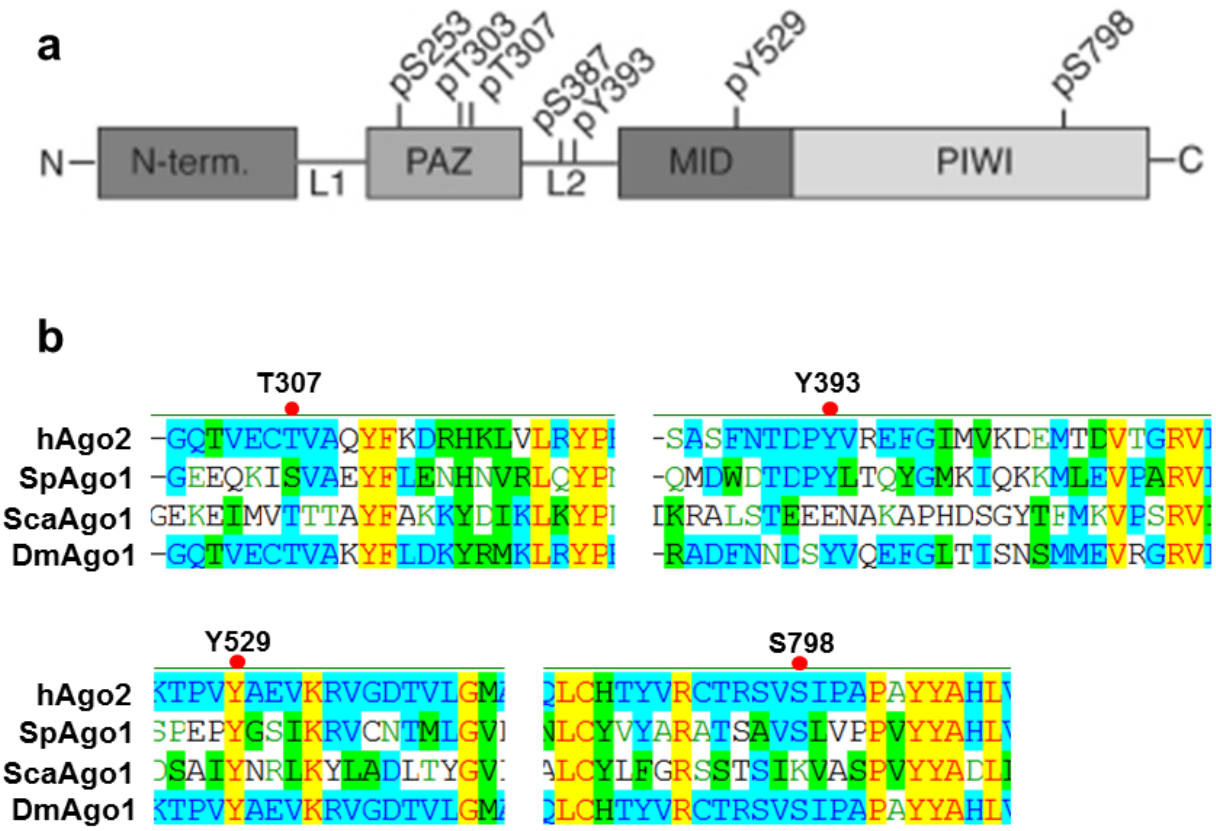

Figure. 1.6 The majority of phosphorylated amino acid residues in human Ago2 are conserved in Argonaute proteins in other eukaryotes. **(A)** Seven phosphorylated amino acid residues were identified by mass spectrometry and are schematically represented on hAgo2. **(B)** The alignments of Argonaute proteins from humans (hAgo2), fruit flies (DmAgo1), and fission (SpAgo1) and budding yeast (ScaAgo1) showed that the majority of these sites are conserved (Figure 1.6A is cited from Rüdel et al. 2011).

1.4.2. Kinases affect Argonaute expression, stability and activity

Co-immunoprecipitation and mass spectrometric analyses revealed that hAgo2 interacts with the kinase domain of epidermal growth factor receptor (EGFR) (Shen et al. 2013). During hypoxia, EGFR is internalized and its interaction with hAgo2 is increased, a process that can be blocked by inhibiting the hypoxia-inducible transcriptional factors HIF1α and HIF2α. Subsequent analysis revealed that Y393 of hAgo2 is phosphorylated by EGFR, a process that is enhanced by hypoxic stress (Shen et al. 2013). Crystal structure analysis indicated that the side chain of Y393 protrudes into the Dicer-binding region of hAgo2 and that phosphorylation of this residue may affect interaction with Dicer. Finally, Shen and colleagues noted that maturation of a class of miRNAs with long-loop structures was inhibited by hypoxia. The conclusion from these studies is that EGFR-mediated phosphorylation of hAgo2 at Y393 inhibits interaction with Dicer thereby negatively impacting miRNA biogenesis. Importantly, modulation of miRNA pathways appears to be important for tumor cells to respond to stress, and thus investigation into potential therapeutic targets may be warranted.

The protein tyrosine phosphatase 1B (PTP1B) was shown to dephosphorylate Y393 (Yang et al. 2014). Subsequent analysis revealed that tyrosine phosphorylation of hAgo2 was significantly reduced when PTP1B was expressed in a substrate-trapping mutant (Yang et al. 2014). In summary, the interaction between Ago2 and Dicer and subsequent miRNA biogenesis requires PTP1B activity to prevent phosphorylation of Y393.

MAP (mitogen activated protein) kinase pathways are linked to phosphorylation of Argonaute proteins. For example, inhibition of p38 MAPK, but not SAPK/JNK (c-Jun N-terminal kinase) and MEK (MAPK/extracellular signal regulated kinase) significantly diminishes S387 phosphorylation

(Zeng et al. 2008). Finally, the proto-oncogene Akt-3/PKBγ has also been reported to increase phosphorylation of hAgo2, a process that enhances translational repression of miRNA targets tumor-suppressor genes PDCD1 (programmed cell death 1) and PTEN (phosphatase and tensin homolog) (Asangani et al. 2008; Meng et al. 2007). Phosphorylation of S387 by Akt3 does not affect small RNA loading but rather, facilitates hAgo2 interaction with GW182, a process that has been linked to its localization to PBs (Horman et al. 2013). Therefore, Akt3-mediated phosphorylation at S387 may function as a molecular switch between mRNA cleavage and translational repression, rather than as a regulator of small RNA loading and passenger strand degradation.

1.4.3. Other post-translational modifications of Argonaute proteins

Post-translational modifications are chemical changes that occur on amino acid side chains in a site-specific way. These modifications can temporarily or permanently change the protein function by altering the structure, electrical charge, stability, and localization of the target protein through the recruitment of the modified groups (Mann and Jensen 2003; Blom et al. 2004). Argonaute proteins have been shown to be modified by prolylhydroxylation, ubiquitination, poly-ADP-ribosylation, and SUMOlyation (Qi et al. 2008; Rybak et al. 2009; Pratt et al. 2009; Jee and Lai 2014; Sahin et al. 2014; Josa-Prado et al. 2015).

It was reported that hAgo2 associated with collagen prolyl 4-hydroxylase I (C-P4H) (Qi et al. 2008). Further analysis identified that proline 700 is a target of proxyl 4-hydroxylation, which stabilized hAgo2 and increases its association with small RNA duplexes (Qi et al. 2008; Wu et al. 2011). Blocking of hydroxylation at P700 leads to decreased hAgo2 levels and subsequent reduction in RNAi efficiency (Wu et al. 2011).

Ubiquitination of mouse Ago2 by the ligase Lin-41 was shown to lead to a loss of the protein in embryonic stem cells (Rybak et al. 2009). In *C. elegans*, the miRNA-target interaction between let-7 miRNA and lin-41 is crucial for the transition from larval to adult (Reinhart et al. 2000). This pathway is highly conserved, from invertebrates to vertebrates. Depletion of the ubiquitin-activating enzyme 1 stabilizes *Drosophila* AGO1, and treatment of mammalian cells with the proteasome inhibitor MG132 stabilizes hAgo2 (Johnston et al. 2010; Smibert et al. 2013). However, the identity of the E3 ubiquitin ligase that is required for the conserved feedback loop between Argonaute proteins and certain miRNAs is not known. Autophagy was also reported to decrease Argonaute stability in some conditions (Gibbings et al. 2012; Martinez and Gregory 2013). Together, these studies indicate that Argonaute levels are modulated by a variety of mechanisms. Ubiquitylation is probably more important for Argonaute protein degradation than for its function.

Recent data indicates that cellular stress leads to a global remodeling of Argonaute binding and its localization pattern (Karginov and Hannon 2013). During cellular stress, mammalian Argonaute proteins that are loaded with small RNAs become enriched in SGs and PBs (Baumberger et al. 2007). Several poly (ADP-ribose) polymerases and glycohydrolases are also recruited to SGs, and a portion of the Argonaute pool at these sites becomes PARylated (Leung et al. 2011). Poly-ADP-ribosylation (PARylation) of Argonaute correlates with inhibition of their cleavage activities. It is likely that post-translational modifications differentially influence the subcellular localization and activities of Argonaute proteins in response to different cellular stresses. Table 1.1 summarizes the effects of known post-translational modifications on hAgo2.

Table 1.1 Post-translational modifications of human Argonaute 2

Argonaute modification	Regulatory impact
P700 prolyl 4-hydroxylation	Increased Ago stability, increased miRNA levels/activity during hypoxia
S253, T303, T307, S798 phosphorylation	Unknown
S387 phosphorylation (MAPK or Akt3)	Localization to P-bodies; increased translational repression versus target-cleavage mode
Y529 phosphorylation	Impaired miRNA binding; transient relief of miRNA activity during macrophage activation
Y393 phosphorylation (EGFR)	Inhibited maturation of long-loop pre-miRNAs during hypoxia; increased cell survival/invasiveness
Ubiquitination	Destabilization of unloaded Ago; also promotes turnover and remodeling of miRISC pool during T cell activation
PARylation	Suppression of RNA silencing

(Modified from Johnston and Hutvagner 2011; Jee and Lai 2014)

1.5. Rationale and Objective

RNAi pathways are thought to directly and indirectly regulate more than half of all human genes (Friedman et al. 2009). Moreover, RNAi-mediated gene silencing is crucial for diverse biological processes, including antiviral defence, transposon silencing, metabolic control, cell proliferation, differentiation, development and death (Friedman et al. 2009; Carthew and Sontheimer 2009; Kim et al. 2009). However, the current understanding on the regulatory mechanisms of RNAi via its core components is quite limited compared to the mechanisms by which RNAi represses gene expression.

The finding that RNAi pathway can be reconstituted in *S. cerevisiae* brings this extremely well-characterized experimental organism into the study of the mechanism and regulation of RNAi pathways. Part of my PhD studies focused on restoring the RNAi pathway in *S. cerevisiae* by introducing Argonaute and Dicer genes from *S. castellii* and humans. By generating inter-species pairs of Argonaute and Dicer, with or without the expression of co-facotrs, this study may reveal the minimum requirements for a functional RNAi pathway *in vivo*, and how the RNAi components interact with each other in an evolutionarily conserved manner. *S. cerevisiae* cells containing restored

RNAi pathways can also be used to investigate if the ATPase activity of Hsp90 is required for RNAi-mediated gene silencing.

Emerging data indicate that post-translational modifications (PTMs), especially protein phosphorylation, play vital roles in regulating subcellular localization and function of Argonaute proteins (Qi et al. 2008, Zeng et al. 2008; Rudel et al. 2011). The role of *S. pombe* Ago1, Dcr1, and Rdp1 in transcriptional and post-transcriptional gene silencing are relatively well understood. Moreover, access to a systematic kinase deletion library and dozens of phosphatase deletion strains made *S. pombe* an excellent model system to study phosphorylation/dephosphorylation on Argonaute.

The objective of my thesis research was to identify and characterize factors involved in the regulation of core RNAi components in both budding yeast *S. cerevisiae* and fission yeast *S. pombe*. Since RNAi mechanism and its key components are highly conserved in eukaryotes, our findings in yeast may reveal mechanisms that regulate gene expression in mammalian cells.

Chapter 2

Materials & Methods

2.1. Materials

2.1.1. Reagents

Reagents were purchased from the indicated vendors and used according to the manufacturer's recommendations unless otherwise stated.

Table 2.1 Commercial sources of reagents, chemicals, and other materials

Reagents	Source
β-Mercaptoethanol (β-Me)	BioShop Canada
Acrylamide/Bis-acrylamide solution (40%; 29:1)	Bio-Rad
Adenine hemisulfate dihydrate	MP Biomedicals
Agar	Difco
Acid washed beads (425-600 micron)	Sigma-Aldrich
Acetone (certified ACS)	Fisher Scientific
Acetonitrile	Sigma-Aldrich
Agarose (UltraPure)	Fisher Scientific
Ammonium sulphate	Fisher Scientific
Ampicillin	Sigma-Aldrich
Anti-FLAG M2 magnetic beads	Sigma-Aldrich
Bacto-peptone	Becton, Dickinson and Company (BD)
Bacto-tryptone	Becton, Dickinson and Company (BD)
Bacto-yeast extract	Becton, Dickinson and Company (BD)
Bovine serum albumin (BSA)	Sigma-Aldrich
Butanol	Fisher Scientific
Chloroform	Fisher Scientific
Complete EDTA-free protease inhibitor	Roche
Commassie brilliant blue	Invitrogen
Difco-yeast extract	Becton, Dickinson and Company (BD)
Difco-yeast nitrogen base	Becton, Dickinson and Company (BD)
Deoxyribonucleotide triphosphate (dNTP)	New England BioLabs
Dextrose (D-Glucose)	Fisher Scientific
Dimethyl sulphoxide (DMSO)	Sigma-Aldrich
Dithiothreitol (DTT)	Sigma-Aldrich
Edinburgh minimum medium (EMM)	Sunrise Science
Ethanol	Biochemistry Store(UAlberta)
Ethylenediaminetetraacetic acid (EDTA)	Sigma-Aldrich
5-fluoroorotic acid (5-FOA)	Sigma-Aldrich
G418 (Geneticin)	Sigma-Aldrich
Geldanamycin	LC laboratories
Glycerol	Fisher Scientific

Glycine	Fisher Scientific
Glacial acetic acid	Fisher Scientific
Galactose (D-Galactose)	Fisher Scientific
4-(2-hydroxyethyl)-1-piperazineethanesulfonic acid (HEPES)	Fisher Scientific
Hydroxyurea (HU)	Sigma-Aldrich
Iodoacetamide	Bio-Rad
Isopropanol	Sigma-Aldrich
Kanamycin	Sigma-Aldrich
L-Histidine	MP Biomedicals
L-Isoleucine	ACROS Organics
L-Leucine	ACROS Organics
L-Lysine	ACROS Organics
L-Threonine	MP Biomedicals
L-Tryptophan	MP Biomedicals
L-Tyrosine	Fisher Scientific
Lithium acetate (LiOAc)	Acros Organics
Magnesium chloride ($MgCl_2$)	Fisher Scientific
Methanol	Fisher Scientific
N,N,N',N'-Tetramethylethylenediamine (TEMED)	Sigma-Aldrich
NVP-AUY922	Chemie Tek
Phenol	Fisher Scientific
Phenol: Chloroform: Isoamyl alcohol (25:24:1)	Sigma-Aldrich
Polyethylene glycol (PEG) 3550	Sigma-Aldrich
Polyvinyldene difluoride (PVDF) membrane	Bio-Rad
Ponceau stain	MP Biomedicals
Potassium chloride (KCl)	Fisher Scientific
Protein A sepharose	GE Healthcare
Radicicol	TOCRIS
Raffinose	MP Biomedicals
RNase/DNase free water	Invitrogen
Skim milk powder	Carnation
Sodium cloride (NaCl)	Sigma-Aldrich
Sodium dodecyl sulphate (SDS)	Fisher Scientific
Sodium fluoride (NaF)	Sigma-Aldrich
Sodium hydroxide (NaOH)	Sigma-Aldrich
Sodium orthovandate (Na_3VO_4)	Sigma-Aldrich
Sorbitol	Sigma-Aldrich
Trichloroacetic acid (TCA)	Fisher Scientific
Trifluoroacetic acid (TFA)	Thermo Scientific
Thiabendazole (TBZ)	Sigma-Aldrich
TRIzol reagent	Thermo Fisher Scientific
Tris base (biotechnology grade)	AMRESCO
Triton X-100	VWR International

Trypsin	Promega
Tween 20	Fisher Scientific
Uracil	MP Biomedicals
Zymolyase-20T	Sigma

Table 2.2 Multi-components systems/kits

System	Source
Halt Protease Inhibitor Cocktail (1:100)	Thermo Scientific
Bio-Rad Protein Assay Kit	Bio-Rad
ECL Plus Western Blotting Detection System	GE Healthcare
Expand High Fidelity PCR system	Roche
HiSpeed Plasmid Midi Kit	QIAGEN
Platinum Taq PCR System	Invitrogen
PerfeCTa SYBR Green SuperMix, Low ROX	Quanta Biosciences
QIAEX II Gel Extraction Kit	QIAGEN
QIAprep Spin Miniprep Kit	QIAGEN
QIAquick PCR Purification Kit	QIAGEN
QuikChange Multi Site-Directed Mutagenesis Kit	Agilent
Quick Start Bradford Protein Assay Kit	QIAGEN
SuperScript III Reverse Transcriptase System	Invitrogen

Table 2.3 DNA/RNA modifying enzymes

Enzyme	Source
Calf intestinal alkaline phosphatase	Invitrogen
DNase I, amplification grade	Invitrogen
Restriction endonucleases	New England BioLabs (NEB); Invitrogen
RNase Out	Invitrogen
RNase A	Invitrogen
Shrimp alkaline phosphatase	Invitrogen
T4 DNA ligase	NEB, Invitrogen

Table 2.4 Molecular size standards

Marker	Source
1 kb DNA Ladder	Invitrogen
PageRuler Prestained Protein Ladder, 10 to 180 kDa	Thermo Scientific
PageRuler Plus Prestained Protein Ladder, 10 to 250 kDa	Thermo Scientific

Table 2.5 Detection systems

Equipment	Marker
BlueView Transilluminator	Vernier Technology

Eppendorf Refrigerated Microcentrifuge 5417R	Eppendorf
Eppendorf Mastercycler Pro Thermal Cyclers	Eppendorf
FACSCalibur Flow Cytometer	BD Biosciences
FluorChem Q Imaging System	Cell BioSciences
IPGphor System	Amersham Biosciences
Isotemp 2100 Incubator	Fisher Scientific
LSRFortessa Cell Analyzer	BD Biosciences
MiniBeadbeater-8	Bio Spec Product
Stratagene Mx3005P qPCR System	Agilent Genomics
MicroPulse Electroporator	Bio-Rad
NanoDrop 2000 UV-Vis Spectrophotometer	Thermo Scientific
pH Meter 240	Corning
Planetary Ball Mill PM 100	Retsch
Vortex Genie 2	Fisher Scientific

2.1.2. Commonly used buffers and media

Table 2.6 Buffers and Solutions

Buffers and Solutions	Ingredients
10 x Colony PCR buffer	0.125 M Tris-HCl (pH 8.5); 0.56 M KCl
6 x DNA gel loading buffer	40% (w/v) sucrose; 0.25% (w/v) bromophenol blue; 0.25% (w/v) xylene cyanol
6 x Protein sample buffer	62.5 mM Tris-HCl (pH 6.8); 25% (v/v) glycerol; 2% (v/v) SDS; 0.01% (w/v) bromophenol blue; 5% (v/v) β-mercaptoethanol
5 x TE buffer	50 mM Tris-HCl (pH 7.5); 5 mM EDTA
Alkaline lysis buffer	200 mM NaOH; 1% (w/v) SDS
DNA preparation buffer	50 mM Citrate/Phosphate (pH 5.6) (contains 7.1 g/l Na_2HPO_4 and 11.5 g/l citric acid); 40 mM EDTA (pH 8.0); 1.2 M sorbitol
Equilibration buffer (2D gel)	0.05 M Tris-HCl (pH 8.8); 6 M urea; 30% (v/v) glycerol; 2% (w/v) SDS

LiAc/TE	10 mM Tris (pH 7.2); 100 mm lithium acetate; 1 mM EDTA
Luria-Bertani (LB) broth, Miller	10 g/l Bacto-tryptone; 5 g/l NaCl; 5 g/l Bacto-yeast extract;
Phosphate buffered saline (PBS)	137 mM NaCl; 2.7 mM KCl; 8 mM Na_2HPO_4 (pH 7.4)
PBS-Tween	137 mM NaCl; 2.7 mM KCl; 8 mM Na_2HPO_4 (pH 7.4); 0.05% (v/v) Tween-20
PEG solution	10 mM Tris (pH 7.2); 100 mM lithium acetate; 1 mM EDTA; 40% (w/v) PEG 3550
Protein resuspension buffer	20 mM Hepes (pH 7.4); 1:100 HALT protease inhibitor cocktail; 1:100 sodium fluoride; 5 mM sodium fluoride; 1:500 sodium orthovanadate
Rehydration buffer (2D gel)	8 M Urea; 2% (w/v) CHAPS; a speck of bromophenyl blue. Add 4 mg/ml DTT and 5 µl /ml pH specific IPG buffer prior to use
SDS-PAGE running buffer	250 mM glycine; 0.1% SDS; 100 mM Tris base
SDS-PAGE resolving gel buffer	0.1% SDS; 374 mM Tris-HCl (pH 8.8); 4% acrylamide/bis-acrylamide; 0.1% (w/v) APS; 0.1% (v/v) TEMED
SDS-PAGE stacking gel buffer	0.1% SDS; 250 mM Tris-HCl (pH 6.8); 6%-12% acrylamide/ bis-acrylamide; 0.1% (w/v) APS; 0.1% (v/v) TEMED
Tris, acetic acid and EDTA buffer (TAE)	40 mM Tris-acetate; 1 mM EDTA (pH 8.0)
Tris-buffered saline (TBS)	137 mM NaCl; 2.7 mM KCl; 24 mM

	Tris-HCl (pH 7.4)
TBS-Tween	137 mM NaCl; 2.7 mM KCl; 24 mM Tris-HCl (pH 7.4); 0.05% (v/v) Tween-20
Western blot transfer buffer	20% methanol; 200 mM glycine; 25 mM Tris base (pH 8.3), 0.1% (w/v) SDS
Yeast breaking buffer	2% Triton X-100; 1% SDS; 100 mM NaCl; 10 mM Tris-HCl (pH8.0); 1 mM EDTA

Table 2.7 Yeast media

Yeast Media	**Ingredients**
Edinburg minimum media (EMM)	3 g/l potassium hydrogen phthalate; 2.2 g/l Na_2HPO_4; 5 g/l NH_4Cl; 2% (w/v) glucose **50 x Salts**: 52.5 g/l $MgCl_2 \cdot 6H_20$; 0.735 mg/l $CaCl_2 \cdot 2H_20$; 50 g/l KCl; 2 g/l Na_2SO_4 **1000 x Vitamins**: 1 g/l pantothenic acid; 10 g/l nicotinic acid; 10 g/l inositol ; 10 mg/l biotin **10,000 x Minerals:** 5 g/l boric acid; 4 g/l $MnSO_4$; 4 g/l $ZnSO_4.7H_2O$; 2 g/l $FeCl_2.6H_2O$; 0.4 g/l molybdic acid; 1 g/l KI; 0.4 g/l $CuSO_4.5H_2O$; 10 g/l citric acid
Synthetic complete (SC)	6.7 g/l Yeast nitrogen base without amino acids;

	10 x amino acid dropout: 200 mg/l adenine hemisulfate; 200 mg/ arginine; 200 mg/l histidine monohydrate; 300 mg/l isoleucine; 300 mg/l lysine HCl； 200 mg/l methionine； 500 mg/l phenylalanine； 2000 mg/l threonine； 300 mg/l tyrosine； 200 mg/l uracil； 1500 mg/l valine
Yeast extract (YE)	0.5% (w/v) yeast extract; 3.0% (w/v) glucose
Yeast extract + supplements (YES)	YE medium added with 225 mg/l of each adenine, histidine, leucine, uracil and lysine hydrochloride
Yeast extract + peptone dextrose (YPD)	10 g/l yeast extract; 20 g/l peptone; 20 g/l dextrose
Solid media was made by adding 2% Agar	

2.1.3. Oligonucleotides

Table 2.8 Oligonucleotides

Oligonucleotides	**Sequences**
byr1 knockout sense	5'-TAATTAACCCGGGGATCCGTCGACCTTCTAGCTATTGGCCAAATT -3'
byr1 knockout antisense	5'-AAACGAGCTCGAATTCATCGATGATAATGTGCAAAGGACGCAATG-3'
ckb1 knockout sense	5'-TAATTAACCCGGGGATCCGTCGACCGCTTCGTTCCGATTTACGTTG-3'
ckb1 knockout antisense	5'-AAACGAGCTCGAATTCATCGATGATAAGGCATTTTGCTTAATCTTC-3'
dg forward	5'-TGTGCCTCGTCAAATTATCATCCATCC-3'
dg reverse	5'-ACTTGGAATCGAATTGAGAACTTGTTATGC-3'
gsk3 knockout sense	5'-TAATTAACCCGGGGATCCGTCGACCTATGGATGATGATACAGAAATG-3'
gsk3 knockout antisense	5'-AAACGAGCTCGAATTCATCGATGATAATGTAACGGGTATATGCATTC -3'
hAgo2 sense	5'-GAGAGAATGAGTATGCACCCATTCCAGTGGTG

	TAAC-3’
hAgo2 antisense	5’-GAGAGAGTCGACTCACTAAGCAAAGTACATG GTGCGCAG -3’
hDcr sense	5’-GAGAGAACTAGTATGAAAAGCCCTGCTTTGCA AC -3’
hDcr antisense	5’-GAGAGACTCGAGTCACTATTGGGAACCTGAG GTTGATTAG-3’
hDcr-myc sense	5’-GAGAGACCGCGGCAGCACTCCCCGGGGGTCC TC-3’
hDcr-myc antisense	5’-GAGACTCGAGCTATCACAGATCTTCTTCAGAA ATAAGTTTTTGTTCTTGGAACCTGAGG-3’
KanMX6 sense	5’- GGGTAAGGAAAAGACTCACG -3’
KanMX6 antisense	5’- TGCATGGTTACTCACCACTG -3’
LRP1 knockout sense	5’-GAAATCGATTAATATAAACATATATCTAGCAAC GTAACGGAGTATTAGATCAGTAATGCGTACGCTG CAGGTCGAC-3’
LRP1 knockout antisense	5’-GCTCTCACATCACCTTTAATCATTTTTTCACTCA TGTACCAGTATACGTCGACCTCTAATCGATGAATT CGAGCTCG-3’
MRPL3 knockout sense	5’-ACTAAAATAATCTGAAAAGAATTGGTGAAAAG AAAGCTGTAGTTATATATACAGAATGCGTACGCTG CAGGTCGAC-3’
MRPL3 knockout antisense	5’-GTACAAGAATGTATTCTGGTTAAGGAGTTCTCT ATCTACAAAATGGCAAACACAGAACTAATCGATG AATTCGAGCTCG-3’
PDR5 knockout sense	5’-ATTAAAGACCCTTTTAAGTTTTCGTATCCGCTC GTTCGAAAGACTTTAGACAAAAATGCGTACGCT GCAGGTCGAC -3’
PDR5 knockout antisense	5’-ATTAAAAAAGTCCATCTTGGTAAGTTTCTTTTC TTAACCAAATTCAAAATTCTATTAATCGATGAATT CGAGCTCG-3’
pka1 knockout sense	5’-TAATTAACCCGGGGATCCGTCGACCGAGTACAAA TGTGAAATAGC -3’
pka1 knockout antisense	5’-AAACGAGCTCGAATTCATCGATGATATGTTTTG TGCCACGTTTGTTTTG -3’
pmk1 knockout sense	5’-TAATTAACCCGGGGATCCGTCGACCCCTTGCG ACTTATAGCATGC -3’
pmk1 knockout antisense	5’-AAACGAGCTCGAATTCATCGATGATATACATTG GCAGCAGCTGGTT -3’
RNT1 knockout sense	5’-TAAATGCGCATATAGAAGAGAGCAAAACTGTC CTATTTACAAGCTTTTCAAAACAATGCGTACGCT GCAGGTCGAC-3’
RNT1 knockout antisense	5’-TATGGCTAAAGAAAATCAATGCAAGTTCCATC ATGGTTGTGTAAAAGGAACGTTTCAATCGATGAA

	TTCGAGCTCG -3’
ScaAgo1 sense	5’-GAGAGATGTCATCCAATTCGGAGGAGAACAGT C-3’
ScaAgo1 antisense	5’-GAGAGATCATATGTAGTACATGATGTCAGTG -3’
ScaDcr1 sense	5’-GAGAGAATGAATAGAGAAAAAAGCGCCGATC TAAG -3’
ScaDcr1 antisense	5’-GAGAGATCACAGATTGTTGCAATGCCTCAAG -3’
ScaDcr1-myc antisense	5’-GAGACTCGAGCTATCACAGATCTTCTTCAGAA ATAAGTTTTTGTTCCAGATTGTTGC-3’
ScaDcr1-myc antisense	5’-GAGACTCGAGCTATCACAGATCTTCTTCAGAA ATAAGTTTTTGTTCCAGATTGTTGC-3’
SNF1 knockout sense	5’-AAATAGAAGTTTTTTTTTGTAACAAGTTTTGCT ACACTCCCTTAATAAAGTCAACATGCGTACGCTG CAGGTCGAC -3’
SNF1 knockout antisense	5’-ATACGTTACGATACATAAAAAAAAGGGAACTT CCATATCATTCTTTTACGTTCCACCATCA ATCGATGAATTCGAGCTCG-3’
TIF11 knockout sense	5’-TTATGTAGAAGGTGTACTTGCAAAAGCACTAG TGTAATATAGAGCAAAGTTCATCATGCGTACGCT GCAGGTCGAC-3’
TIF11 knockout antisense	5’-AATAAATTATGAATAGTTGACGCATTAGAAGAT ATTGAGGACACTTGTTCGGCCTAAATTTTAATCGA TGAATTCGAGCTCG -3’
TRBP2 sense	5’-GAGAGAGGATCCATGAGTGAAGAGGAGCAAG GCTC-3’
TRBP2 antisense	5’-GAGAGACTCGAGTCACTACTTGCTGCCTGCCA TGATCTTG -3’
wee1 knockout sense	5’-TAATTAACCCGGGGATCCGTCGACCGTTTTCTG TATGGAAAATGTG -3’
wee1 knockout antisense	5’-AAACGAGCTCGAATTCATCGATGATAACCTTTT AGAGACTCTTGTTC- 3’

2.1.4. Plasmids

Table 2.9 Plasmid vectors

Vectors	**Source**
pFA6a-kanMX6	Addgene plasmid repository
pRS404-P_{TEF}-ScaAgo1	Addgene plasmid repository
pRS404-P_{TEF}-hAgo2	Addgene plasmid repository
pRS405-P_{TEF}-ScaDcr1	Constructed in this study
pRS405-P_{TEF}-hDcr	Constructed in this study

pRS404-P_{TEF}-HA-ScaAgo1	Constructed in this study
pRS404-P_{TEF}-HA-hAgo2	Constructed in this study
pRS405-P_{TEF}-ScaDcr1-myc	Constructed in this study
pRS405-P_{TEF}-hDcr-myc	Constructed in this study
pRS403- P_{GAL1}-weakSC-*GFP*	Addgene plasmid repository
pRS403- P_{GAL1}-strongSC-*GFP*	Addgene plasmid repository
pRS403- P_{GAL1}-SC-*URA3*	Addgene plasmid repository
pRS406-P_{ADH1}-GFP (S56T)	Constructed in this study
pREP3x, pREP3x-ScaAgo1	Dr. Forsburg, University of Southern California
pYES2.1	Addgene plasmid repository

2.1.5. Antibodies

Table 2.10 Primary antibodies

Antibody	Dilution	Application	Source (Product ID)
Goat anti-TRBP2 (C-18)	1:2000	WB	Santa Cruz Biotechnology
Mouse anti-actin	1:1000	WB	Abcam
Mouse anti-c-Myc (9E10)	1:2000	WB, IP	Abcam
Mouse anti-FLAG (F3165)	1:1000	IP	Sigma
Rat anti-HA (3F10)	1:2000	WB, IP	Sigma
WB: Western blot; IP: immunoprecipitation			

Table 2.11 Secondary antibodies

Antibody::Conjugate	Dilution	Application	Source
Donkey anti-goat::HRP (sc-2020)	1:3000	WB	Santa Cruz Biotechnology
Goat anti-mouse::HRP	1:4000	WB	Abcam; Jackson Immuno Research
Goat anti-rabbit::HRP	1:4000	WB	Abcam; Jackson Immuno Research
Goat anti-rat::HRP (ab97057)	1:2000	WB	Abcam
WB: Western blot			

Table 2.12 *S. pombe* strains used and constructed in this study

Strain	Genotype	Source	Institution
TV294	h- *ura*4-D18 DS/E	Dr. T. Volpe	Northwestern University
TV292 (Δ*ago*1)	h- *ago1*::kanMX6 *ura*4-D18 DS/E	Dr. T. Volpe	Northwestern University
TV296	h- *rdp1*::kanMX6 *ura*4-D18 DS/E	Dr. T. Volpe	Northwestern

(Δ*rdp*1)			University
TV293 (Δ*dcr*1)	h- *dcr1*::kanMX6 *ura*4-D18 DS/E	Dr. T. Volpe	Northwestern University
FY254	h- *can*1-1 *leu*1-32 *ade*6-M210 *ura*4-D18	Dr. S. Forsburg	University of Southern California
S51	h+ *otr*1R(*SphI*)::*ura*4+ *ura*4-DS/E *leu*1-32 *ade*6-M210	Dr. Mo Motamedi	Harvard Medical School
S155	h+ *otr*1(*SphI*)::*ura*4+ *ura*4-DS/E *leu*1-32 *ade*6-M210 *ago*1::Nat^r-Ago1promoter -3xFLAG-*ago*1	Dr. Mo Motamedi	Harvard Medical School
AY160-14D	h90 *ade*6-216 *leu*1-32 *lys*1-131 *ura*4-D18	Yeast Genomic Resource Center (Japan)	
FY15177	h90 *ade*6-216 *leu*1-32 *lys*1-131 *ura*4-D18 *ago*1::*ago*1-GFP-HA-Kan^r	Yeast Genomic Resource Center (Japan)	

2.2. Methods

2.2.1. Culturing and handling yeast

Yeast strains were grown at 30°C or as otherwise indicated (*e.g.* mild heat shock at 37°C). Either rich media (YPD for the budding yeast *S. cerevisiae*; YES for the fission yeast *S. pombe*) or synthetic media (SC for *S. cerevisiae*; EMM for *S. pombe*) were used (**Table 2.7**). Rich media contains yeast extract which provides ample metabolites, whereas synthetic media (complete or amino acid dropout) contain known types and amounts of carbon and nitrogen sources.

Yeast cells were grown in liquid media at 30°C for 16–18 hours. The optical density (O.D.) of cell cultures was measured using a NanoDrop 2000 UV-Vis Spectrophotometer (Thermo Scientific) until it reached stationary phase ($OD_{600} > 1.5$). In general, the doubling time of most yeast strains growing in synthetic media (*e.g.* SC or EMM) was twice as long as in rich media (*e.g.* YPD or YES).

For short-term storage (up to two months), yeast strains were kept at 4°C as patches on

appropriate plates wrapped with plastic paraffin film. For long term storage, yeast cells in rich media were mixed with equal volume of 25% glycerol in screw cap microcentrifuge tubes, and stored at –80°C indefinitely.

2.2.2. Transformation protocols

2.2.2.1. Transformation of competent *E. coli*

For *E. coli* transformation, 50 ng of plasmid DNA was added into 50-100 µl ice-thawed DH5α competent cells. The mixture was incubated on ice for 30 minutes, heat shocked at 42°C for 45 seconds, and then incubated on ice for 2 minutes to let cells recover. Next, 950 µl of LB liquid medium with no antibiotic was added and incubated at 37°C for 1 hour. Around 100 µl of the mixture was spread onto a fresh LB agar plate with appropriate antibiotics (*e.g.* ampicillin, kanamycin). Plates were incubated at 37°C for 12-16 hours until colonies appeared.

2.2.2.2. Transformation of budding yeast *S. cerevisiae*

Lithium acetate transformation protocol was modified for *S. cerevisiae* transformation (Ito et al. 1983; Hill et al. 1991; Gietz et al. 1992). Single colonies of experimental strains were grown in liquid media with required nutrients at 30°C. Overnight cultures were diluted to an OD_{600} of 0.3 with fresh media, and then incubated for 4 hours at 30°C to reach exponential growth phase. Next, 1 ml of each cell culture was centrifuged at 3,000 x g for 3 minutes, resuspended in 1 ml sterilized water and centrifuged at 3,000 x g for 3 minutes again. Cell pellets were resuspended in 1 ml LiAc/TE (**Table 2.6**) and centrifuged at 3,000 x g for 3 minutes. Supernatant was aspirated until about 100 µl left in the tube. Next, 10 µl of freshly boiled salmon sperm DNA (10 µg/µl), 0.5–2 µg plasmid DNA or 1–7

µg linear DNA, 300 µl of PEG solution (**Table 2.6**), and 6 µl of DMSO were added sequentially. The mixtures were incubated in a 30°C water bath for 1 hour, heat shocked at 42°C for 15 minutes, centrifuged at 3,000 x g for 3 minutes, washed with 1 ml of 1M sorbitol, and then resuspended in 1 ml YPD medium. The YPD-sorbitol (1:1) liquid cultures were grown at 30°C overnight. The next morning, cells were collected and washed with sterile water, and plated on appropriate synthetic dropout media. Plates were incubated at 30°C for 3-5 days until colonies appeared.

2.2.2.3. Transformation of fission yeast *S. pombe*

Transformation of *S. pombe* cells was conducted either by the lithium acetate protocol as described above or by electroporation. Cell cultures were grown at 30°C to early-stationary phase (OD_{600} = 1.2–1.5), incubated on ice for 5 minutes, and then centrifuged at 1,600 x g at 4°C for 5 minutes. Cells were resuspended in equal volume of ice-cold sterile water, vortexed well, centrifuged at 8,000 x g at 4°C for 10 seconds and carefully aspirated the supernatant. Cells were then resuspended in 200 µl of 1 M sorbitol, 0.5-1 µg of plasmid or linear DNA was added and mixed well by pipetting. The mixtures were transferred to an electroporation cuvette, incubated on ice for 5 min before being placed into a Bio-Rad MicroPulse Electroporator (**Table 2.5**). The mixtures were pulsed at 1.5 kV, 200 Ω, 25 µF for 4.0-6.0 ms using "*fungi*" > "*ShS*" program. Immediately after the electrical pulse, 800 µl of ice-cold 1M sorbitol was added. The cell suspensions were mixed well, transferred into microcentrifuge tubes, and incubated for 1 hour at 30°C. Up to 200 µl volume of the mixture was spread on plates with appropriate antibiotics or nutrient drop-outs. Plates were then incubated at 30°C for 3-5 days until single colonies appeared.

2.2.3. Construction of plasmids for RNAi reconstitution in *S. cerevisiae*

Vectors pRS404-P_{TEF}-ScaAgo1 and pRS405-P_{TEF}-ScaDcr1 were purchased from Addgene plasmid repository (https://www.addgene.org/). Vector pRS404-P_{TEF}-hAgo2 and pRS405-P_{TEF}-hDcr were constructed by ligating the coding sequence into the multiple cloning sites (hAgo2 between SpeI and XhoI; hDcr between XbaI and XhoI).

The stability of transformants was examined to confirm the chromosomal integration of the plasmids. After transformants were first selected on the appropriate synthetic dropout media, multiple individual colonies were then picked and streaked on synthetic complete media to recover. Subsequent, individual colonies were plated back on synthetic dropout media to select for the integration of the introduced module. If the gene of interest was integrated, the phenotype (auxotrophic in this situation) was maintained after relaxing the selection on synthetic complete media. On the other hand, if the gene of interest was not integrated and lost in the absence of selection pressure, the colonies would not grow when plated back on the selective media. Furthermore, it was necessary to grow yeast cells transformed with extrachromosomal plasmids in appropriate synthetic dropout media to keep the selection pressure.

2.2.4. Serial dilution assay to measure *URA3* silencing in *S. cerevisiae*

Genetic constructed *S. cerevisiae* strains harbouring *S. castellii* or human RNAi components, *URA3* as the reporter gene, and the corresponding silencing construct were grown overnight in liquid synthetic complete media with 2% raffinose as the carbon source. Cell cultures were diluted to an OD_{600} of 0.1, and 10 µl volume of 1:10 serial dilutions were spotted onto the appropriate plates (SC, SC-ura, or 5-FOA) containing either 2% glucose (*URA3* silencing construct not induced) or 2%

galactose (*URA3* silencing construct induced). Plates were incubated at 30 °C for 3 days before taking images.

2.2.5. Fluorescence-activated cell sorting (FACS) analysis of *GFP* in *S. cerevisiae*

The relative *GFP* fluorescence in constructed *S. cerevisiae* strains was measured by flow cytometry. Briefly, each strain was grown overnight in the appropriate synthetic dropout media with 2% raffinose as a carbon source. Overnight cultures were seeded into 10 x volume of fresh liquid media with either 2% glucose (*GFP* silencing constructs repressed) or 2% galactose (*GFP* silencing constructs induced) and cells were grown for 3-5 hours to early log-phase. Cell cultures were diluted to an OD_{600} of 1.0 and 100 µl of volume was taken out and centrifuged at 960 × g for 2 minutes. The cell pellet was then washed twice with 1 ml of 1 x PBS buffer. Cells of constructed *S. cerevisiae* strains were analyzed by using either FACSCalibur (BD Biosciences) or LSRFortessa flow cytometer (BD Biosciences) at 488 nm wavelength. Raw data were processed with CellQuest Pro (BD Biosciences) or FlowJo (Tree Star).

2.2.6. Phenotypic assessment of nonessential *S. pombe* protein kinase mutants

Selected *S. pombe* kinase deletion strains were cultured in liquid YES media at 30°C overnight to stationary phase. Cell cultures were diluted to an OD_{600} of 0.1, and 5 µl volume of 1:10 serial dilutions were spotted onto YES plates incubated at 30°C containing 20 µg/ml TBZ or 10 mM HU, or simple YES plates incubated at 37°C (mild heat shock). Fresh stocks of TBZ (20 mg/ml) and HU (1 M) were prepared in DMSO. Plates were monitored after 3-5 days of incubation. The phenotype of kinase deletion mutants were compared to wildtype cells. Specifically, mutants exhibiting similar

growth to wildtype cells at the same dilution was designated as “not sensitive” and “-”; mutants exhibiting growth comparable to wildtype cells at 1 dilution factor lower was designated as “sensitive” and “+”; 2 dilution factors lower than wildtype as “very sensitive” and “++”; and 3 (or more) dilution factors lower than wild-type as “hypersensitive” and “+++”.

2.2.7. DNA techniques

2.2.7.1. Isolation of yeast genomic DNA

Small volume (up to 10 ml) yeast cultures were grown in the appropriate liquid media overnight at 30°C. Yeast cultures were centrifuged at 2,400 x g for 5 minutes yielded 30-50 µl volume of cell pellet, resuspended in 0.5 ml of sterile water, and transferred into 1.5 ml microcentrifuge tubes. After centrifugation at 10,000 x g for 5 seconds, sequentially added with 200 µl of yeast breaking buffer (**Table 2.6**), 200 µl of phenol: chloroform: isoamyl alcohol (25:24:1) pH 8.0, and ~250 µl of acid-washed glass beads (Sigma, 425-600 µm in diameter) to the level of the meniscus of the solution. The mixtures were vortexed vigorously for 1 minute and then placed on ice for 1 minute to prevent overheating. This vortex-rest cycle was repeated at least 5 times for each sample. The upper aqueous layer collected by centrifuging at 10,800 x g for 5 minutes was carefully transferred to microcentrifuge tubes containing 200 µl of chloroform. The mixtures were vortexed for 1 minute and then placed on ice for 1 minute. The upper layer was transferred to fresh microcentrifuge tubes containing 500 µl of 100% ethanol (ice-cold). The mixtures were incubated at -20°C for at least 1 hour and centrifuged at 12,400 x g for 10 minutes. Cell pellets were washed once with 70% ethanol, and then centrifuged at 12,400 x g for 10 minutes. Next, cell pellets were air-dried for 5-10 minutes, resuspended in 30 µl TE buffer containing 1 ng of RNase A, and incubated for 30 minutes at 37°C.

DNA concentration of each sample was measured using a NanoDrop 2000 UV-Vis Spectrophotometer (**Table 2.5**).

For large-scale DNA isolation, up to 2 L yeast cell cultures were grown in appropriate liquid media to late stationary phase (OD_{600} = 2-3) with constant agitation at 30°C. Cells were harvested by centrifuging at 2,400 x g for 5 minutes and resuspended in 1/20 volume of DNA preparation buffer (**Table 2.6**). 15 mg of Zymolyase-20T (Sigma) was added to the mixture and incubated at 37°C for 30-60 minutes. The digestion of cell walls was monitored under a phase contrast microscope on 10 µl of sample. The mixtures were centrifuged at 2,400 x g for 5 minutes, and the pellets were resuspended in 15 ml of 5 x TE buffer (**Table 2.6**). Next, 1.5 ml of 10% SDS and 5 ml of 5M potassium acetate was added, mixed well, and then placed on ice for 30 minutes. The mixture was centrifuged at 4,400 x g for 15 minutes. The supernatant was passed through gauze, added with 20 ml ice cold isopropanol, and incubated for 5 minutes at -20°C. The mixtures were centrifuged at 8, 600 x g for 10 minutes, the tube drained, air-dried the pellet, resuspended in 3 ml of 5 x TE with RNAse (20 µg/ml), and incubated for 2 hours at 37°C. Subsequently, 3 ml of phenol/chloroform (1:1) was added, mixed well, transferred to a 15 ml Falcon tube, and centrifuged at 8,600 x g for 10 minutes. The upper aqueous phase was transferred to a fresh 15 ml Falcon tube, added with 0.3 ml of 3 M sodium acetate and 7.5 ml of ethanol, and incubated on dry ice for 1 hour. Next, DNA was precipitated by centrifugation at 8,600 x g for 10 minutes, washed with 5 ml of cold 70% ethanol, and air-dried for 10-15 minutes at room temperature. Finally, DNA was resuspended in 0.2 ml of sterile water. DNA concentration was measured on a NanoDrop 2000 UV-Vis Spectrophotometer. High quality DNA should have an $OD_{260/280}$ ratio above 1.8.

2.2.7.2. Plasmid DNA isolation from *E. coli*

Isolation of plasmid DNA from *E. coli* was performed by following the manufacturer's instruction of the commercial preparation kit (QIAGEN QIAprep Spin Miniprep Kit). DH5α *E. coli* competent cells transformed with plasmids containing the gene of interest were grown overnight in 5 ml of LB liquid media with appropriate antibiotics at 37°C. Cell cultures were divided into 1.5 ml microcentrifuge tubes, and centrifuged at 12,000 x g for 2 minutes. Cell pellets were resuspended in 400 µl of buffer P1, added with 250 µl of alkaline lysis buffer P2, inverted 3-5 times until the solution was clear, incubated on ice for 5 minutes to complete cell lysis, and then neutralized by 300 µl of neutralization buffer P3. After centrifugation at 12,000 x g for 10 minutes, the supernatant was transferred to the columns provided with the kit, and the insoluble materials were discarded. The membranes of the columns were washed once with 750 µl of binding buffer PB. Plasmid DNA bound to the column membrane was eluted by 1 ml of elution buffer PE. DNA concentrations were measured by using a NanoDrop 2000 UV-Vis Spectrophotometer. Aliquots of plasmid DNA were stored at -20°C until use.

2.2.7.3. Polymerase chain reaction (PCR)

DNA was amplified using specific primers according to the manufacturers' instructions for multi-components systems TopTaq Master Mix Kit (QIAGEN) or Platinum Taq DNA Polymerase (Thermo Scientific). A single 50 µl PCR reaction normally contains ~100 ng of plasmid DNA or 1 µg of genomic DNA as amplification templates, 10 µM each of dNTPs, 0.5 to 2 units of Taq polymerase, and 1 x PCR reaction buffer. Reactions were run for 25-35 cycles in an Eppendorf Mastercycler Pro Thermal Cycler (**Table 2.5**).

2.2.7.4. Colony PCR

Colony PCR was conducted to check plasmid integration. A typical colony PCR reaction includes the following components: 5 µl of 10 x colony PCR buffer (**Table 2.6**), 3 µl of 25 mM $MgCl_2$, 1 µl of dNTPs (10 mM of each), 1 µl of forward and reverse primer (20 µM of each), and sterile water to fill up to 50 µl volume. A small amount of bacterial colony was picked by sterile toothpicks, inoculated in the above mentioned reaction, and mixed by pipetting up and down. Reactions in PCR tubes were boiled at 95°C to lyse yeast cells. Next, 2 units of Taq DNA polymerase were added. Colony PCR reactions were performed in an Eppendorf Mastercycler Pro Thermal Cyclers (**Table 2.5**), followed by DNA separation on agarose gel to examine amplified products.

2.2.7.5. DNA agarose gel electrophoresis

Products of PCR amplification and restriction endonuclease digestion were separated by agarose gel electrophoresis. Agarose at 0.6-1.5% (w/v) was completely dissolved in 1 x TAE buffer by microwaving. After the solution cooled down to ~60°C, 3-5 µl of SYBR Safe DNA Gel Stain (Thermo Scientific) was added to the solution prior to pour into the gel casting tray. DNA samples were mixed with 6x DNA gel loading buffer (**Table 2.6**), and then run at voltage of 80-100 V for 30-45 minutes. DNA agarose gels were visualized using a FluorChem Q imaging system (Cell BioSciences).

2.2.7.6. Restriction endonuclease digestion and DNA purification

Restriction endonuclease digestions were conducted by following manufacturer's

recommendations. A typical 50 µl reaction was assembled with 1-3 µg of plasmid DNA, 5 units of restriction endonuclease, 1 x restriction digestion buffer. The reactions were incubated for 1-3 hours at 37°C or otherwise indicated.

The digestion reactions were run on agarose gel to separate DNA segments by their molecular size. QIAquick PCR Purification kit (QIAGEN) was used to collect and purify the digested DNA segments. Gels were visualized using a BlueView Transilluminator (Vernier Technology).

2.2.7.7. DNA extraction from agarose gel

QIAquick Gel Extraction Kit (QIAGEN) was used to recover DNA from excised agarose gel bands using a clean scalpel. No more than 500 mg of gel slice was then transferred into microcentrifuge tubes containing 750 ml of buffer QG (QIAGEN), and incubated on a block heater at 50°C for at least 10 minutes until all gel slices were completed dissolved. The tubes were briefly vortexed every 3 minutes during the incubation. The mixtures were applied onto QIAquick Spin Columns (QIAGEN) which bind DNA, and centrifuged at 11,000 x g for 1 minute. The column was washed with 750 ml of buffer PE (QIAGEN) and centrifuged at 11,000 x g for 1 minute. The columns were centrifuged at 11,000 x g for 1 minute to completely drain the flow-through. The columns were placed into microcentrifuge tubes; 20-50 µl of sterile water or elution buffer (QIAGEN) was added to the center of the column membrane, left for 1 minute to equilibrium, and centrifuged at 11,000 x g for 1 minute. DNA concentration was measured using a NanoDrop 2000 UV-Vis Spectrophotometer. Proper DNA aliquots were stored at -20°C.

2.2.7.8. DNA Ligation

DNA fragments with compatible cohesive-ends were ligated by T4 DNA ligase (Invitrogen) according to the manufacturer's specifications. Typically, a single 20 µl ligation reaction contains insert (~50 ng) and vector segments in 3:1 molar ratio, 2 µL of 10 x ligation buffer and 2-3 units of T4 DNA ligase. Ligation reactions were incubated at room temperature for 3 hours. For DNA fragments with blunt-ends, the ligation usually requires a higher molar ratio of insert to vector (*e.g.* 6:1) and a longer incubation time (*e.g.* overnight at room temperature), or at 16°C for at least 3 hours which lead to optimal ligation efficiency.

To minimize self-ligation of the vectors, DNA segments was dephosphorylated before ligation by adding calf intestinal alkaline phosphatase (CIP) or shrimp alkaline phosphatase according to the manufacturer's instruction (New England Biolabs). The phosphatases were deactivated by heating at 65°C for 15 minutes.

2.2.7.9. DNA sequencing

DNA sequencing was conducted by The Centre for Applied Genomics (University of Alberta).

2.2.7.10. Epitope tagging of Argonaute and Dicer genes

The HA epitope tag was added to the N-terminal of hAgo2 or ScaAgo1 by ligating a complementary segment comprised of an ATG start codon and the HA coding sequence into the single SpeI digestion site on vector pRS404-P_{TEF}-hAgo2 or pRS404-P_{TEF}-ScaAgo1. The orientation of insertion was identified by subsequent restriction digestion and/or DNA sequencing. The resultant plasmids were named as pRS404-P_{TEF}-HA-hAgo2 and pRS404-P_{TEF}-HA-ScaAgo1.

The c-Myc epitope tag was added to the C-terminal of hDcr or ScaDcr1. For hDcr, the sequence of C-terminal region was amplified by a sense primer that contains a SacII site and an antisense primer that contains the c-Myc coding sequence and an XhoI site. The PCR product was ligated onto SacII and XhoI digested pRS405-P_{TEF}-hDcr to form pRS405-P_{TEF}-hDcr-myc. For ScaDcr1, the same epitope tagging strategy was utilized, but the specific restriction digestion sites on primers and vector pRS405-P_{TEF}-ScaDcr1 were NheI and XhoI.

2.2.7.11. Site-directed mutagenesis

Site-directed mutagenesis was conducted by using QuikChange II Site-Directed Mutagenesis Kit (Agilent). A typical reaction includes 10-50 ng of target vector containing the gene of interest, 125 ng of sense and antisense primers, 1 µl of dNTP mix (10 mM of each), 3 µl of Quick Solution, 1 µl of PfuUltra High-Fidelity DNA polymerase (2.5 U/µl), 5 µl of 10 x reaction buffer, and add sterile water to 50 µl. Cycling parameters were set as denaturing at 95°C for 1 minute; 12-18 cycles of 95°C for 50 seconds, 60°C for 50 seconds, 68°C per 1 kb of plasmids. Following temperature cycling, the reactions were placed on ice for 2 minutes. Successful point mutations, single amino acid changes, or multiple amino acid deletions or insertions were examined by DNA sequencing.

2.2.8. RNA techniques

2.2.8.1. Isolation of total RNA from yeast cell cultures

Total RNA was isolated from yeast cells by using TRIzol reagent (Thermo Fisher Scientific) as recommended by the manufacturer. Small volume (5-10 ml) of yeast cultures were grown overnight to stationary phase. Yeast cells (~100 µl) were collected by centrifuging at 3,000 x g for 5 minutes,

and then resuspended in 1 ml of TRIzol. After 300 µl of acid-washed glass beads (Sigma, 425-600 µm in diameter) were added, the mixtures were subjected to at least 5 homogenization cycles (1 min of each) by vigorously shaking and rotating microcentrifuge tubes in Mini Bead Beater-8 (BioSpec Products). Samples were placed on ice in between homogenization cycles to prevent overheating of samples. The mixtures were incubated at room temperature for 5 minutes, added with 0.2 ml of chloroform per 1 ml TRIzol, shaken vigorously for 15 seconds, incubated at room temperature for 3 minutes, and centrifuged at 12,000 x g at 4°C for 15 minutes. The top aqueous phase (~400 µl) was transferred to clean microcentrifuge tubes containing 500 µl of ice-cold isopropanol. Samples were incubated at room temperature for 10 minutes followed by centrifuging at 12,000 x g for 10 minutes at 4°C. The pellet, which may not be visible, was washed with 1 ml of pre-cold 75% ethanol, centrifuged at 7,500 x g for 5 minutes at 4°C, air-dried for at least 10 minutes until it is transparent and dissolved in 50 µl of RNase-free sterile water. RNA concentration was measured by a NanoDrop 2000 UV-Vis Spectrophotometer. RNA aliquots were stored at -20°C for short term storage or at -80°C for long term storage..

2.2.8.2. RNA agarose gel electrophoresis

The integrity of TRIzol extracted RNA samples was examined by the agarose gel electrophoresis method described above. Moreover, RNA gel electrophoresis was run at a higher voltage (up to 150 V) for a shorter period of time (<15 minutes) to minimize RNA degradation. The appearance of non-smeared ribosomal RNA bands at the size of 1.8 and 3.5 kb indicated successful extraction of high quality RNA from yeast cells.

2.2.8.3. Reverse transcription and quantitative PCR assay

Typically, each reverse transcription reaction contained 3 µg of total RNA extract, 1 µl of DNase I (amplification grade, Invitrogen), 1 µl of 10 x reaction buffer (**Table 2.6**), and RNase-free water to a final volume of 10 µl. The reactions were incubated at 37°C for at least 1 hour to let DNase degrade DNA contamination, and then added with 1 µl of 25 mM EDTA (pH 8.0) to inactive the enzyme. The mixtures were then incubated at room temperature for 5 minutes, 10 minutes at 65°C, and finally 2 minutes on ice. Next, 9 µl of DNase treated RNA sample was added with 1 µl of dNTPs (25 mM of each), 4 µl of 5 x reverse transcription first strand buffer (**Table 2.6**), 2 µl of 0.1 M DTT, 1 µl of RNase OUT (Invitrogen), 1 µl each of *dg* and actin forward (named FF, Act-F-qPCR and *dg*-For) or reverse (named RR, Act-R-qPCR and *dg*-Rev) primers (**Table 2.8**). The reactions were incubated at 42°C for 3 minutes, added with 1 µl of SuperScript III reverse transcriptase (Thermo Fisher Scientific), incubated at 55°C for 1 hour, 70°C for 15 minutes, and chilled on ice for 5 minutes. The cDNA samples were either stored at -80°C or used for the qPCR assay directly.

2.2.8.4. Data analysis of quantitative PCR

Relative abundance of pericentromeric transcripts of different kinase deletion mutants were normalized to actin mRNA by running quantitative PCR in a Stratagene Mx3005P qPCR System (Agilent Genomics) using the PerfeCTa SYBR Green SuperMix, UNG, Low Rox (Quanta BIOSCIENCES). Each sample was run in triplicate to minimize the variation. To ensure the specificity of qPCR amplification and the effective removal of genomic DNA, no template (NTC) and no reverse transcriptase (NRT) control samples were included in each assay. Standard curves were established to measure the efficiency of qPCR reaction. Ideally, qPCR amplification should

form a perfect linear curve when cDNA concentration increases. Therefore, the R squared (Rsq) value, which denotes the linearity of standard curve, should be close to 1. A standard curve was accepted for further quantification analysis only when its Rsq value > 0.985. In addition, a dissociation curve was also used to determine if the gene of interest is the only product been amplified in the reaction. Data were analyzed with the two standard curve methods (Livak and Schmittgen 2001) to quantify the abundance of the forward and reverse pericentromeric transcripts relative to the β-actin mRNA control. The comparison of *dg* forward and reverse transcript levels in kinase deletions and its parental control allowed us to determine the effect of certain kinases on the silencing of pericentromeric transcription.

2.2.9. Protein techniques

2.2.9.1. Small scale protein preparation

Yeast cell cultures were grown in the appropriate liquid culture until the OD_{600} reached 1.0–1.2. Samples were always kept on ice to minimize protein cleavage and degradation during the process. For each culture, cells in 5 ml liquid media were harvested by centrifuging at 4,000 x g for 5 minutes at 4°C. The cells were washed twice with equal volume of ice-cold sterile water, and then resuspended in 500 µl of sterile water containing 0.2 mM of sodium orthovanadate (Na_3VO_4), 5 mM sodium fluoride (NaF), and 90 µl of freshly made 1 x protein lysis buffer (**Table 2.6**). The cell walls were broken by vortexing for 30 seconds at least three times and incubated on ice in between each cycle, and then incubated on ice for another 10 minutes. Subsequently, 250 µl of pre-chilled 100% TCA was added, followed by incubation on ice for 10 minutes, centrifuged at 14,000 x g for 10 minutes at 4°C, and washed twice with 500 µl of pre-chilled 80% acetone to remove traces of TCA.

Finally, pellets were air-dried for 15 minutes and then dissolved in ~50 µl of 1x protein sample buffer (**Table 2.6**), boiled for 5 minutes at 95°C, and then run on protein gel or stored at -20°C.

2.2.9.2. Large scale cryogenic disruption of yeast cells

Yeast cell cultures were grown in at least 1 L of rich media until OD_{600} reached 1.5. Cells were harvested by centrifugation at 5,000 x g for 5 minutes at 4°C using a JLA 10.5 rotor (Beckman), washed twice with equal and 1/10 volumes of sterile water, respectively. Centrifuge bottles were weighted and balanced before every spinning. The cell pellets were then resuspended in resuspension buffer (**Table 2.6**), and centrifuged at 5,000 x g for 5 minutes at 4°C. At this stage, yeast cells should be dry and resemble a thick paste. The cell pellets were quickly scooped by liquid nitrogen chilled spatulas into 30 ml syringes and slowly discharged into 50 ml Falcon tubes filled with liquid nitrogen to snap freeze yeast cells into spaghetti-shaped "yeast noodles" (avoid to form clumps or ball-shaped frozen yeast, which are more difficult to grind into fine powders). Excess liquid nitrogen in Falcon tubes was discarded. The frozen "yeast noodles" were transferred into metal jars and filled to at least 50% volume for proper grinding. Two grinding jars containing frozen yeast cells were stacked and the balanced with the counterweight of the Planetary Ball Mill PM 100 Grinding Machine (Retsch). The frozen yeast cells were ground for at least 5 cycles for 3 min/cycle at 400 x g. In between cycles, the metal jars were submerged into liquid nitrogen. The powder on the sides of each jar was scraped with a liquid nitrogen chilled spatula. After every two grinding cycles, a fingertip sized yeast powder was diluted in sterile water to monitor the breakage of cell walls under a microscope. Once >95% cell breakage was complete, the powder was transferred to 50 ml Falcon tubes pre-chilled in liquid nitrogen. The powder was weighted and immediately stored at -80°C. This grinding protocol

typically yielded 2-3 g of fine yeast powder from a 1 L overnight culture.

2.2.9.3. Sodium dodecyl sulphate polyacrylamide gel electrophoresis (SDS-PAGE)

Protein samples were mixed with equal volumes of 2x protein sample buffer and boiled at 95°C for 5 minutes to allow protein denaturation. Total proteins were separated by discontinuous gel electrophoresis (Laemmli 1970; Shapiro and Vinuela 1967). Resolving gel was prepared by adding acrylamide/bis-acrylamide to an appropriate final concentration (from 6% to 12%) into the resolving buffer (**Table 2.6**). The stacking gel was prepared by mixing acrylamide/bis-acrylamide to a final concentration of 4% into the stacking buffer (**Table 2.6**). Electrophoresis was performed using a Mini-protean III system (Bio-Rad) in 1x SDS-PAGE running buffer (**Table 2.6**) at 80–120 V for 60-80 minutes until the bromophenol blue indicator reached to the bottom of the gel gasket.

2.2.9.4. Western transfer and immunoblotting

After SDS-PAGE, proteins were transferred from gel to either polyvinylidene fluoride (PVDF) or nitrocellulose membranes. Protein transfer was conducted using the Mini Trans-Blot Electrophoresis Transfer Cell (Bio-Rad) apparatus filled with 1x Western transfer buffer (**Table 2.6**) with 10% methanol. Pre-chilled ice-packs were used to keep transfer buffer cold during the process. The transfer was conducted at a constant current of 250 mA for 90 minutes. After protein transfer, the membranes were blocked with 1x PBS-Tween containing 5% (w/v) skim milk or 2.5% (w/v) BSA for 1 hour at room temperature or overnight at 4°C on a rocking device.

The membranes were further incubated with the appropriate primary antibodies in 1x PBS-T (**Table 2.6**) containing 5% (w/v) skim milk or 2.5% (w/v) BSA for 1-2 hours at room temperature or

overnight at 4°C. The membranes were then washed three time (15 minutes of each) with 1x PBS-T to remove the excess primary antibodies. Next, the membranes were incubated with the secondary antibodies in 1x PBS-T containing 5% (w/v) skim milk or 2.5% (w/v) BSA for up to 3 hours at room temperature with constant agitation. The membranes were then washed three times with 1xPBS-T (15 minutes of each). Finally, the membranes were immunoblotted by enhanced chemiluminescence (ECL) solutions (**Table 2.2**), and visualized under a FluorChem Q System. The images were converted and saved as JPEG format.

2.2.9.5. Immunoprecipitation of FLAG-SpAgo1

About 0.5 g cell powder generated by yeast cell cryogenic disruption described above was resuspended in 1.5 ml of lysis buffer (**Table 2.6**) containing Halt Protease Inhibitor Cocktail (Roche). The mixtures were incubated on ice for 30 minutes and vortexed for 15 seconds every 5 minutes. Insoluble debris was removed by centrifuging at 14,000 x g for 10 minutes at 4°C. Protein concentration was measured by using QuickStart Bradford Protein Assay kit (QIAGEN).

Meanwhile, 50-100 µl of anti-FLAG M2 Magnetic Beads (Sigma) slurries were prepared in microcentrifuge tubes, and equilibrated by washing twice with 10 volumes of 1 x TBS buffer. The end of the pipette tips were cut off to reduce physical damage to the magnetic beads during pipetting. The beads were collected and excess buffer was discarded. Prepared cell lysates were added to the equilibrated anti-FLAG beads (named PRE, pre immunoprecipitation sample). All samples were gently agitated for 1 hour at room temperature or overnight at 4°C for epitope specific protein binding. Next, anti-FLAG beads were collected, and the supernatant was removed and saved (named POST, post immunoprecipitation sample). The resin was washed three times with 1x TBS at room

temperature. Proteins bound to anti-FLAG beads were eluted with either 100 µl of 0.1 M glycine-HCl (pH 2.5) and then neutralized by adding 5 µl of 1 M Tris-base (pH 10), or by 1x protein sample buffer and heated up at 95°C for 5-10 minutes (named IP, immunoprecipitation sample). The eluted epitope-specific binding proteins can be immediately run on SDS-PAGE gel or stored at -20°C.

2.2.9.6. Two dimensional gel electrophoresis

The first dimensional of protein separation was conducted using an IPGphor System (Amersham Biosciences). 7 cm IPG gel strips with a linear separation range of pH 3-10 (Amersham Biosciences) were immersed in rehydration buffer (**Table 2.6**) overnight at room temperature in a DryStrip Reswelling Tray (Amersham Biosciences). Strips were prevented from dehydration by covering with ~750 µl mineral oil. The focusing protocol for up to 150 µg protein per strip was set as 150 V for 1h, 300 V for 2h, 600 V for 1h, gradient from 600 V to 8000 V for 1h, and 8000 V for 3 hours. Next, the strips were equilibrated twice for 15 minutes in 10 ml equilibration buffer (**Table 2.6**). First equilibration step was added with 65 mM DTT (reduction step) and second with 135 mM iodoacetamide (alkylation step). Proteins in strips were migrated into SDS-PAGE gels to further separate proteins by their molecular weight. Electrophoresis conditions were set as 5 W per cm of gel for 45 minutes and 15 W per cm of gel until the bromophenol blue indicator reached to the bottom. The protein transfer and immunoblotting protocol discussed above was employed.

2.2.9.7. Mass spectrometry

The gel piece was treated for 40 minutes with 5 mM of DTT dissolved in 25 mM NH_4HCO_3 at

room temperature, and then alkylated for 40 minutes in the dark with 15 mM iodoacetamide in dissolved 25 mM NH_4HCO_3. The samples were digested overnight at 37°C with trypsin (Promega) in a 1:50 enzyme-to-substrate ratio. The peptide mixtures were extracted with 50% acetone and 0.1% trifluoroacetic acid (TFA) for 2 hours at 37°C. The peptide sample was further air-dried and dissolved in 10 µl of 0.1% formic acid in water and subjected to LC-MS/MS analysis. The raw MS files were analyzed and searched against the UniProt *S. pombe* protein sequence database (http://www.uniprot.org/taxonomy/4896) using Proteome Discoverer 1.2 (Thermo Scientific). Only high-confidence peptides were chosen for downstream protein modification analysis.

Chapter 3

Reconstitution of RNAi pathways in budding yeast *Saccharomyces cerevisiae* and the regulation by Hsp90

A version of this chapter was published in
"Wang Y, Mercier R, Hobman TC, LaPointe P. (2013). Regulation of RNA interference by Hsp90 is an evolutionarily conserved process. *Biochim Biophys Acta.* 1833(12):2673-81."

3.1. Rationale

The introduction of budding yeast *S. castellii AGO1* and *DCR1* genes into the RNAi-deficient experimental organism *S. cerevisiae* successfully restores RNAi-mediated silencing of both reporter genes and endogenous retrotransposons (Drinnenberg et al. 2009). With a large number of genetic resources and tools available, *S. cerevisiae* would be a useful complementation to the arsenal of experimental organisms employed in the study of the mechanism and regulation of RNAi pathways. It was of interest to find out whether the introduction of human RNAi components can reconstitute RNAi in *S. cerevisiae.*

The comparative study of classical and non-canonical RNAi systems in *S. cerevisiae*, represented by humans and budding yeast components respectively will shed light on the understanding of how RNAi evolved in different phyla of eukaryotes as a highly conserved mechanism. Restored RNAi pathways in *S. cerevisiae* can also be used to further investigate how Dicer and Argonaute proteins interact with each other to transfer dsRNAs between them.

Our laboratory and others reported that the ATPase activity of Hsp90 facilitates conformational changes of Argonaute proteins to accommodate dsRNA loading in *Drosophila* and humans (Pare et al. 2009, 2011; Iwasaki et al. 2010). However, it was unknown whether Hsp90 regulation of RNAi is conserved in simpler eukaryotes like budding yeast. Therefore, it would be of interest to determine whether the restored RNAi pathways in *S. cerevisiae* are dependent on the ATPase activity of endogenous Hsp90.

3.2. Results

3.2.1. Introduction of *S. castellii AGO1* and *DCR1* restores RNAi in *S. cerevisiae*

3.2.1.1. The silencing constructs against the reporter genes transcribe into dsRNA substrates

Until very recently, it was generally considered that all budding yeast species are RNAi deficient like the model organism *S. cerevisiae* (Harrison et al. 2009; Camblong et al. 2009) since no canonical Dicer was ever identified. The groundbreaking work conducted by Drinnenberg and colleagues identified non-canonical Dicer proteins in some budding yeasts including *S. castellii*, a close relative of *S. cerevisiae* (Drinnenberg et al. 2009). These newly identified non-canonical Dicers are required for retrotransposon silencing (Drinnenberg et al. 2009). Furthermore, the integration of *S. castellii* Argonaute (Sca*AGO1*) and Dicer (Sca*DCR1*) genes into the genome of RNAi-deficient *S. cerevisiae* successfully restored the silencing of both exogenous reporter genes (*e.g. GFP*) and endogenous retrotransposons (Drinnenberg et al. 2009).

To employ *S. cerevisiae* as an experimental system for further studies on the regulatory mechanism of RNAi pathways, I constructed a series of strains by sequentially integrating Sca*AGO1* and Sca*DCR1*genes, *GFP* and *URA3* as reporter genes, and their corresponding silencing constructs into the genome of the *S. cerevisiae* strain W303a (**Table 3.1**). Sca*AGO1* and Sca*DCR1* genes were driven by the constitutive promoter P_{TEF}, *GFP* by the constitutive promoter P_{ADH1}, and *URA3* by its endogenous promoter.

The silencing constructs against *GFP* or *URA3* mRNAs were driven by a galactose-inducible promoter P_{GAL1} (**Figure 3.1A-C**). This allowed us to compare the expression levels of a reporter gene under non-inducing (glucose) and inducing (galactose) conditions of the corresponding silencing constructs. Two *GFP* silencing constructs were employed to mimic the precursors of miRNA and

siRNA, respectively. The strong *GFP* silencing construct (strongSC-*GFP*) produces a long single-stranded RNA (ssRNA) transcript containing two inverted *GFP* segments and an unpaired linker loop in between, which naturally folds into a stem-loop structure (**Figure 3.1A**). The weak *GFP* silencing construct (weakSC-*GFP*) generates two reverse complemented ssRNAs by the opposite directed P_{GAL1} and P_{URA3} promoters. These two transcripts hybridized to form perfectly matched long dsRNA substrates (**Figure 3.1B**). To elaborate the terminology of the strong and the weak silencing construct: the strong silencing construct only requires a single transcription event to produce dsRNA substrates; the weak silencing construct produces two separate ssRNA transcripts and a subsequent annealing step is required. Moreover, the strength of P_{URA3} is much less potent than P_{GAL1} under inducing conditions. Thus the terms "strong" and "weak" are intended to refer to the abundance of the dsRNA substrates, not necessarily the efficiency with which they act on their targets. The *URA3* silencing construct (SC-*URA3*) contains two inverted repeats of a *URA3* fragment which naturally folds into a stem-loop structure (**Figure 3.1C**).

Table 3.1 Budding yeast *S. cerevisiae* strains used in this study

Strain	Genotype	Reference
W303a	*MATa leu2-3,112 trp1-1 can1-100 URA3-1 ade2-1 his3-11,15*	Thomas and Rothstein 1989
YW1	*MATa leu2-3,112 trp1-1 can1-100 URA3-1 ade2-1 his3-11,15* pRS*406-*P_{ADH1}*-GFP*(*S65T*)	This study
YW2	*MATa leu2-3,112 trp1-1 can1-100 URA3-1 ade2-1 his3-11,15* pRS*406-*P_{ADH1}*-GFP*(*S65T*) pRS*403-*P_{GAL1}*-SC-URA3*	This study
YW3	*MATa leu2-3,112 trp1-1 can1-100 URA3-1 ade2-1 his3-11,15* pRS*404-*P_{TEF}*-ScaAgo1* pRS*405-*P_{TEF}*-ScaDcr1*	This study
YW4	*MATa leu2-3,112 trp1-1 can1-100 URA3-1 ade2-1 his3-11,15* pRS*404-*P_{TEF}*-ScaAgo1* pRS*405-*P_{TEF}*-ScaDcr1* pRS*406-*P_{ADH1}*-GFP*(*S65T*)	This study
YW5	*MATa leu2-3,112 trp1-1 can1-100 URA3-1 ade2-1 his3-11,15* pRS*404-*P_{TEF}*-ScaAgo1* pRS*405-*P_{TEF}*-ScaDcr1* pRS*406-*P_{ADH1}*-GFP*(*S65T*) pRS*403-*P_{GAL1}*-SC-URA3*	This study
YW6	*MATa leu2-3,112 trp1-1 can1-100 URA3-1 ade2-1 his3-11,15* pRS*404-*P_{TEF}*-HA-ScaAgo1* pRS*405-*P_{TEF}*-ScaDcr1-myc*	This study
YW7	*MATa leu2-3,112 trp1-1 can1-100 URA3-1 ade2-1 his3-11,15* pRS*404-*P_{TEF}*-HA-ScaAgo1* pRS*405-*P_{TEF}*-ScaDcr1-myc* pRS*406-*P_{ADH1}*-GFP*(*S65T*)	This study
YW8	*MATa leu2-3,112 trp1-1 can1-100 URA3-1 ade2-1 his3-11,15* pRS*404-*P_{TEF}*-HA-ScaAgo1* pRS*405-*P_{TEF}*-ScaDcr1-myc* pRS*406-*P_{ADH1}*-GFP*(*S65T*) pRS*403-*P_{GAL1}*-SC-URA3*	This study
YW9	*MATa leu2-3,112 trp1-1 can1-100 URA3-1 ade2-1 his3-11,15* pRS*404-*P_{TEF}*-HA-hAgo2* pRS*405-*P_{TEF}*-ScaDcr1-myc*	This study
YW10	*MATa leu2-3,112 trp1-1 can1-100 URA3-1 ade2-1 his3-11,15* pRS*404-*P_{TEF}*-HA-hAgo2* pRS*405-*P_{TEF}*-ScaDcr1-myc* pRS*406-*P_{ADH1}*-GFP*(*S65T*)	This study
YW11	*MATa leu2-3,112 trp1-1 can1-100 URA3-1 ade2-1 his3-11,15* pRS*404-*P_{TEF}*-HA-hAgo2* pRS*405-*P_{TEF}*-ScaDcr1-myc* pRS*406-*P_{ADH1}*-GFP*(*S65T*) pRS*403-*P_{GAL1}*-SC-URA3*	This study
YW12	*MATa leu2-3,112 trp1-1 can1-100 URA3-1 ade2-1 his3-11,15* pRS*404-*P_{TEF}*-HA-ScaAgo1* pRS*405-*P_{TEF}*-hDcr-myc*	This study
YW13	*MATa leu2-3,112 trp1-1 can1-100 URA3-1 ade2-1 his3-11,15* pRS*404-*P_{TEF}*-HA-ScaAgo1* pRS*405-*P_{TEF}*-hDcr-myc* pRS*406-*P_{ADH1}*-GFP*(*S65T*)	This study
YW14	*MATa leu2-3,112 trp1-1 can1-100 URA3-1 ade2-1 his3-11,15* pRS*404-*P_{TEF}*-HA-ScaAgo1* pRS*405-*P_{TEF}*-hDcr-myc* pRS*406-*P_{ADH1}*-GFP*(*S65T*) pRS*403-*P_{GAL1}*-SC-URA3*	This study
YW15	*MATa leu2-3,112 trp1-1 can1-100 URA3-1 ade2-1 his3-11,15* pRS*404-*P_{TEF}*-HA-hAgo2* pRS*405-*P_{TEF}*-hDcr-myc*	This study
YW16	*MATa leu2-3,112 trp1-1 can1-100 URA3-1 ade2-1 his3-11,15* pRS*404-*P_{TEF}*-HA-hAgo2* pRS*405-*P_{TEF}*-hDcr-myc* pRS*406-*P_{ADH1}*-GFP*(*S65T*)	This study
YW17	*MATa leu2-3,112 trp1-1 can1-100 URA3-1 ade2-1 his3-11,15* pRS*404-*P_{TEF}*-HA-hAgo2* pRS*405-*P_{TEF}*-hDcr-myc* pRS*406-*P_{ADH1}*-GFP*(*S65T*) pRS*403-*P_{GAL1}*-SC-URA3*	This study

YW18	*MATa leu2-3,112 trp1-1 can1-100 URA3-1 ade2-1 his3-11,15* pRS*404-*P_{TEF}*-HA-hAgo2* pRS*405-*P_{TEF}*-hDcr-myc* pRS*401-*P_{TEF}*-TRBP2-natNT2*	This study
YW19	*MATa leu2-3,112 trp1-1 can1-100 URA3-1 ade2-1 his3-11,15* pRS*404-*P_{TEF}*-HA-hAgo2* pRS*405-*P_{TEF}*-hDcr-myc* pRS*401-*P_{TEF}*-TRBP2-natNT2* pRS*406-*P_{ADH1}*-GFP*(*S65T*)	This study
YW20	*MATa leu2-3,112 trp1-1 can1-100 URA3-1 ade2-1 his3-11,15* pRS*404-*P_{TEF}*-HA-hAgo2* pRS*405-*P_{TEF}*-hDcr-myc* pRS*401-*P_{TEF}*-TRBP2-natNT2* pRS*406-*P_{ADH1}*-GFP*(*S65T*) pRS*403-*P_{GAL1}*-SC-URA3*	This study
YW21	*MATa leu2-3,112 trp1-1 can1-100 URA3-1 ade2-1 his3-11,15* pRS*404-*P_{TEF}*-HA-ScaAgo1* pRS*405-*P_{TEF}*-hDcr-myc* pRS*401-*P_{TEF}*-TRBP2-natNT2*	This study
YW22	*MATa leu2-3,112 trp1-1 can1-100 URA3-1 ade2-1 his3-11,15* pRS*404-*P_{TEF}*-HA-ScaAgo1* pRS*405-*P_{TEF}*-hDcr-myc* pRS*401-*P_{TEF}*-TRBP2-natNT2* pRS*406-*P_{ADH1}*-GFP*(*S65T*)	This study
YW23	*MATa leu2-3,112 trp1-1 can1-100 URA3-1 ade2-1 his3-11,15* pRS*404-*P_{TEF}*-HA-ScaAgo1* pRS*405-*P_{TEF}*-hDcr-myc* pRS*401-*P_{TEF}*-TRBP2-natNT2* pRS*406-*P_{ADH1}*-GFP*(*S65T*) pRS*403-*P_{GAL1}*-SC-URA3*	This study
YW24	*MATa leu2-3,112 trp1-1 can1-100 URA3-1 ade2-1 his3-11,15* pRS*404-*P_{TEF}*-ScaAgo1* pRS*405-*P_{TEF}*-ScaDcr1* pRS*406-*P_{ADH1}*-GFP*(*S65T*) pRS*403-*P_{GAL1}*-weakSC-GFP*	This study
YW25	*MATa leu2-3,112 trp1-1 can1-100 URA3-1 ade2-1 his3-11,15* pRS*404-*P_{TEF}*-ScaAgo1* pRS*405-*P_{TEF}*-ScaDcr1* pRS*406-*P_{ADH1}*-GFP*(*S65T*) pRS*403-* P_{GAL1}*-strongSC-GFP*	This study
YW26	*MATa leu2-3,112 trp1-1 can1-100 URA3-1 ade2-1 his3-11,15* pRS*404-*P_{TEF}*-HA-ScaAgo1* pRS*405-*P_{TEF}*-ScaDcr1-myc* pRS*406-*P_{ADH1}*-GFP*(*S65T*) pRS*403-*P_{GAL1}*-weakSC-GFP*	This study
YW27	*MATa leu2-3,112 trp1-1 can1-100 URA3-1 ade2-1 his3-11,15* pRS*404-*P_{TEF}*-HA-ScaAgo1* pRS*405-*P_{TEF}*-ScaDcr1-myc* pRS*406-*P_{ADH1}*-GFP*(*S65T*) pRS*403-*P_{GAL1}*-strongSC-GFP*	This study
YW28	*MATa leu2-3,112 trp1-1 can1-100 URA3-1 ade2-1 his3-11,15* pRS*404-*P_{TEF}*-HA-hAgo2* pRS*405-*P_{TEF}*-ScaDcr1-myc* pRS*406-*P_{ADH1}*-GFP*(*S65T*) pRS*403-*P_{GAL1}*-weakSC-GFP*	This study
YW29	*MATa leu2-3,112 trp1-1 can1-100 URA3-1 ade2-1 his3-11,15* pRS*404-*P_{TEF}*-HA-hAgo2* pRS*405-*P_{TEF}*-ScaDcr1-myc* pRS*406-*P_{ADH1}*-GFP*(*S65T*) pRS*403-*P_{GAL1}*-strongSC-GFP*	This study
YW30	*MATa leu2-3,112 trp1-1 can1-100 URA3-1 ade2-1 his3-11,15* pRS*404-*P_{TEF}*-HA-hAgo2* pRS*405-*P_{TEF}*-hDcr-myc* pRS*401-*P_{TEF}*-TRBP2-natNT2* pRS*406-*P_{ADH1}*-GFP*(*S65T*) pRS*403-*P_{GAL1}*-weakSC-GFP*	This study
YW31	*MATa leu2-3,112 trp1-1 can1-100 URA3-1 ade2-1 his3-11,15* pRS*404-*P_{TEF}*-HA-hAgo2* pRS*405-*P_{TEF}*-hDcr-myc* pRS*401-*P_{TEF}*-TRBP2-natNT2* pRS*406-*P_{ADH1}*-GFP*(*S65T*) pRS*403-*P_{GAL1}*-strongSC-GFP*	This study

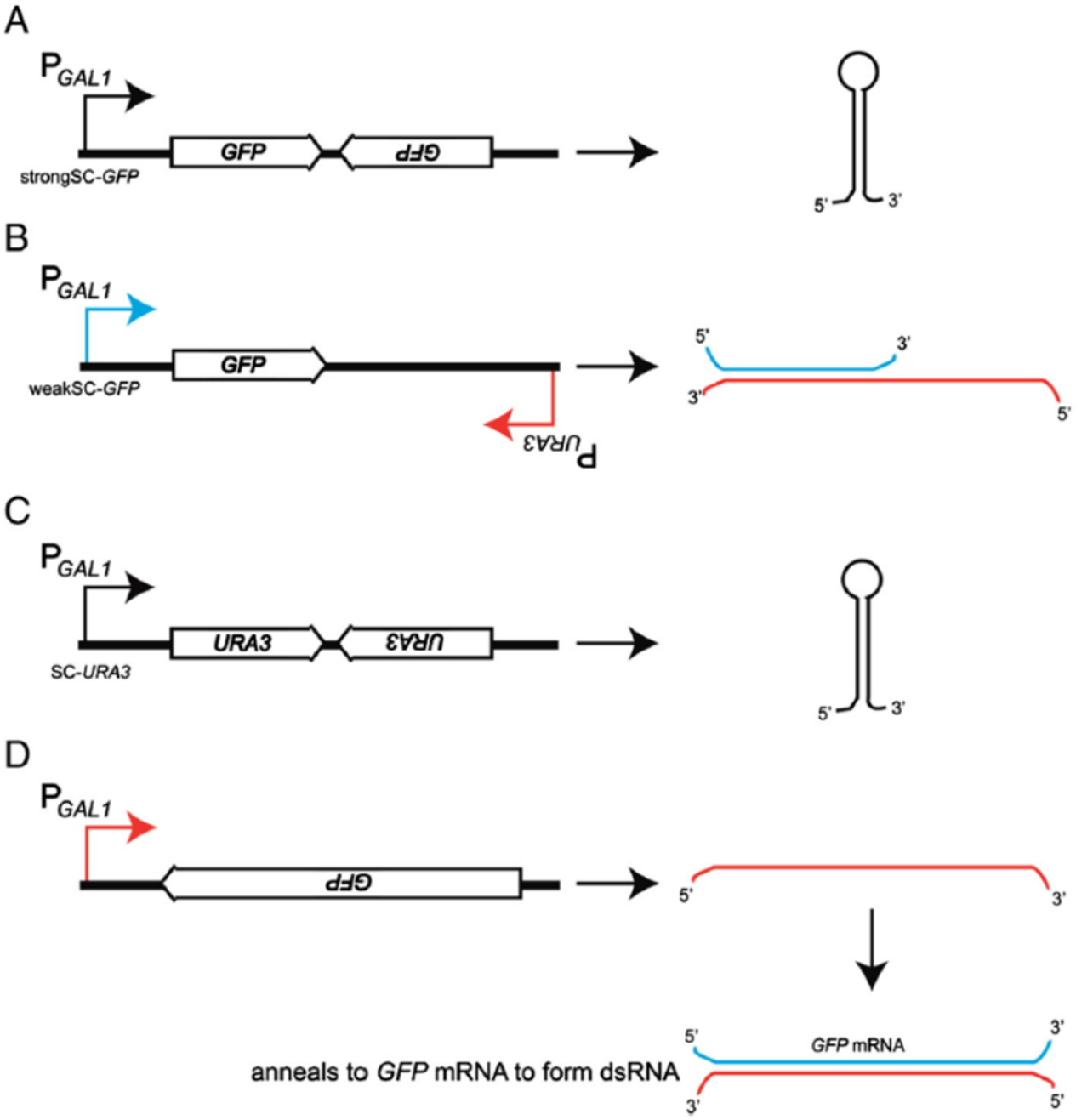

Figure 3.1 Schematic for silencing constructs directed against *GFP* and *URA3*. (A) The transcripts of the strong silencing construct against *GFP* (strongSC-*GFP*) harbouring two inverted *GFP* fragments connected by a link region. **(B)** The sense and antisense transcripts of the weak silencing construct against *GFP* (weakSC-*GFP*) anneal to form perfectly complemented dsRNAs. The sense transcript (blue) is driven by the galactose-inducible *GAL1* promoter (P_{GAL1}) and the antisense transcript (red) is constitutively driven from the weaker *URA3* promoter (P_{URA3}). **(C)** The transcripts of the silencing construct directed against *URA3* (SC-*URA3*) are single transcripts harbouring two inverted repeats of *URA3* and forms a dsRNA hairpin structure. The transcription of this construct is driven by P_{GAL1}, which is the same as used in the strongSC-*GFP*. **(D)** The silencing construct used by Suk and colleagues produces single-stranded antisense transcripts (red) that anneal directly to the *GFP* mRNA to form dsRNA substrates (Wang et al. 2013).

3.2.1.2. RNAi-mediated silencing of *URA3* in *S. cerevisiae*

URA3 is a gene located on chromosome V of the *S. cerevisiae* genome, which encodes orotidine 5'-phosphate decarboxylase (ODCase), an enzyme that catalyzes an essential step of uracil synthesis (Loison et al. 1980). Meanwhile, ODCase also converts the anti-metabolite 5-fluoroorotic acid (5-FOA) into the toxic 5-fluorouracil (5-FU) that inhibits cell growth (Wagner and Heidelberger 1962). Therefore, *S. cerevisiae* cells expressing uracil can grow on media lacking uracil, but not on media containing uracil and 5-FOA. Conversely, *S. cerevisiae* cells with mutated or deleted *URA3* can grow on media containing uracil and 5-FOA, but not on media lacking uracil. Therefore, the RNAi-mediated silencing of *URA3* can be measured by plating serial dilutions of *S. cerevisiae* cells on synthetic media containing uracil, lacking uracil, or containing both uracil and 5-FOA.

The parental strain W303a is uracil auxotrophic which lacks *URA3* gene; W303a cells transformed with either *URA3* only (YW1), or *URA3* and the SC-*URA3* construct (YW2) allow the comparison of uracil levels with and without the expression of its silencing construct. When grown under galactose conditions, the above-mentioned three strains were comparable on synthetic complete media (Patch 1 in **Figure 3.2**). Uracil auxotrophic W303a strain grew on synthetic complete media with 5-FOA but not on media lacking uracil, whereas the two derivative strains containing *URA3* grew on minus uracil but not on 5-FOA media (Patch 1 in **Figure 3.2**). This indicates the induction of the SC-*URA3* silencing construct did not confer detectable negative effects on cell growth, and the expression of the silencing construct alone cannot trigger the target gene silencing in the absence of the RNAi apparatus.

Next, the three *S. cerevisiae* strains mentioned above were all sequentially integrated with Sca*AGO1* and Sca*DCR1* genes. Again, all three strains grew similarly on synthetic complete media, and the growth is comparable to the strains without RNAi components (Patch 2 in **Figure 3.2**). This

indicates the expression of ScaAgo1 and ScaDcr1 proteins did not negatively affect cell growth. The strain expressing ScaAgo1 and ScaDcr1 (YW3) is uracil auxotrophic, which grew on 5-FOA but not on minus uracil media; the strain expressing ScaAgo1, ScaDcr1 and Ura3 proteins (YW4) showed exactly the opposite, which grew on minus uracil but not on 5-FOA media. Comparing to YW4, the strain expressing ScaAgo1, ScaDcr1, Ura3p proteins, and the SC-*URA3* silencing construct (YW5) exhibited reduced growth on both minus uracil and increase growth on 5-FOA media (Patch 2 in **Figure 3.2**). This suggests *URA3* mRNA was partially silenced under the induction of the SC-*URA3* construct. Thus, the expression of ScaAgo1 and ScaDcr1, and the induction of the SC-*URA3* silencing construct are both required for RNAi-mediated silencing of *URA3* in *S. cerevisiae.* Therefore, my study confirmed that the integration of Sca*AGO1* and Sca*DCR1* genes restored RNAi-mediated gene silencing in RNAi-deficient *S. cerevisiae*. However, it is unknown whether one or more unidentified endogenous factor(s) is required for the restored RNAi pathways.

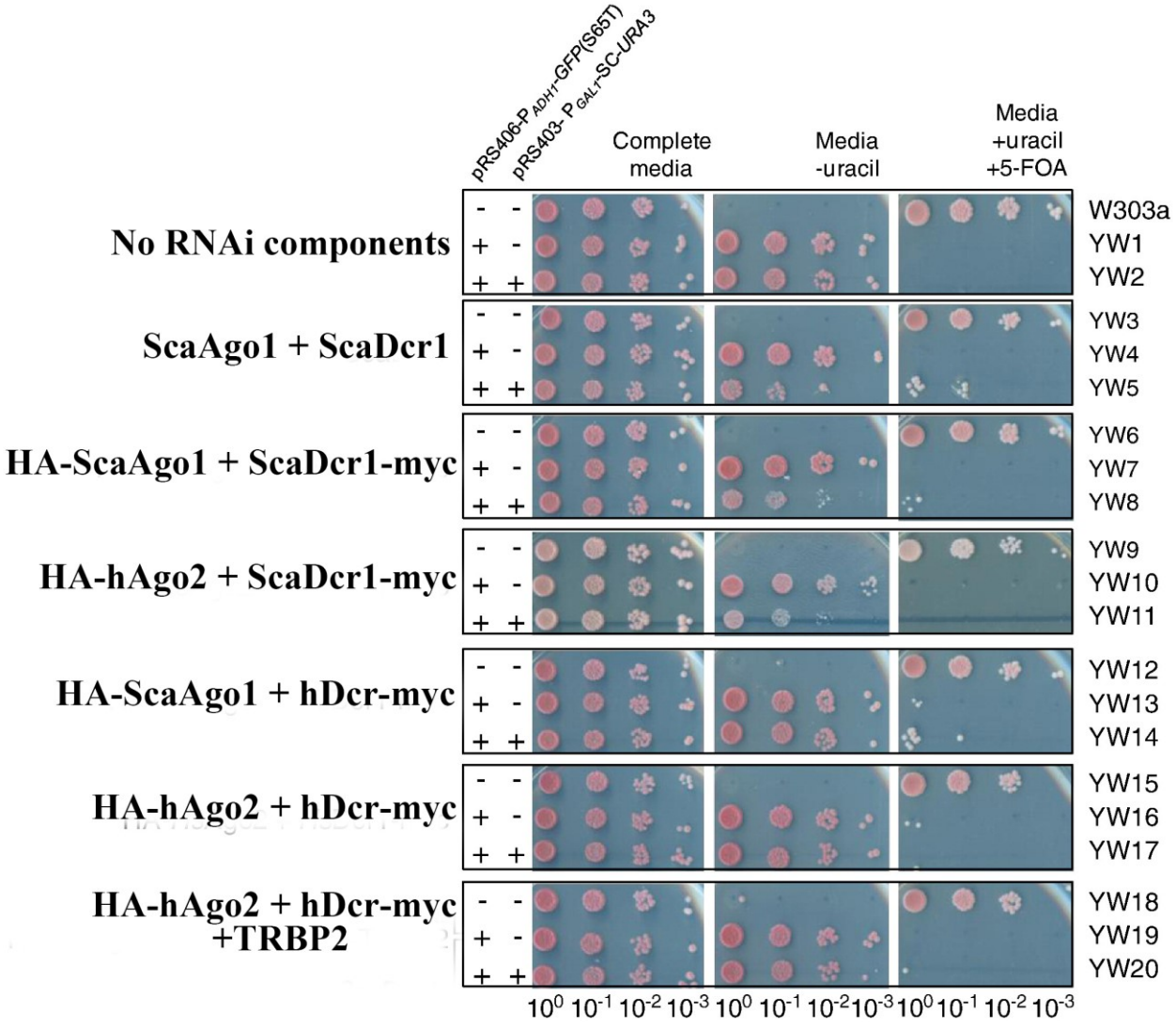

Figure 3.2 *URA3* silencing in transformed *S. cerevisiae* strains to express mixed combinations of Argonaute and Dicer. *S.cerevisiae* strains transformed with different Argonaute and Dicer genes from human and *S.castellii* were plated on a series of media. Each group has three strains; *S. cerevisiae* strains lacking both the pRS406$_{(URA3)}$-P$_{ADH1}$-*GFP* reporter construct and the pRS403-P$_{GAL1}$-SC-*URA3* silencing construct, strains harbouring only the reporter construct, and strains harbouring both the reporter and silencing constructs. Each strain was grown on synthetic complete media containing uracil (left image), media lacking uracil (centre image), and media containing uracil and 5-FOA (right image). Cells were grown overnight in appropriate media and then diluted to 1 x 10^8 cells per ml. 10-fold serial dilutions were prepared and 5 µl aliquots were spotted on indicated plates and grown for 3 days at 30°C.

3.2.1.3. RNAi-mediated silencing of *GFP* in *S. cerevisiae*

Another assay using *GFP* as reporter gene was conducted to investigate if the integration of Sca*AGO1* and Sca*DCR1* genes can successfully restore RNAi-mediated gene silencing in *S. cerevisiae*. A set of four strains were used to compare the relative fluorescence of GFP under non-inducing and inducing conditions of the silencing constructs against GFP. The parental strain W303a transformed with Sca*AGO1* and Sca*DCR1* genes was used as the negative control of the GFP fluorescence (YW3), whereas the integration of Sca*AGO1*, Sca*DCR1*, and *GFP* genes into W303a (YW4) led to a robust expression of GFP protein. These two strains set the baseline of the GFP fluorescence since the former has no GFP expression (filled gray trace in in **Figure 3.3A**) while the latter has active GFP expression (filled green trace in **Figure 3.3A**). Moreover, no difference in relative GFP fluorescence in the above described two strains was observed between glucose (non-inducing) and galactose (inducing) conditions (**Figure 3.3A**). Subsequently, strains YW4 was further transformed with either the strongSC-*GFP* construct (YW25) or the weakSC-*GFP* construct (YW24) to generate two derivative strains with GFP silencing constructs. Since these two constructs were driven by a galactose-inducible promoter P_{GAL1}, we compared the relative *GFP* fluorescence in strains YW24 and YW25 under glucose (non-inducing) and galactose (inducing) conditions to investigate the potential RNAi-mediated *GFP* silencing.

Interestingly, the strain harboring the strongSC-*GFP* construct (YW25) did not show any detectable GFP fluorescence even under non-inducing glucose conditions of the silencing construct (red lines in **Figure 3.3A**). Multiple studies have shown that a mammalian RISC can go through more than twenty rounds of target mRNA cleavage before the disassociation of the loaded guide strand (Hutvágner and Zamore 2002; Gregory et al. 2005). This suggests that RNAi-mediated gene silencing is a highly efficient process. The small amount of "leaky" transcription of the strong *GFP*

silencing construct under the non-inducing conditions was sufficient to completely silence *GFP* mRNAs.

Under non-inducing glucose conditions, no reduction of the relative *GFP* fluorescence was observe in strain harboring the weakSC-*GFP* silencing construct (YW24) (blue line in **Figure 3.3A top**) compared to the strain expressing GFP but has no silencing construct (YW4) (filled green trace in **Figure 3.3A top**). Conversely, induction of the weakSC-*GFP* silencing construct under galactose condition resulted in a significant reduction in the *GFP* fluorescence in strain YW24 (blue line in **Figure. 3.3A bottom**). The induction of weak silencing construct did not completely eliminate *GFP* expression, which suggests a dynamic balance between *GFP* synthesis rate and turnover rate was reached.

To conclude, the induction of the silencing constructs against *GFP* led to partial or complete reduction of the relative fluorescence of GFP. Moreover, this RNAi-mediated gene silencing requires the expression of ScaAgo1 and ScaDcr1 proteins.

Figure 3.3 Relative fluorescence of GFP in transformed *S. cerevisiae* strains. The relative *GFP* fluorescence was measured in *S. cerevisiae* strains transformed with mixed Argonaute and Dicer genes from human and *S. castellii*, when the expression of the silencing constructs was uninduced (glucose) and induced (galactose). (**A**) *S. cerevisiae* cells expressing untagged ScaAgo1 and ScaDcr1; (**B**) *S. cerevisiae* cells expressing HA-ScaAgo1 and ScaDcr1-myc; (**C**) *S. cerevisiae* cells expressing HA-hAgo2 and hDcr-myc; (**D**) *S. cerevisiae* expressing HA-hAgo2, hDcr-myc, and TRBP2. Each panel shows four traces for GFP fluorescence in yeast grown under inducing (glucose, left) and non-inducing (galactose, right) conditions: *S. cerevisiae* strains lacking the *GFP* reporter (filled gray trace; A-YW3, B-YW6, C-YW9, D-YW18) served as negative controls, strains expressing the *GFP* reporter but lacking any silencing construct (filled green trace; A-YW4, B-YW7, C-YW10, D-YW19) served as positive controls, strains harbouring both the *GFP* reporter and the weakSC-*GFP* construct (blue trace; A-YW24, B-YW26, C-YW28, D-YW30), and strains expressing both the *GFP* reporter and the strongSC-*GFP* construct (red trace; A-YW25, B-YW27, C-YW29, D-YW31). Each strain was analyzed on a BD FacsCalibur flow cytometer to measure GFP fluorescence intensity.

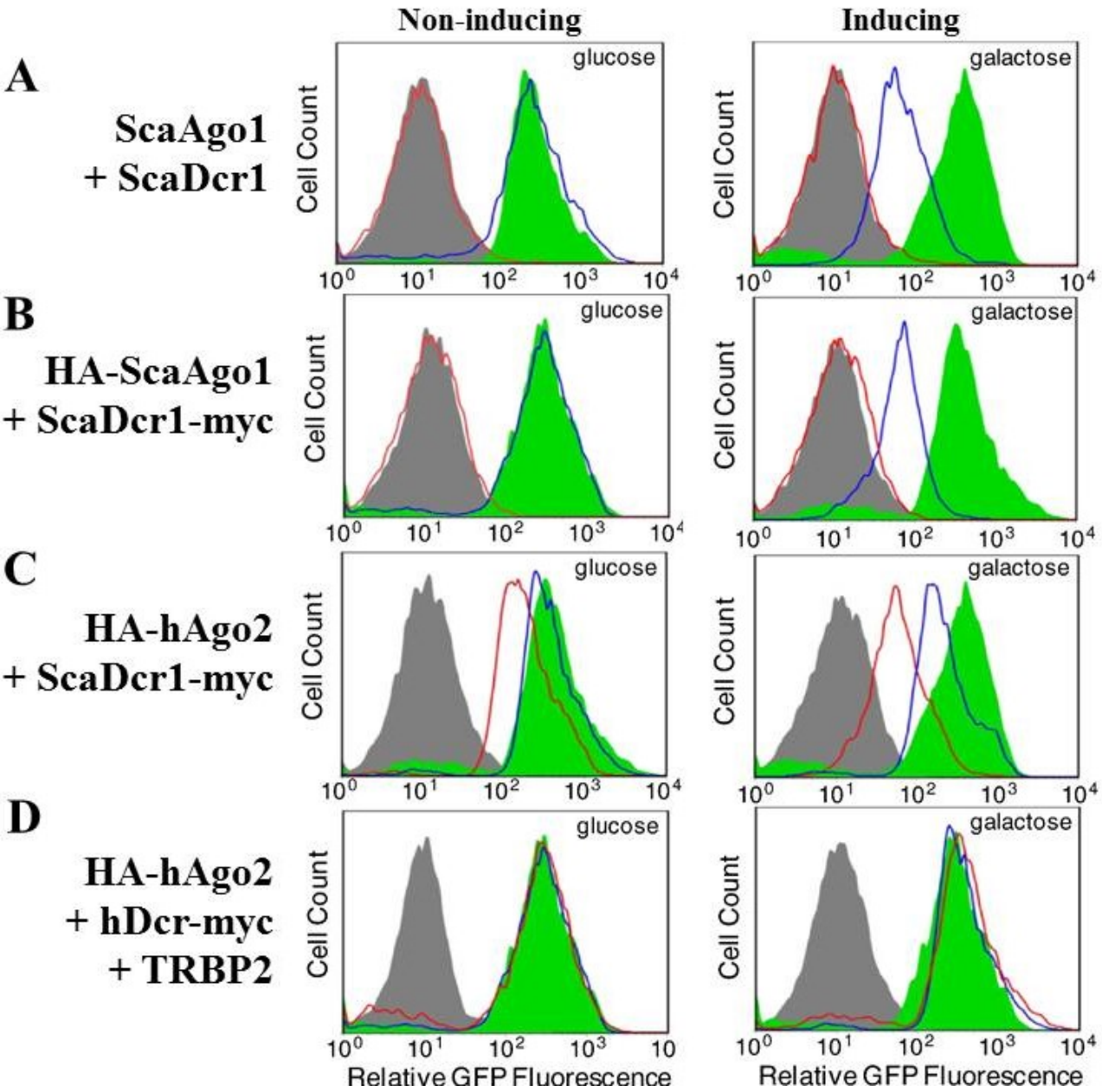
Non-inducing
Inducing
A
ScaAgo1
+ ScaDcr1
B
HA-ScaAgo1
+ ScaDcr1-myc
C
HA-hAgo2
+ ScaDcr1-myc
D
HA-hAgo2
+ hDcr-myc
+ TRBP2
glucose
galactose
Cell Count
Relative GFP Fluorescence

3.2.1.4. Epitope tagged ScaAgo1 and ScaDcr1 effectively silence reporter genes

During the construction of *S. cerevisiae* strains for RNAi investigation, a major obstacle was the random loss of the transformed Sca*AGO1* or Sca*DCR1* genes. A publication two years after I started this research project reported that RNAi pathways are incompatible with the killer RNA virus harboured in some fungi including *S. cerevisiae* (Drinnenberg et al. 2011). RNAi-mediated sequence-specific silencing confers protection against viral infection, whereas the satellite dsRNA of the killer RNA virus encodes a protein toxin that kills nearby cells and provides self-protection to the host (Schmitt and Breinig 2006; Breinig et al. 2006). Furthermore, whole-genome sequencing showed that RNAi components were absent in all species known to possess dsRNA killer, whereas killer virus was absent in every fungi species that retained an RNAi pathway (Drinnenberg et al. 2011). Therefore, the restored RNAi pathways may interfere with the killer RNA virus in *S. cerevisiae*. It eventually leads to the loss of one of these two incompatible mechanisms. Another explanation for the random loss of transformed RNAi components is that the expression vector series I employed to transform Sca*AGO1*, Sca*DCR1*, reporter genes, and the corresponding silencing constructs into the genome of *S. cerevisiae* share the common plasmid backbone. This could lead to undesired homologous recombination that disrupts or discards genes of interest while leaving the selectable markers intact.

Without commercial antibodies available for ScaAgo1 and ScaDcr1 proteins, an epitope tagging strategy was utilized to detect protein expression levels and to examine protein-protein interactions. Previous experimental results from our laboratory suggest that the N-terminal tagging of Argonaute and C-terminal tagging of Dicer proteins posed the least effect on their function in RNAi-mediated silencing. Therefore, we epitope tagged ScaAgo1 with hemaglutinin (HA) at its N-terminus, and

tagged ScaDcr1 with myc epitope at its C-terminus. Protein immunoblotting confirmed the robust expression of HA-ScaAgo1 and ScaDcr1-myc (YW8 in **Figure 3.4**).

The efficiency of *GFP* silencing under the induction of the strong or weak silencing constructs was comparable between the strains expressing epitope tagged HA-ScaAgo1 and ScaDcr1-myc (**Figure 3.3B**) and untagged ScaAgo1 and ScaDcr1, respectively (**Figure 3.3A**). The growth assay also exhibited that *URA3* silencing triggered by HA-ScaAgo1 and ScaDcr1-myc (patch 3 in **Figure 3.2)** was comparable to, or slightly less effective than, untagged ScaAgo1 and ScaDcr1 pair (patch 2 in **Figure 3.2)**. The results of these two parallel assays demonstrated that epitope tagged ScaAgo1 and ScaDcr1 largely preserved their function when expressed in *S. cerevisiae*. Therefore, the N-terminal tagged Argonaute and C-terminal tagged Dicer proteins were used in the subsequent studies to allow further analysis on protein expression and protein-protein interactions.

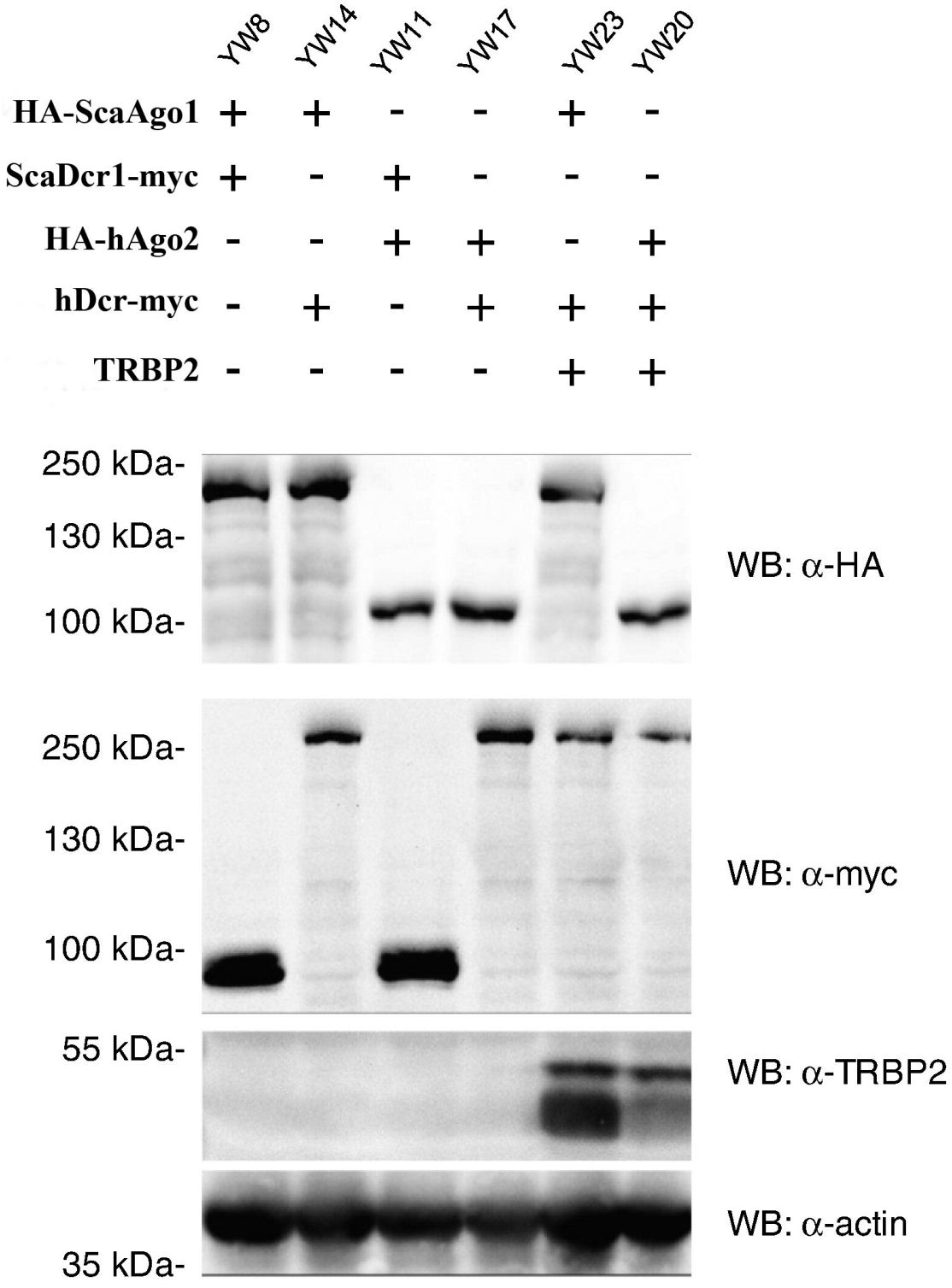

Figure 3.4 Detection of Argonaute, Dicer, and TRBP2 proteins by Western blot. The expression of HA-tagged Argonaute proteins, myc-tagged Dicer proteins, and untagged human TRBP2 were detected by anti-HA, anti-myc, anti-TRBP2 antibodies, respectively. Anti- β-actin antibody was used to detect *S. cerevisiae* actin, which used as a positive control of protein expression and extraction. Strains analyzed are indicated above each lane.

3.2.2. Introduction of human RISC cannot restore RNAi in *S. cerevisiae*

The reconstitution of RNAi in *S. cerevisiae* by RNAi components from closely related budding yeast piqued our interests to investigate whether the introduction of human RNAi system would restore RNAi-mediated reporter gene silencing in *S. cerevisiae*. Previous publications showed that purified human Argonaute 2 (hAgo2), Dicer (hDcr), and co-factor TRBP2 proteins can form a functional RISC *in vitro* (MacRae et al. 2008).

I constructed a number of *S. cerevisiae* strains using W303a as the parental strain. Plasmids containing HA-Hs*AGO2*, Hs*DCR1*-myc, and *TRBP2* genes were sequentially integrated into the genome of W303a (YW18), which grew on 5-FOA but not minus uracil media (Patch 7 in **Figure 3.2**) and had no GFP expression (filled grey trace in **Figure 3.3D**). Conversely, the strain expressing HA-hAgo2, hDcr-myc, TRBP2, and Ura3 proteins (YW19) grew on minus uracil but not 5-FOA media (Patch 7 in **Figure 3.2**) and had robust expression of GFP (filled green trace in **Figure 3.3D**). The subsequent integration of the corresponding silencing constructs into the genome of strain YW19 generated three strains to examine the potential RNAi-mediated *URA3* or *GFP* silencing: SC-*URA3* (YW20), weakSC-*GFP* (YW30), or strongSC-*GFP* (YW31). Surprisingly, the introduction of encoding genes of three human RISC components did not trigger any detectable silencing of *URA3* or *GFP* as reporter genes under inducing conditions of the corresponding silencing constructs (Patch 7 in **Figure 3.2;** red and blue lines in **Figure 3.3D**).

We also examined whether the expression of HA-hAgo2 and hDcr-myc, without TRBP2 could restore the RNAi pathway in *S. cerevisiae*. Strain W303a was integrated with HA-Hs*AGO2* and Hs*DCR1*-myc genes and the resultant strain, YW15, grew on 5-FOA but not minus uracil media (Patch 6 in **Figure 3.2**), whereas the strain transformed with HA-Hs*AGO2*, Hs*DCR1*-myc, and *URA3*

genes grew on minus uracil but not on 5-FOA media. The subsequent integration of SC-*URA3* construct (YW17) into strain YW16 showed no detectable *URA3* silencing (Patch 7 in **Figure 3.2**). Protein immunoblot confirmed the expression of HA-hAgo2, hDcr-myc, and TRBP2 (YW20), or HA-hAgo2 and hDcr-myc (YW17) in my *S. cerevisiae* strains (**Figure 3.4**).

To rule out the possibility that the epitope tags fused to hAgo2 and hDcr interfere with their function in RNAi-mediated gene silencing, I conducted GFP fluorescence and uracil growth assays in strains expressing untagged hAgo2, hDcr, with or without hDcr cofactor TRBP2. As was the case with strains expressing epitope-tagged human RISC components, no RNAi-mediated silencing of reporter genes were observed in strain expressing untagged human RISC components (data not shown). This suggests that the introduction of human RISC genes cannot reconstitute the RNAi pathway in budding yeast *S. cerevisiae.*

Interestingly, Suk and colleagues reported that the expression of hAgo2, hDcr, and TRBP2 in *S. cerevisiae* cells reduced the relative fluorescence of GFP protein (Suk et al. 2011). However, the silencing construct in their studies produced single-stranded antisense *GFP* that hybridized with *GFP* mRNA to form dsRNA substrates for hDcr cleavage (**Figure 3.1D**). This hybridization process blocks GFP protein expression by inhibiting mRNA translation. Therefore, it is not clear whether the reduced GFP fluorescence was a result of *bona fide* RNAi-mediated silencing or antisense-based silencing.

3.2.3. Human Argonaute 2 and *S. castellii* Dicer restore RNAi in *S. cerevisiae*

While conserved in a functional sense to process long dsRNA substrates into small RNA duplexes, there are significant structural differences in the Dicer homologues between humans and

budding yeast (**Figure 1.2A**). In contrast, Argonaute proteins are highly conserved across eukaryotes (**Figure 1.3A**). To further investigate at which step (*e.g.* dsRNA recognition, Dicer processing, Argonaute loading, or target mRNA silencing) that the human RNAi apparatus failed to restore RNAi in *S. cerevisiae*, I constructed *S. cerevisiae* strains harboring epitope tagged pairs of Argonaute and Dicer proteins from *S. castellii* and humans. Strains expressing three cross-species Argonaute-Dicer pairs were constructed from the parental strain W303a: (1) HA-hAgo2 and ScaDcr1-myc; (2) HA-ScaAgo1 and hDcr-myc; (3) HA-ScaAgo1, hDcr-myc, and TRBP2. RNAi-mediated reporter gene silencing was measured in the assays described above. Protein immunoblots probed with antibodies against corresponding epitope tags and TRBP2 confirmed the expression of Argonaute, Dicer, and TRBP2 proteins in above mentioned strains harbouring cross-species Argonaute-Dicer pairs (**Figure 3.4**). For each cross-species Argonaute-Dicer pair, a set of five strains were generated using W303a as the parental strain. Transformation of only Argonaute and Dicer genes generated the uracil auxotrophic strains which also had no GFP expression. Conversely, integration of Argonaute, Dicer, *URA3*, and *GFP* genes produced strains survived on minus uracil but not on 5-FOA media, and had robust GFP expression. Subsequently, corresponding silencing constructs against *URA3* and *GFP* described above were introduced to generate three strains each harbouring a unique silencing construct to examine potential RNAi-mediated reporter gene silencing.

Interestingly, both cell growth and GFP fluorescence assays exhibited that the only cross-species pairs induced *URA3* and *GFP* silencing in *S. cerevisiae* is HA-hAgo2 and ScaDcr1-myc (patch 4 in **Figure 3.2; Figure 3.3C**). In contrast, expression of HA-ScaAgo1 and hDcr-myc, with or without TRBP2 was unable to activate the silencing of *URA3* and *GFP* (patch 5 in

Figure 3.2). It is worth mentioning that *GFP* silencing induced by HA-hAgo2 and ScaDcr1-myc proteins was less potent compared to the levels induced by HA-ScaAgo1 and ScaDcr1-myc (**Figure 3.3B, C**). However, levels of *URA3* silencing by these two Argonaute-Dicer pairs were comparable (patch 3, 4 in **Figure 3.2**).

To conclude, the non-canonical ScaDcr1 can restore RNAi-mediated silencing in RNAi-deficient *S. cerevisiae* with either ScaAgo1 or hAgo2. Conversely, hDcr cannot restore RNAi-mediated silencing with either ScaAgo1 or hAgo2, even with the expression of the co-factor TRBP2.

3.2.4. Human and *S. castellii* Dicer proteins interact with Argonaute by distinct mechanisms

Details about how Dicer processed small RNA duplexes are transferred and incorporated into Argonaute are largely unknown. Human TRBP2 was proposed to function as a structural bridge to connect Dicer to Argonaute proteins (Lau et al. 2009). To examine why Dicer from *S. castellii* but not human reconstituted *URA3* and *GFP* silencing in *S. cerevisiae*, I investigated the protein-protein interactions between transformed Argonaute and Dicer proteins by co-immunoprecipitation in *S. cerevisiae*.

Five strains expressing different Argonaute and Dicer proteins were used in co-IP analysis: (1) HA-ScaAgo1 and ScaDcr1-myc; (2) HA-hAgo2 and ScaDcr1-myc; (3) HA-ScaAgo1 and hDcr-myc; (4) HA-hAgo2 and hDcr-myc; (5) HA-hAgo2, hDcr-myc, and TRBP2. The total cell lysates of these strains were collected and incubated with agarose beads coupled to anti-myc antibodies. C-terminally myc-tagged Dicer proteins were bound to, and then eluted off the anti-myc beads. To confirm the epitope-specific immunoprecipitation of Dicer proteins and binding partners, the samples were run

on SDS-PAGE gels, and probed with an antibody against myc (left panel in **Figure 3.5**). The co-immunoprecipitation of HA-tagged Argonaute proteins was probed with an antibody against HA (right panel in **Figure 3.5**).

When the SC-*URA3* silencing construct was not induced, none of the examined five strains showed Argonaute co-immunoprecipitation with Dicer proteins (top right panel in **Figure 3.5**). Conversely, HA-hAgo2 was detected in hDcr pull downs only when the SC-*URA3* construct was induced (bottom right panel in **Figure 3.5**). Interestingly, the co-immunoprecipitation between human Argonaute and Dicer in *S. cerevisiae* was independent on the expression of TRBP2. Moreover, no immunoprecipitation was observed between other Argonaute-Dicer pairs. ScaDcr1 protein triggers reporter gene silencing with either *S. castellii* or human Argonaute, but neither one of the Argonaute was observed to co-immunoprecipitate with ScaDcr1.

To rule out the possibility that the detected hAgo2 in the pull downs of hDcr was due to non-specific binding, two strains expressing either HA-ScaAgo1 or HA-hAgo2 but no Dicer protein was incubated with agarose beads coupled with anti-myc antibodies. Immunoblotting of proteins eluted from the beads with and anti-HA antibody showed no detectable signal (**Figure 3.5**).

To conclude, hDcr forms a stable protein complex with hAgo2 but not with ScaAgo1. Moreover, the association between hDcr and hAgo2 is dependent on the induction of dsRNA substrates, but does not require Dicer co-factor TRBP2. Conversely, ScaDcr1 did not form a stable protein complex with either ScaAgo1 or hAgo2 although these two pairs restore reporter gene silencing in *S. cerevisiae*. This suggests that the canonical and non-canonical Dicer proteins interact with Argonaute by distinct mechanisms, and the formation of a stable complex between Argonaute and Dicer is not necessary for effective RNAi-mediated gene silencing.

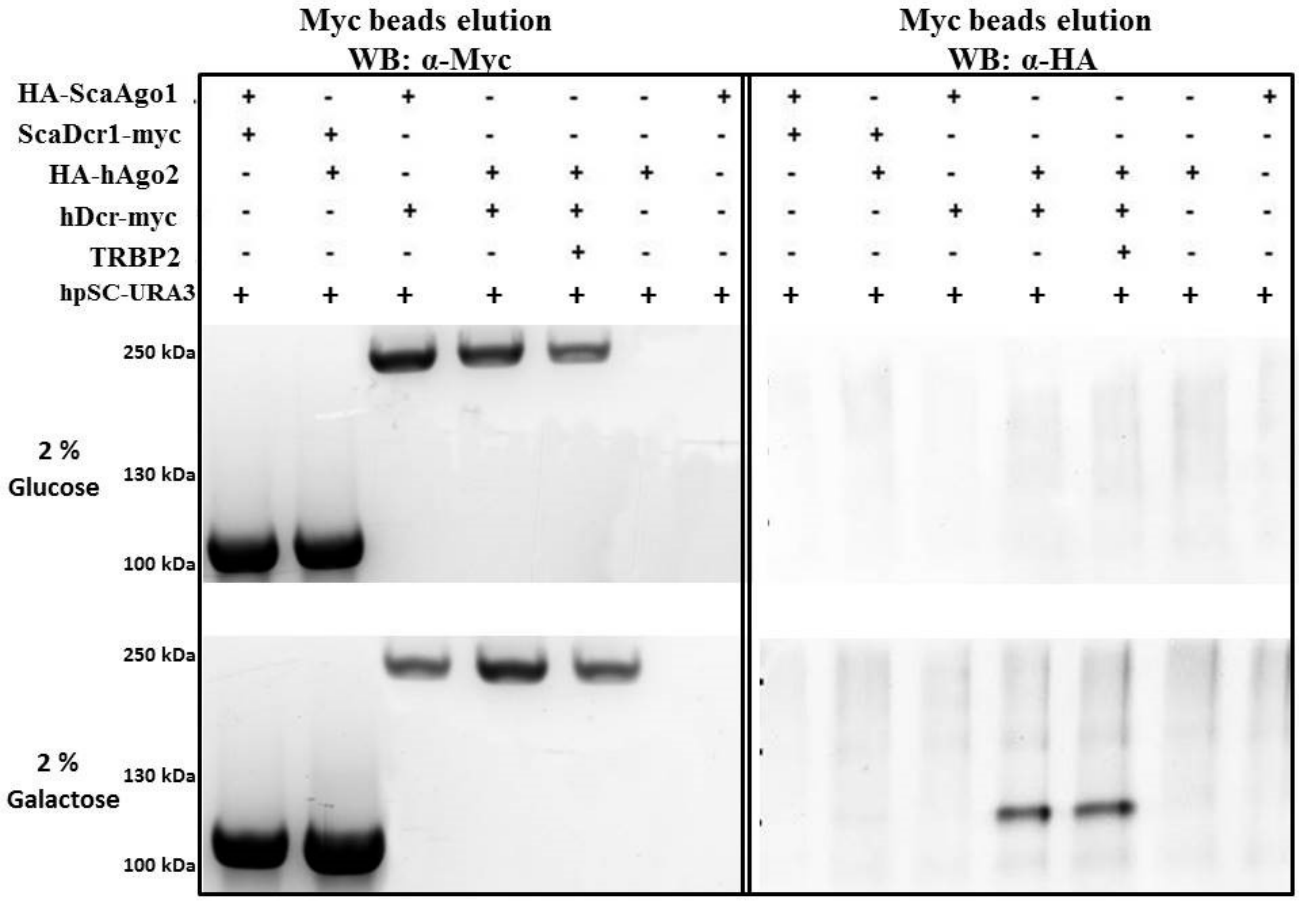

Figure 3.5 Co-immunoprecipitation of human Argonaute 2 with human Dicer is dsRNA substrate dependent. The epitope-specific immunoprecipitation of *S. castellii* and human Dicer proteins were probed by antibody against myc tag. The potential co-immunoprecipitation of Argonaute proteins with Dicer was examined by probing Dicer pull down with antibody against HA with and without the presence of *URA3* silencing construct. Strains expressing HA-ScaAgo1 or HA-hAgo2 but no Dicer gene were served as negative controls of unspecific binding to myc coupled agarose beads. The expression of HA-tagged Argonaute proteins and myc-tagged Dicer proteins were probed by antibodies against HA and myc tags.

3.2.5. Human and *S. castellii* Argonaute proteins are subject to Hsp90 regulation in *S. cerevisiae*

Previous studies from our lab and others reported that the molecular chaperone Hsp90 facilitates small RNA duplex loading into Argonaute in *Drosophila* and humans (Pare et al. 2009, 2013; Johnston et al. 2010; Miyoshi et al. 2010; Iwasaki et al. 2010). The inhibition of Hsp90 ATPase activity significantly reduces the efficiency of RNAi-mediated gene silencing.

There are two Hsp90 homologues in *S. cerevisiae*, the constitutively expressed Hsc82 and the inducible Hsp82, which share high similarity with their respective mammalian counterparts, Hsp90α and Hsp90β (Erkine et al. 1995; Kamal et al. 2003). Since both Argonaute and Hsp90 proteins are highly conserved across eukaryotic phyla, I investigated whether human and *S. castellii* Argonaute transformed into *S. cerevisiae* are subject to the regulation of endogenous Hsp90 machinery.

My initial attempt at human or *S. castellii* Argonaute co-immunoprecipitation with *S. cerevisiae* Hsp90 did not yield strong evidence to conclude that exogenous Argonaute proteins directly interact with endogenous Hsp90 in *S. cerevisiae*. Therefore, we examined if RNAi-induced *URA3* silencing was affected with the addition of Hsp90 inhibitors. Preliminarily, silencing of *URA3* was partially inhibited on plates added with 10 or 20 μM of the Hsp90 inhibitor geldanamycin (GA) (data not shown). However, the poor solubility of GA in media caused uneven distribution of the drug which formed visible yellow particles. Therefore, we examined several other Hsp90 inhibitors including 17-AAG (17-N-allylamino-17-demethoxygeldanamycin), radicicol (RD), and NVP-AUY922. Among these inhibitors, RD has the best solubility and distribution so we chose it for subsequent assays. It is worth mentioning that the inhibition of Hsp90 ATPase activity could potentially lead to cell cycle arrest and apoptosis since numerous client proteins of Hsp90 are kinases and hormone receptors crucial for cell growth. Thus, an ideal concentration of Hsp90 inhibitor in this assay should

be high enough to show a difference in RNAi-mediated silencing, but also low enough to avoid negatively effecting *S. cerevisiae* cell growth.

I examined a range of RD concentrations from 25 to 150 μM, and found that 75 μM is the optimal concentration that revealed the role of Hsp90 activity in *URA3* gene silencing while no adverse effect on cell growth was posed. We examined the entire set of strains expressing distinct pairs of Argonaute and Dicer proteins: (1) no RNAi apparatus; (2) untagged ScaAgo1 and ScaDcr1; (3) HA-ScaAgo1 and ScaDcr1-myc; (4) HA-hAgo2 and ScaDcr1-myc; (5) HA-ScaAgo1 and hDcr-myc; (6) HA-hAgo2 and hDcr-myc; (7) HA-hAgo2 and hDcr-myc, and TRBP2. Each set contains three strains: no *URA3* and SC-*URA3*; has *URA3* but not SC-*URA3*; has both *URA3* and SC-*URA3.*

The cell growth of examined strains was similar on complete media added with either 75 μM RD or the same volume of the solvent dimethyl sulfoxide (DMSO) (**Figure 3.6**). Furthermore, the previously identified functional RNAi pairs, *S. castellii* Dicer paired with either *S. castellii* or human Argonaute, still triggered *URA3* silencing (patch 2, 3, 4 in **Figure 3.6**). This suggested cell growth on complete media was not noticeably affected with the addition 75 μM of RD or its solvent DMSO, and *URA3* silencing on minus uracil media was maintained when DMSO was supplemented.

Most importantly, *URA3* silencing in strains that *S. castellii* Dicer paired with either *S. castellii* or human Argonaute was greatly diminished, if not completely abolished with the addition of 75 μM of RD (patch 2, 3, 4 in **Figure 3.6**). In conclusion, the inhibition of Hsp90 activity by 75 μM of RD significantly diminished the RNAi-mediated *URA3* silencing.

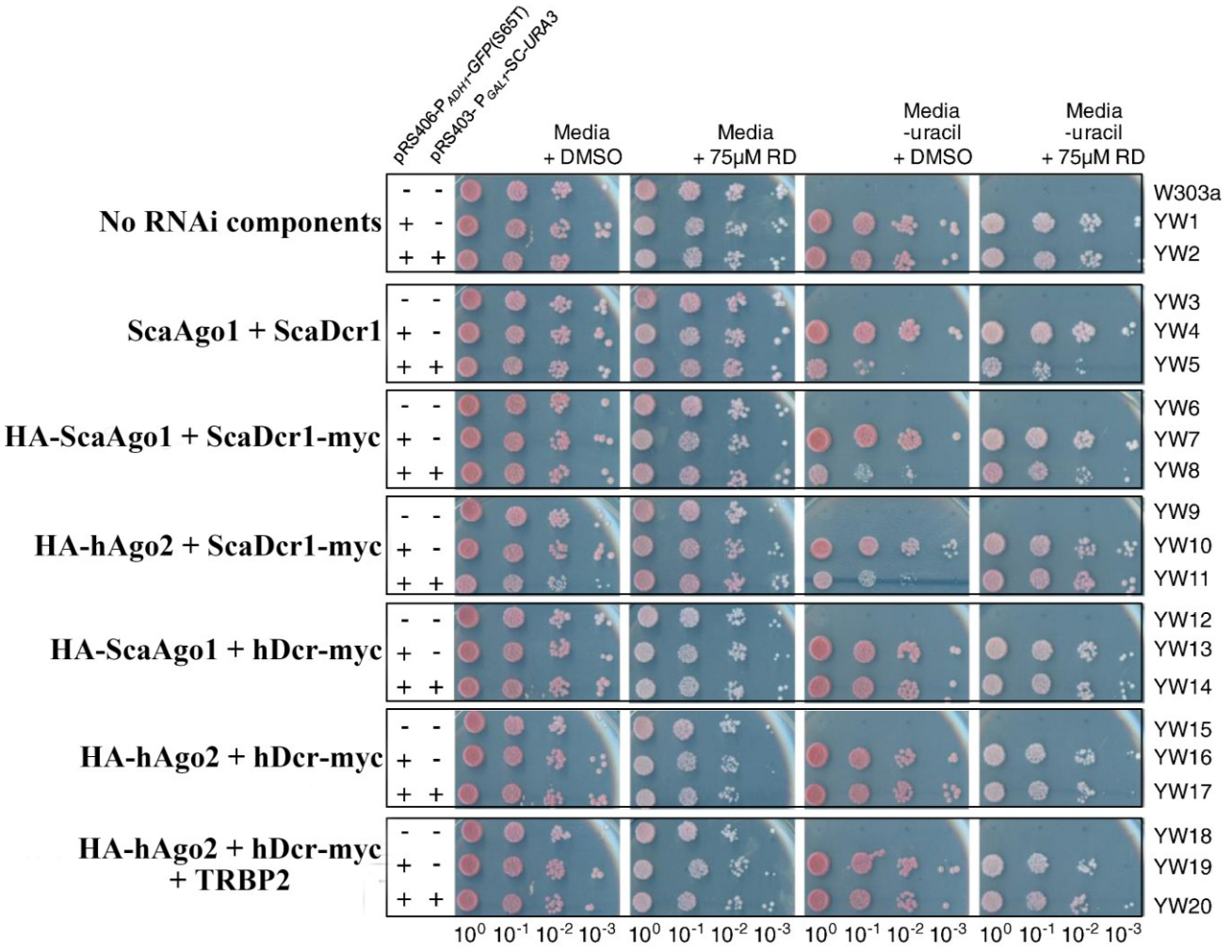

Figure 3.6 RNAi-mediated gene silencing is less potent with the addition of the Hsp90 inhibitor radicicol. *S. cerevisiae* strains containing different Argonaute and Dicer genes from human and *S. castellii.* Each group has three strains; yeast lacking both the pRS406-P_{ADH1}-*GFP* reporter construct and the pRS403-P_{GAL1}-SC-*URA3* silencing construct, yeast harbouring only the reporter construct, and yeast harbouring both the reporter and silencing constructs. Each strain was grown on media containing uracil and DMSO control (left panel), media containing uracil and 75 μM radicicol (centre left panel), media lacking uracil with DMSO control (centre right panel), and media lacking uracil with 75 μM radicicol (right panel). Cells were grown overnight in appropriate media and then diluted to 1 x 10^8 cells per ml. 10-fold serial dilutions were prepared and 5 ul aliquots were spotted on indicated plates and grown for 2 days at 30°C.

3.2.6. Endogenous protein factors play roles in restored RNAi pathways in *S. cerevisiae*

Although the expression of ScaDcr1 paired with either ScaAgo1 or hAgo2 effectively reconstituted RNAi in *S. cerevisiae*, it is possible that one or more endogenous protein factors are also required for the restored RNAi pathways. The majority of identified RNAi co-factors are double-stranded RNA-binding proteins (*e.g.* TRBP2 in mammalian cells, and R2D2 in *Drosophila*). I interrogated the *S. cerevisiae* genome for genes encoding confirmed or predicted double-stranded RNA binding proteins. Five genes containing one or more dsRBD domains, *RNT1* (YMR239C), *LRP1* (YHR081W), *MRPL3* (YMR024W), *TIF11* (YMR260C), and *SUA5* (YGL169W) were identified. The corresponding ORFs of *RNT1*, *LRP1*, *MRPL3*, and *TIF11* were deleted by homologous recombination with the nourseothricin (natNT2) selectable marker. However, none of the four deletion strains exhibited noticeable changes in RNAi-mediated gene silencing (data not shown).

SNF1 (YDR477W) encodes a serine/threonine protein kinase that is required for transcription of glucose-repressed genes, thermal tolerance, sporulation, peroxisome biogenesis, and filamentous growth in response to starvation (Celenza and Carlson 1989). Lo and colleagues further reported that Snf1 and the acetyltransferase Gcn5 respectively activate histone H3 serine-10 phosphorylation and lysine-14 acetylation to enhance the transcription of *INO1*, a structural gene for inositol-1-phosphate synthase in *S. cerevisiae* (Lo et al. 2001). Thus, these coordinated modifications of histone H3 by promoter-specific regulation could relate to the deacetylation and methylation of histone H3 during RNAi-mediated heterochromatic silencing in *S. pombe* (Rea et al. 2000).

To examine if Snf1 proteins could play a role in restored RNAi pathways in *S. cerevisiae*, I generated *SNF1* deletion strains containing ScaDcr1-myc paired with either HA-ScaAgo1 or

HA-hAgo2. All examined strains grew similarly under non-inducing condition of *URA3* silencing construct, whereas the *URA3* silencing triggered by RNAi was more severe in both Argonaute-Dicer pairs when *URA3* silencing construct presented (**Figure 3.7A**). The more robust *URA3* silencing in *SNF1* deletion strains suggests the phosphorylation catalyzed by this kinase has a negative effect on the RNAi pathway.

Piper and colleagues reported that sensitivity to Hsp90 inhibitors can be modified with mutation to Hsp90, its co-chaperones, and plasma membrane transporters of yeast (Piper et al. 2003). The deletion of *PDR5* (YOR153W) could prevent yeast cells from pumping certain chemicals out of the cell, which would lead to cytoplasmic retention of Hsp90 inhibitors in *S. cerevisiae*. *PDR5* (YOR153W) encodes an ATP-binding cassette transporter on the plasma membrane involved in cellular detoxification, cation resistance, and steroid transport (Lepper et al. 1990; Mamnun et al. 2004; Ernst et al. 2005). *S. cerevisiae* cells lacking Pdr5 protein were more sensitive to the addition of Hsp90 inhibitors (**Figure 3.7B**).

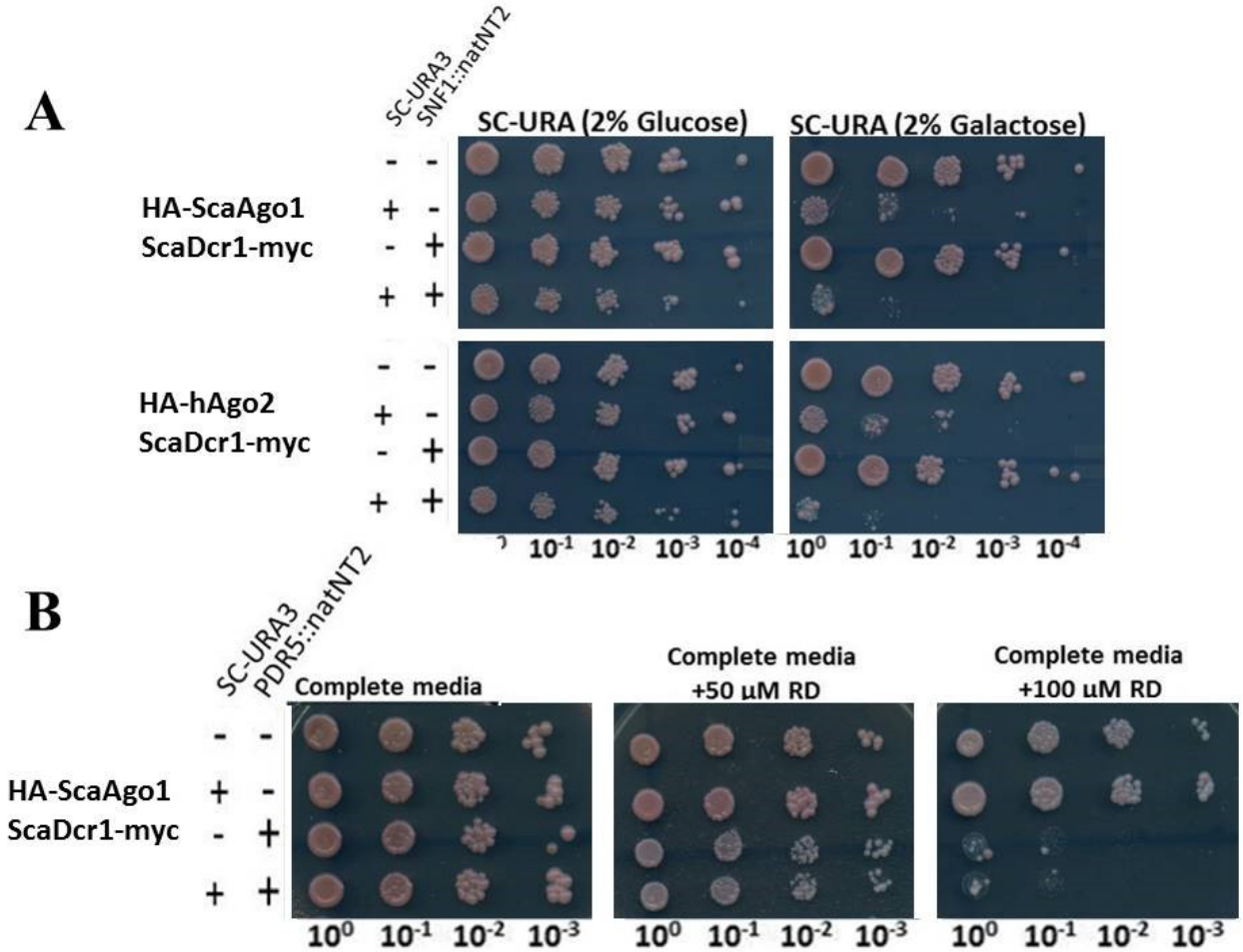

Figure 3.7 Deletion of *SNF1* and *PDR5* affects *URA3* silencing and Hsp90 inhibition. *S. cerevisiae* strains integrated with HA-Sca*AGO1* and Sca*DCR1*-myc genes, and pRS406$_{(URA3)}$-P_{ADH1}-*GFP* silencing construct. Each group contains four strains. The expression of the *URA3* silencing contruct and the deletion of *SNF1* or *PDR5* were marked on the left panel. **(A)** Deletion effect of SNF1 was measured by comparing the *URA3* silencing of strains with and without *SNF1* gene. **(B)** Deletion effect of *PDR5* was measured by growing cells on media containing uracil and 0 µM, 50 µM, 75 µM radicicol. Cells were grown overnight in appropriate media and then diluted to 1 x 10^8 cells per ml. 10-fold serial dilutions were prepared and 5 ul aliquots were spotted on indicated plates and grown for 2 days at 30°C.

3.3. Summary

As described in this chapter, RNAi-mediated gene silencing was restored in *S. cerevisiae* by introducing genes encoding *S. castellii* Dicer and *S. castellii* or human Argonaute (**Figure 3.2; Figure 3.3**). In contrast, introduction of genes encoding human Dicer and Argonaute did not reconstitute RNAi regardless of whether the Dicer co-factor TRBP2 was present or not (**Figure 3.2; Figure 3.3**). The alignments of amino acid sequences of Argonaute and Dicer proteins across eukaryotes revealed that Argonaute proteins are highly conserved while Dicer proteins are more divergent.

Investigation of the associations between epitope tagged Argonaute and Dicer proteins revealed that ScaDcr1 does not establish a strong interaction with either Argonuate protein even though RNAi-mediated gene silencing was restored. Conversely, hAgo2 but not ScaAgo1 co-immunoprecipitated with hDcr protein, and this interaction was independent on the presence of hDcr cofactor TRBP2. Moreover, the induction of dsRNA substrates strongly stimulated the interaction between human Dicer and Argonaute, indicating that hDcr interacts with dsRNA substrates in an as yet unidentified manner. This finding demonstrated that human and *S. castellii* RNAi machineries are not only sequentially and structurally different, but also process dsRNA substrates and pass mature RNA duplexes to Argonaute by distinct mechanisms.

My research also revealed that the restored RNAi pathways were dependent on the ATPase activity of Hsp90 (**Figure 3.6)**. One explanation is that the ATP hydrolysis catalyzed by Hsp90 facilitates the conformation changes of *S. castellii* and human Argonaute proteins which is crucial for subsequent dsRNA loading. This finding is in accordance with the growing body of evidence that Hsp90-mediated structural rearrangements of Argonaute are well conserved and functionally crucial

to small RNA duplex loading.

It is possible that one or more endogenous protein factor(s) are necessary for RNAi-mediated gene silencing in *S. cerevisiae*. Based on previous research in Drosophila and mammals, proteins containing multiple dsRBD are the most likely candidates. However, single deletion of a number of genes encoding dsRBP proteins did not noticeably affect silencing of reporter genes in *S. cerevisiae.* Snf1, a serine/threonine protein kinase, was identified as a repressor of restored RNAi pathways in *S. cerevisiae.* This suggests that the restored RNAi pathways may be activated or repressed by endogenous factors in *S. cerevisiae*. The deletion of *PDR5*, a gene encodes an ATP-binding cassette transporter, made RNAi-mediated reporter gene silencing more sensitive to Hsp90 inhibition.

Chapter 4

Multiple kinases are required for RNAi-mediated heterochromatin assembly at centromeres in fission yeast *Schizosaccharomyces pombe*

4.1. Rationale

Post-translational modification (PTM) increases the functional diversity of proteins by covalently and reversibly adding functional groups. Therefore, identifying and understanding specific PTMs is critical in the study of protein functions. Argonaute proteins have been reported to be modified by phosphorylation, hydroxylation, and ubiquitination (Qi et al. 2008; Kirino et al. 2010; Kim et al. 2009; Heo and Kim et al. 2010; Rudel et al. 2011). Human Ago2, the most extensively studied Argonaute protein, is phosphorylated on at least 7 amino acid residues but we are only beginning to understand the consequences of these modifications on its function. Moreover, we know comparatively little about the protein kinases` and phosphatases that modify Argonautes and other effectors of RNAi. A complicating factor regarding the study of Argonaute phosphorylation in mammalian systems is the presence of multiple paralogues in the genome, some with overlapping functions. Since the genome of *S. pombe* harbours a single copy of each *ago1, dcr1, and rdp1* gene, functional redundancy is not an obstacle (Volpe et al. 2002; Jia et al. 2004; Verdel et al. 2004). *S. pombe* is, therefore, an excellent model system to study the effect of post-translational modifications on core RNAi components, especially phosphorylation on Argonaute.

RNAi-mediated gene silencing is required for heterochromatin assembly at centromeres, telomeres, and mating type loci in fission yeast *S. pombe* (Volpe et al. 2002; Motamedi et al. 2004). I hypothesized that if phosphorylation/dephosphorylation reactions on specific amino acid residues are crucial for *S. pombe* Ago1 function in RNAi pathways, then the deletion of kinases or phosphatases catalyzing these reactions should result in de-repression of heterochromatic transcription. Quantitative measurements of pericentromeric transcripts in viable kinase or phosphatase deletion

strains should identify genes required for heterochromatin assembly. However, further analysis is necessary to find out which kinases/phosphatases regulate pericentromeric silencing in RNAi dependent ways, and which are in RNAi-independent mechanisms.

4.2. Results

4.2.1. Multiple kinases are required for pericentromeric silencing

There are at least 106 genes encoding kinase catalytic-domain-containing proteins that have been identified in the fission yeast *S. pombe* genome (http://www.genedb.org; http://www.pombase.org) (Bimbó et al. 2005). Among these genes, 17 are essential for cell viability, 45 are as yet uncharacterized putative protein kinase (*ppk*) genes, and 58 have well-defined homologues in humans. The first step of my *S. pombe* research project was to identify kinases that are required for pericentromeric silencing, a process that depends on RNAi pathways.

The levels of forward and reverse pericentromeric transcripts from *dg* repeats in each of 89 kinase deletion strains were quantitatively measured by qRT-PCR. The pericentromeric transcript levels were then normalized against actin mRNA in each strain, which was served as an internal control. The parental strain MBY192 was used to set up the baseline of pericentromeric transcription, whereas *ago1* deletion strain was employed as a positive control for de-repression of pericentromeric silencing. Although it is possible that the identified kinases may affect pericentromeric silencing in an RNAi-independent manner, this screen still narrowed down the list of candidates that may phosphorylate *S. pombe* Ago1.

The majority of the single kinase deletion strains exhibited less than two fold variation in the levels of pericentromeric transcripts compared to the parental strain. The most significant increases

in both *dg* forward (>15 fold increase) and reverse (>5 fold increase except *Δppk8*) transcripts were observed in 13 kinase deletion strains (**Figure 4.1**). It is worth mentioning that in the *Δppk8* strain, the levels of *dg* forward transcript were significantly higher than the parental strain, while the *dg* reverse transcript levels were virtually unchanged.

Figure 4.1 Relative abundance of pericentromeric transcripts in 89 kinase deletion strains. The levels of forward and reverse transcripts of pericentromeric *dg* repeats normalized to actin mRNA are shown for each kinase deletion strain. To establish a baseline, forward and reverse transcripts of the parental strain MBY192 were set to 10 on a $\log_{10}$ scale (y-axis). The *ago1* deletion strain was used as a positive control in which increased levels of pericentromeric transcripts were greatly elevated. The qRT-PCR assays were conducted in triplicate. Bars represent standard error of the mean (SEM).

Relative abundance of perfectromerfc transcripts
100000
10000
1000
100
10
1
dg forward
dg reverse
MBY192
Δago1
Δgsk3
Δwee1
Δbyr1
Δpka1
Δpmk1
Δdsk1
Δmak3
Δckb1
Δnph1
Δwin1
Δppk8
Δppk27
Δppk33
Δppk15
Δikh1
Δppk2
Δkln1
Δcsk1
Δcdr1
Δppk5
Δbub1
Δssp2
Δppk36
Δppk35
Δgad8
Δoca2
Δgsk31
Δppk31
Δppk30
Δppk29
Δppk25
Δppk24
Δppk22
Δppk16
Δppk14
Δplt1
Δfin1
Δckl3
Δcds1
Δmik1
Δmak1
Δckl1
Δcdr2
Δssp1
Δppk6
Δckl2
Δrad3
Δppk26
Δppk34
Δppk32
Δppk28
Δppk18
Δpck1
Δcek1
Δspk1
Δppk13
Δppk11
Δppk10
Δsrb10
Δpek1
Δpsk1
Δmek1
Δppk9
Δsck2
Δhri1
Δppk34
Δppk38
Δppk1
Δwis4
Δspo4
Δsfk2
Δpka2
Δmde3
Δhhp2
Δcmk2
Δbyr2
Δmkh1
Δmak2
Δppk3
Δpdk1
Δppk19
Δisk1
Δhri2
Δchk1
Δpom1
Δpck2
Δpef1
Δwis1

Furthermore, the majority of these 13 kinase genes that are required for pericentromeric silencing have homologues in humans and/or budding yeast *S. cerevisiae* (**Table 4.1**). This may indicate that the phosphorylation reactions catalyzed by these kinases are functionally important across eukaryotes. Since the ultimate goal of my research is to utilize findings in *S. pombe* to better understand the posttranslational modifications on human Argonaute proteins, I focused mainly on *S. pombe* kinases with human homologues in this study.

Table 4.1 Kinase genes required for pericentromeric repression in *S. pombe* and their homologues in humans and *S. cerevisiae*

Identified kinase gene in *S. pombe*	dg forward/reverse increase (fold) in deletion strains	Human homologue	*S. cerevisiae* homologue
gsk3	733 / 99	*GSK3A, B*	*MRK1, RIM11*
wee1	56 / 41	*WEE1*	*SWE1*
byr1	121 / 12	*MAP2K1, 2*	/
pka1	44 / 10	*PRKAC-A, -B, -C*	*TRK1, 2, 3*
pmk1	51 / 6	*MAPK7*	*SLT2*
mak3	29 / 17	/	/
dsk1	15 / 8	*SRPK1, 2, 3*	*SKY1*
ckb1	90 / 24	*CSNK2B*	*CKB1, 2*
win1	50 / 21	*MAP3K4*	*SSK2, 22*
mph1	46 / 19	*TTK*	*MPS1*
ppk8	47 / 2	/	*RTK1, PRR2, NPR1*
ppk27	48 / 17	/	*PRR1*
ppk33	51 / 9	/	/

Our laboratory and others reported that *S. pombe ago1, dcr1, or rdp1* deletion strains were hypersensitive to the microtubule-destabilizing drug thiabendazole (TBZ) and the DNA synthesis inhibitor hydroxyurea (HU). Sensitivity of TBZ is linked to the role of RNAi pathways in heterochromatin assembly at centromeres whereas sensitivity of HU links RNAi to cell cycle checkpoints (Carmichael et al. 2004; Janbon et al. 2010; Ard et al. 2014). To investigate if any of the

kinase deletion strains also exhibit sensitivity to these drugs, *Δago1, Δdcr1, Δrdp1,* and selected kinase deletion strains were cultured on rich media containing either TBZ or HU at 30°C, or subjected to mild heat shock at 37°C. As expected, *ago1, dcr1,* and *rdp1* deletion strains were all hypersensitive to the addition of TBZ and HU, but interestingly, only *dcr1* and *rdp1* deletion strains were sensitive to mild heat shock (**Figure 4.2**). Whereas most of the examined kinase deletion strains were sensitive to HU treatment, only a few were affected by TBZ or mild heat shock. The phenotype of one deletion strain (Δ*mph1*) was remarkably similar to Δ*ago1* in terms of its sensitivity to various stresses, wherease Δ*wee1* and Δ*pka1* showed comparable sensitivity to stresses as Δ*dcr1* and Δ*rdp1* (**Figure 4.2**).

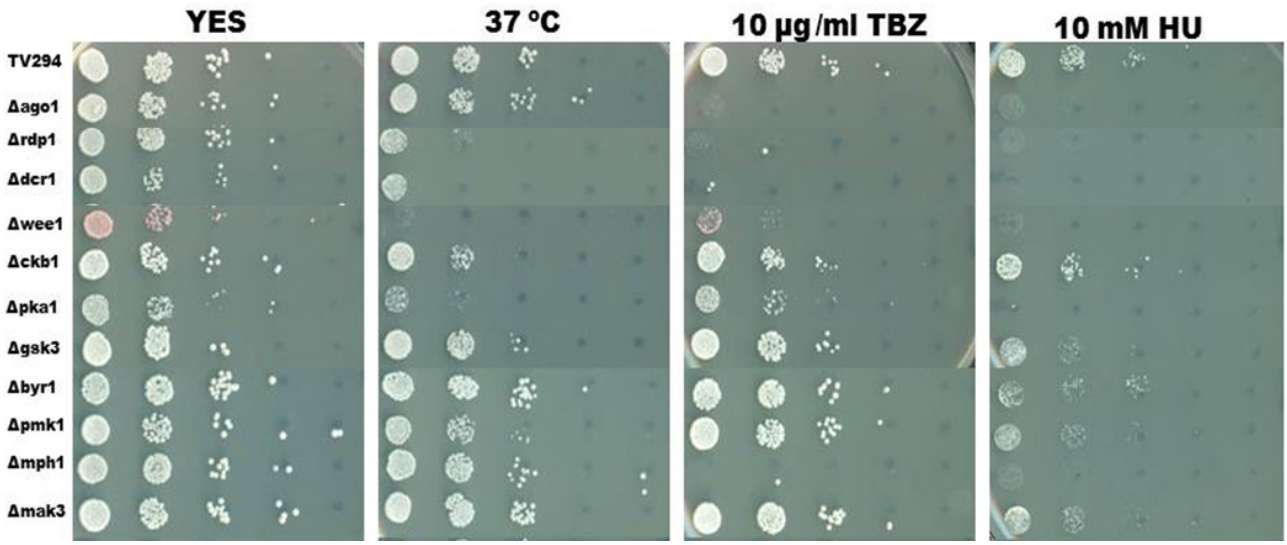

Figure 4.2 Phenotypic assessments of RNAi-defective kinase deletion mutants under various stress conditions. Ten-fold serial dilutions of the three mutants of core RNAi components and eight kinase deletion strains were spotted on YES plates with or without TBZ (10 µg/ml) or HU (10 mM) grown at 30°C, or on YES plates with mild heat shock stress at 37°C. The images were taken after growing for three days.

4.2.2. Non-essential phosphatases are not required for heterochromatic silencing in *S. pombe*

The number of known phosphatases and regulatory subunits is much lower than protein kinases in *S. pombe*. Since no systematic phosphatase deletion library was available (to our knowledge at least), I searched the *S. pombe* genome for phosphatase-catalytic-domain-containing genes and 20 genes were identified (http://www.pombase.org/search/ensembl/phosphatase). Among them, deletion mutants for 13 of the phosphatase genes were available and obtained from the Bioneer *S. pombe* Genome-wide Deletion Mutant Library (South Korea). In this mutant collection, phosphatase-catalytic-domain-containing genes were replaced by kanamycin resistance cassettes (KanMX4) (http://us.bioneer.com/products/spombe/spombeoverview.aspx) (**Table 4.3**).

Forward and reverse pericentromeric *dg* repeat transcripts from 13 phosphatase deletion strains were measured and compared to their parental strain ED666 using qRT-PCR assay as described above. To my surprise, none of these phosphatase deletion strains showed more than a three-fold increase of either *dg* forward or reverse transcripts comparing to the parental strain (**Figure 4.3**).

Table 4.2 Phosphatase-catalytic-domain-containing genes identified from the genome of *S. pombe*

Gene	Product	Synonyms
Deletion strains of 13 phosphatase genes from Bioneer (South Korea):		
SPAC1556.03	serine/threonine protein phosphatase Azr1	*azr1*
SPAC1782.09c	Cdc14-related protein phosphatase Clp1/Flp1	*clp1*
SPBC839.07	Cdc25 family phosphatase Ibp1	*ibp1*
SPAC11E3.09	protein-tyrosine phosphatase Pyp3	*pyp3*
SPBC1685.01	dual-specificity MAP kinase phosphatase Pmp1	*pmp1*
SPAC57A7.08	serine/threonine protein phosphatase Pzh1	*Pzh1*
SPAC823.15	minor serine/threonine protein phosphatase Ppa1	*ppa1*
SPBC16H5.07c	serine/threonine protein phosphatase Ppa2	*ppa2*
SPCC1739.12	serine/threonine protein phosphatase Ppe1	*ppe1*
SPBP4G3.02	acid phosphatase Pho1	*pho1*
SPAC19D5.01	tyrosine phosphatase Pyp2	*pyp2*
SPAC26F1.10c	tyrosine phosphatase Pyp1	*pyp1*
SPCC31H12.05c	serine/threonine protein phosphatase PP1 subfamily, Sds21	*sds21*
No deletion strains available for another 7 phosphatase genes:		
SPBC776.02c	serine/threonine protein phosphatase PP1 subfamily, Dis2	*dis2*
SPAC19B12.05c	CTD phosphatase Fcp1	*fcp1*
SPAC824.08	guanosine-diphosphatase Gda1	*gda1*
SPAC1952.13	lipin, phosphatidate phosphatase Ned1	*ned1*
SPBC428.03c	thiamine-repressible acid phosphatase Pho4	*pho4*
SPAC1071.12c	protein tyrosine phosphatase Stp1	*stp1*
SPAC19G12.15c	trehalose-6-phosphate phosphatase Tpp1	*tpp1*

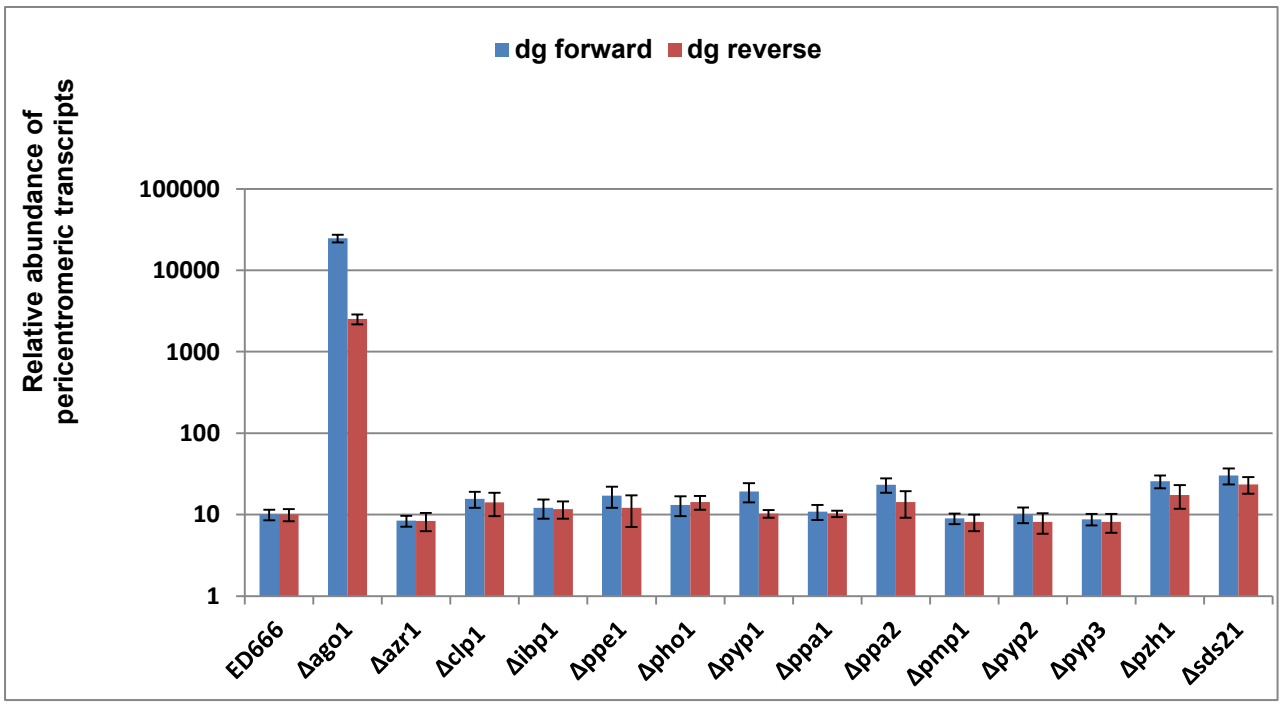

Figure 4.3 Levels of pericentromeric transcripts are unaffected by loss of phosphatase genes. The *dg* forward and reverse transcripts were quantitated in 13 phosphatase haploid deletion strains. The relative abundance of *dg* forward and reverse transcripts were normalized to actin mRNA as the internal control. Forward and reverse transcription levels of *dg* in the parental strain ED666 were set to 10 on a $\log_{10}$ scale (y-axis). The *ago1* deletion strain was used as a positive control for de-repression of pericentromeric transcription. qRT-PCR assayes were conducted in duplicates for this figure. The error bars represent standard errors of the mean (SEM).

Recently, a fellow graduate student in our laboratory used siRNA screening to determine the potential importance of kinases and phosphatases in human Ago2 function (Lopez-Orozco, in preparation). Among the 25 human phosphatases that were found to have effects on hAgo2 activity, eight appear to have corresponding orthologues in *S. pombe.* Conveniently, the haploid deletion strains of six out of these eight phosphatases were available from Bioneer Genome-wide Deletion Library (**Table 4.4**). The pericentromeric transcripts in these phosphatase deletion strains were measured and compared to their parental strain ED666 by qRT-PCR as described above. Unexpectedly, none of these examined strains exhibited more than a two-fold change in *dg* forward or reverse transcripts (**Figure 4.4**). Together, these data indicate that none of the 19 non-essential phosphatase genes examined to date is required for RNAi-mediated heterochromatin assembly at centromeres in *S. pombe.*

Table 4.3 Homologues of human phosphatases affect hAgo2 function in *S. pombe*

Human phosphatase	Gene Locus	*S. pombe* homologues	Gene Locus	Bioneer Label
PDXP	NM_202315	pho2, 4-nitrophenylphosphatase	SPBC15D4.15	BG-H1004
DUSP12	NM_007240	phosphoprotein phosphatase (predicted)	SPBC17A3.06	BG-H1067
ACP6	NM_016361	acid phosphatase (predicted)	SPBC2G2.02	BG-H2505
SYNJ1	NM_003895	syj1,inositol-1,4,5-trisphosphate 5-phosphatase 1	SPBC4.06	BG-H2158
PPM2C	NM_018444	mitochondrial pyruvate dehydrogenase (lipoamide) phosphatase	SPAC10F6.17C	BG-H4185
PPP3R2	NM_147180	calcineurin regulatory subunit (predicted)	SPCC830.06	BG-H4697
PPA2	NM_176865	inorganic pyrophophatase (predicted)	SPAC23C11.05	/
PPP3CA	NM_000944	ppb1, serine/threonine protein phosphatase	SPBP4H10.04	/

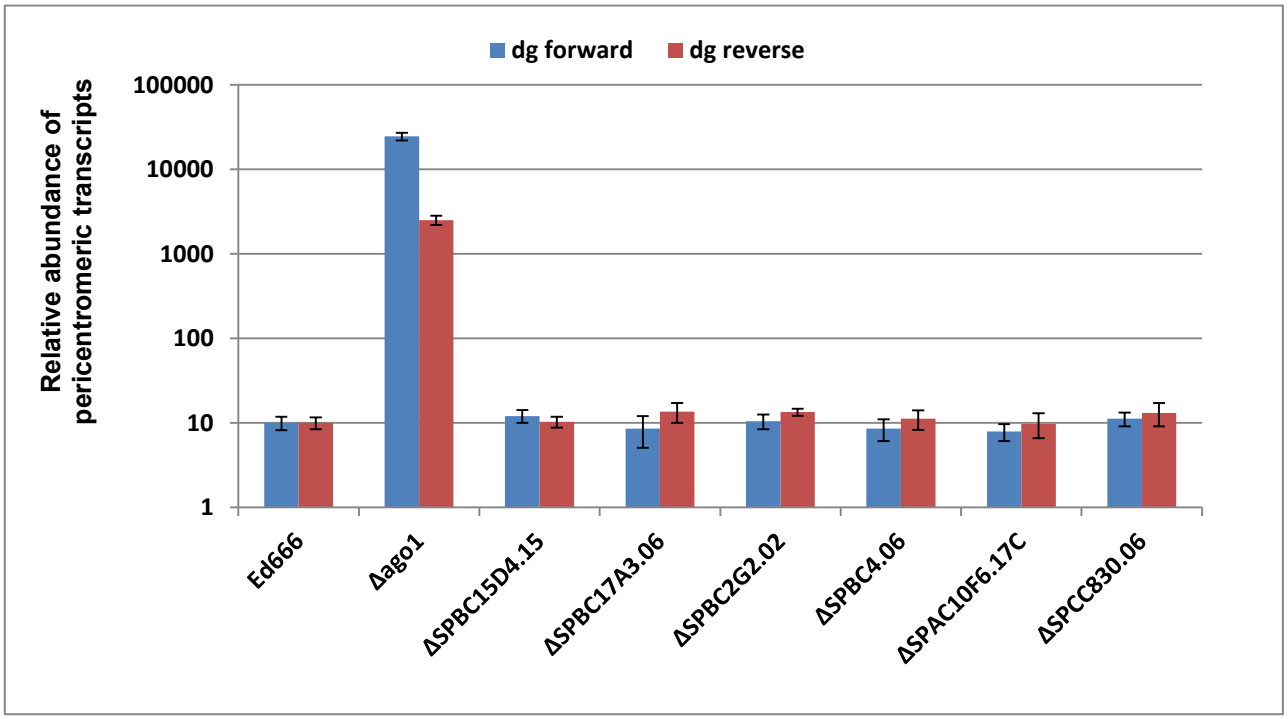

Figure 4.4 Pericentromeric transcript levels in *S. pombe* are not affected by loss of genes encoding orthologues of phosphatases known to affect RNAi in human cells. The *dg* forward and reverse transcripts were measured in six phosphatase deletion strains. The relative abundance of *dg* forward and reverse transcripts was normalized to actin mRNA as the internal control. Forward and reverse transcript levels of *dg* by the parental strain ED666 were set to a baseline of 10, and the *ago1* deletion strain was used as a positive control. Data were collected by conducting qRT-PCR in duplicates. The y-axis shows relative abundance of pericentromeric transcripts in $\log_{10}$ scale. The bars represent standard error of the mean (SEM).

4.2.3. Genetic complementation of the kinase deletion mutants restores RNAi

To verify that the RNAi defects (de-repression of pericentromeric transcription) in the kinase deletion mutants was indeed due to loss of the kinase genes and not due to second site mutations, I used genetic complementation to introduce the appropriate kinase genes into the corresponding deletion mutants.

My first strategy was to subclone the full-length open reading frames of the appropriate kinases into the expression vector pSLF273, which places the kinase genes under the control of a strong thiamine inducible promoter P_{nmt1} (Bahler et al. 1998). The PCR-amplified cDNAs containing the kinase gene and kanamycin resistance cassette (KanMX6) were integrated into the genomes of appropriate *S. pombe* deletion mutants at the *ade6* locus by homologous recombination. The kanamycin-resistant transformants were selected by growing in the presence of geneticin (G418), an aminoglycoside similar to kanamycin. Subsequently, the levels of forward and reverse pericentromeric transcripts from the complemented strains were measured by qRT-PCR as described above. Unexpectedly, none of the rescued strains suppressed the expression of the pericentromeric transcripts (**Figure 4.5A**). This result led me to question "normal" expression of the kinase genes was important for their function RNAi.

The kinase deletion mutants employed in my studies were generated by using *ura4* to disrupt the kinase genes (Bimbó et al. 2005). To reintroduce kinase genes under the control of their natural promoters into the corresponding deletion strains, I employed the following complementation strategy. PCR amplified segments encoding kinase genes and including their natural promoters flanked by homologous sequences to the integrated *ura4* selectable marker were transformed into the kinase deletion strains. Transformants in which the *ura4* modules were replaced by the kinase genes cassettes were counter-selected on synthetic complete media added with 5-FOA for uracil auxotroph

as discussed in Chapter 3. The resulting colonies were re-streaked onto non-selective media to recover, and then subjected twice through 5-FOA selection to enrich for stable integration events. Integration of the kinase genes into the appropriate loci was confirmed by sequencing of diagnostic PCR products from the transformants. Unlike when the kinase genes were overexpressed, expression of the re-introduced kinases from their natural promoters resulted in complementation of the RNAi defects in the kinase deletion strains. Specifically, I observed that levels of pericentromeric transcription in seven of the eight kinase complementation strains were reduced to levels that were comparable to the parental strain (<2 folds fluctuation) (**Figure 4.5B**). The only kinase deletion strain that was not fully complemented using this strategy was Δ*pmk1*. The reason is not clear as sequencing and restriction digestions by endonucleases confirmed the integration of the kinase cassette in the right location. It is possible that second site mutations in the Δ*pmk1* strain affect pericentromeric transcription.

Figure 4.5 Rescue of the RNAi defects in kinase deletion strains requires expression of the kinases at endogenous levels. A. Kinase gene cassettes were introduced into deletion strains under the control of the strong *nmt*$_1$ promoter at the *ade4* locus. **B.** Kinase cassettes driven by their natural promoters were introduced into the deletion strains. The relative abundance of *dg* transcripts was compared with the parental strain TV294 and an *ago1* deletion strain. For the data shown here, qRT-PCR assays were conducted in duplicate. The y-axis shows the relative abundance of pericentromeric transcripts in $\log_{10}$ scale. The error bars represent standard error of the mean (SEM).

A

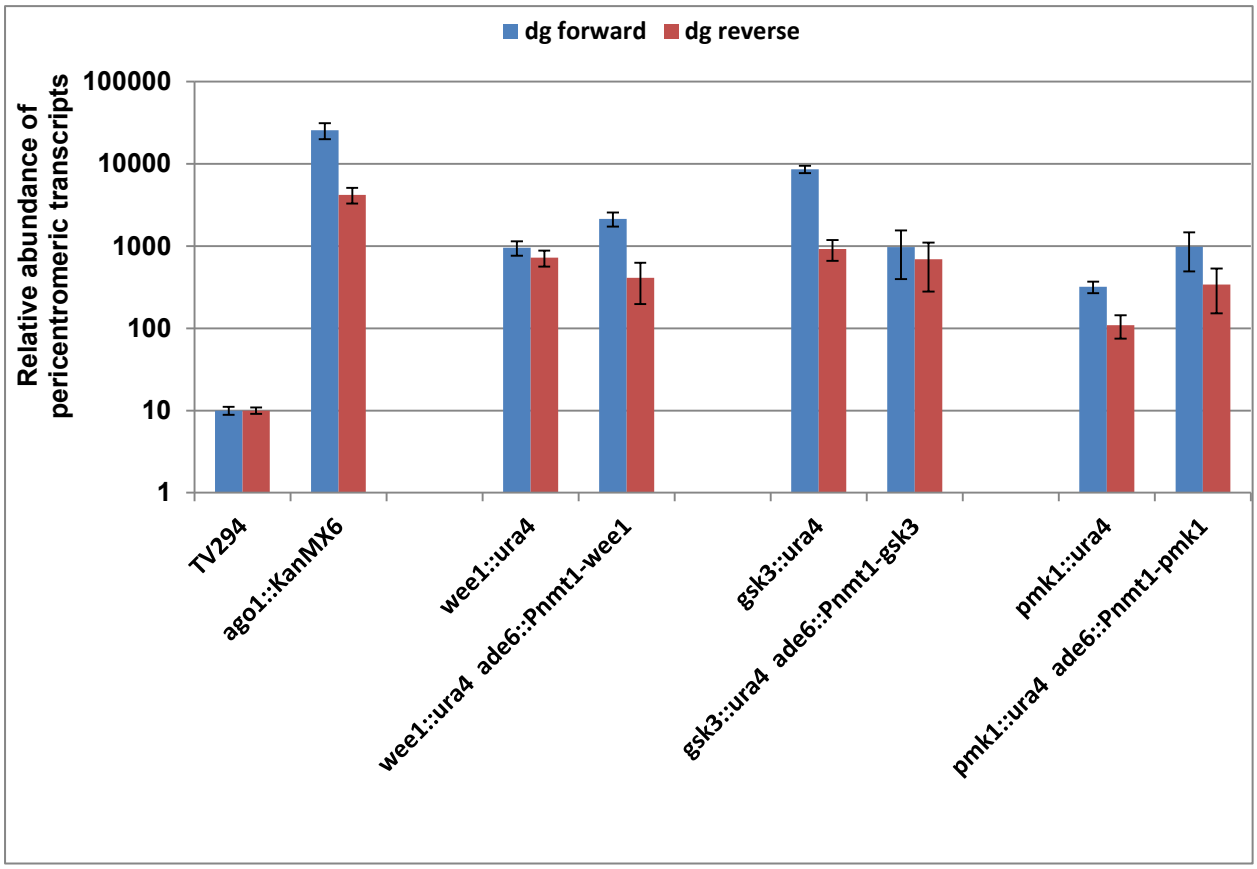
dg forward
dg reverse
Relative abundance of pericentromeric transcripts
100000
10000
1000
100
10
1
TV294
ago1::KanMX6
wee1::ura4
wee1::ura4 ade6::Pnmt1-wee1
gsk3::ura4
gsk3::ura4 ade6::Pnmt1-gsk3
pmk1::ura4
pmk1::ura4 ade6::Pnmt1-pmk1

B

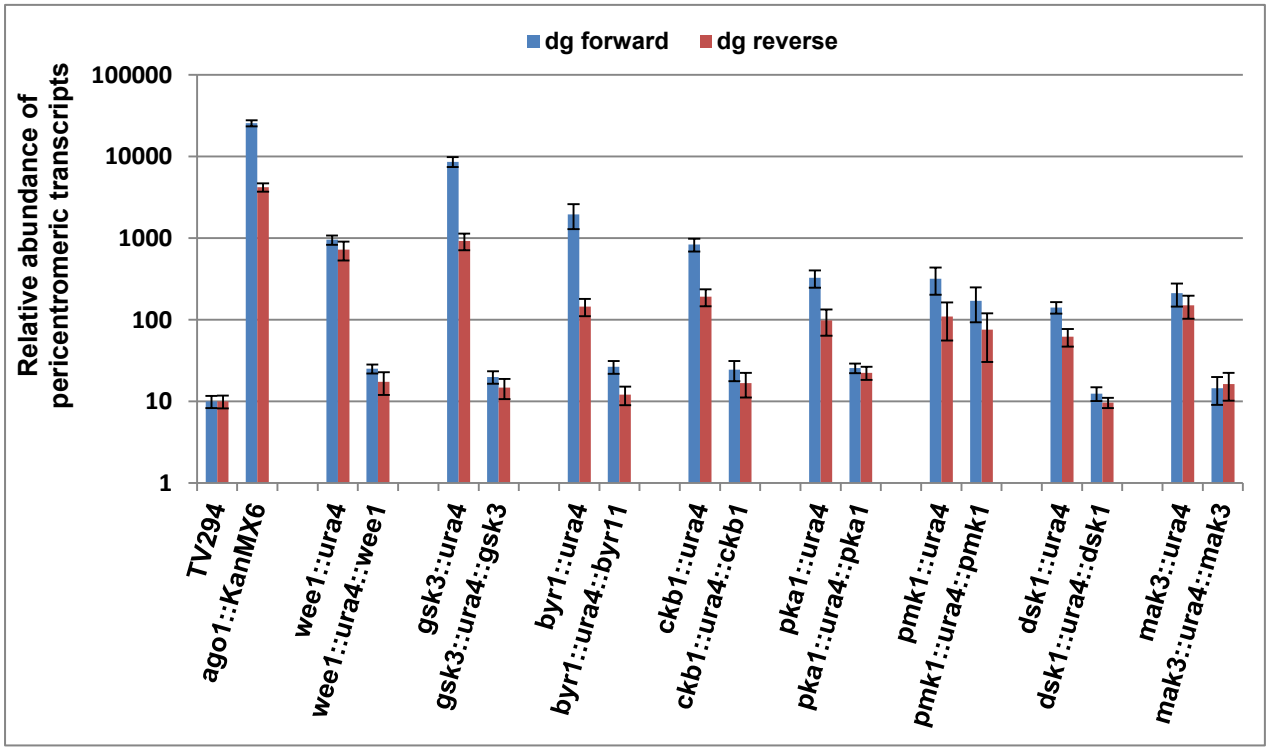
dg forward
dg reverse
Relative abundance of pericentromeric transcripts
100000
10000
1000
100
10
1
TV294
ago1::KanMX6
wee1::ura4
wee1::ura4::wee1
gsk3::ura4
gsk3::ura4::gsk3
byr1::ura4
byr1::ura4::byr11
ckb1::ura4
ckb1::ura4::ckb1
pka1::ura4
pka1::ura4::pka1
pmk1::ura4
pmk1::ura4::pmk1
dsk1::ura4
dsk1::ura4::dsk1
mak3::ura4
mak3::ura4::mak3

4.2.4. Computational prediction of phosphorylation sites in SpAgo1

Identifying the serine, threonine and tyrosine residues in SpAgo1 that are subject to phosphorylation and their corresponding kinases is important for understanding how RNAi is regulated in fission yeast. To my knowledge, protein phosphorylation databases for fission yeast do not exist. Therefore I used the PhosphoMotif Finder from the Human Protein Reference Database (http://www.hprd.org/index_html).

The results of the computational predictions are shown in **Table 4.5**. In total, there were 14 human kinases recognize motifs in SpAgo1 containing serine/threonine residues that could be phosphorylated, 5 different kinases (or kinase families) and 2 phosphatases recognize motifs containing phosphotyrosine residues (**Table 4.5**).

More than half of human kinases and phosphatases that recognize conserved motifs in SpAgo1 have homologues in *S. pombe* (http://www.uniprot.org). Among them, four kinase genes (*gsk3*, *byr1*, *ckb1*, *pka1*) were identified to be required for RNAi-mediated heterochromatin assembly at centromeres in the qRT-PCR assay conducted above (**Figure 4.1**).

Table 4.4 Computational prediction of phosphorylation sites in SpAgo1

Human Kinases or Phosphatases	Recognizing motif	Motifs in SpAgo1	Homologous genes in *S. pombe*
AMP-activated protein kinase	[M/V/L/I/F][R/K/H]XX[pS/pT]XX X[M/V/L/I/F]	4	*cbs2* (SPAC1556.08c); SPCC1919.03c
ATM kinase	pSQ	5	*tel1* (SPCC23B6.03c)
Calmodulin-dependent protein kinase II	[M/V/L/I/F]X[R/K]XX[pS/pT]XX	21	*cmk1*(SPAC25D11.02c); *cmk2* (SPAC23A1.06c)
Calmodulin-dependent protein kinase IV	[M/I/L/V/F/Y]XRXX[pS/pT]	5	
Casein Kinase I	[E/D]XX[pS/pT]	20	*cki1* (SPBC1347.06c); *cki2* (SPBP35G2.05c); *cki3* (SPAC1805.05)
Casein Kinase II	[pS/pT]XX[E/D]	15	***ckb1*** (SPAC1851.03); *ckb2* (SPAC23C11.11)
DNA dependent Protein kinase	P[pS/pT]X	6	*dna2* (SPBC16D10.04c)
G protein-coupled receptor kinase 1	X[pS/pT]XXX[A/P/S/T]	17	*sck1* (SPAC1B9.02c)
GSK3, ERK1, ERK2	X[pS/pT]P	4	***gsk3*** (SPAC1687.15); ***byr1*** (SPAC1D4.13); *spk1* (SPAC31G5.09c)
MAPKAPK2 kinase	pSXXX[pS/pT]	8	/
PKA kinase	[R/K][R/X]X[pS/pT]	15	***pka1*** (SPBC106.10)
PKC kinase	[R/K]XX[pS/pT]	12	*pck1* (SPAC17G8.14c); *pck2* (SPBC12D12.04c)
Pyruvate dehydrogenase kinase	XpSXXDXX	4	*pkp1* (SPAC644.11c)
b-Adrenergic Receptor kinase	[E/D][pS/pT]XXX	8	/
ALK kinase	**pY**XXXX[F/Y]	4	/
EGFR kinase	X[E/D]**pY**X	4	/
JAK2 kinase	**pY**XX[L/I/V]	10	/
Src family kinase	[I/V/L/S]X**pY**XX[L/I]	4	/
Src kinase	**pY**[A/G/S/T/E/D]	15	/
SHP1 phosphatase	[E/D]X**pY**	4	/
TC-PTP phosphatase	[E/D/Y]**pY**	4	/

The sequence alignments of Argonaute proteins from a wide range of eukaryotes showed that at least four phosphorylation sites identified in hAgo2 have corresponding sites in SpAgo1 (**Table 4.6**). Computational analyses of these SpAgo1 residues did not reveal kinase or phosphatase that may act on tyrosine residues Y329 and Y513. In contrast, multiple kinases in *S. pombe* could potentially phosphorylate serine residues S288 and S779 (**Table 4.6**).

Table 4.5 Conserved phosphorylation sites in SpAgo1 and cognate kinases and phosphatases

Human Ago2 phosphorylation sites	**Corresponding sites in *S. pombe* Ago1**	**Predicted human kinases/phosphatases recognize the residues**	**Homologous genes in *S. pombe***
T307	S288	PKA kinase; PKC kinase; Casein kinase II	*pka1* (SPBC106.10); *pck1* (SPAC17G8.14c); *pck2* (SPBC12D12.04c); *ckb1* (SPAC1851.03); *ckb2* (SPAC23C11.11)
Y393	Y371	SHP1 phosphatase	/
Y529	Y513	SHP1 phosphatase; Src kinase; JAK2 kinase	/
S798	S779	Casein Kinase II	*ckb1* (SPAC1851.03); *ckb2* (SPAC23C11.11)

4.2.5. Lack of phosphorylation on epitope-tagged SpAgo1

There are a number of commercial and laboratory antibodies to SpAgo1 but unfortunately, none of these reagents worked very well in my studies. Therefore, I elected to epitope-tag SpAgo1 in order to detect it in protein complexes by immunoprecipitation and immunoblotting. Several different epitope tagging strategies were compared to find out which one was least disruptive to SpAgo1 function in heterochromatin assembly at centromeres. Strain S155, which harbours an N-terminal FLAG-tagged endogenous SpAgo1 suppressed pericentromeric transcripts to the same low levels as

its parental strain S51 (which expresses non-tagged SpAgo1). Therefore, I employed strain S155 and S51 for my subsequent experiments.

Specificity in the immunoprecipitation of FLAG-SpAgo1 from strain S155 was demonstrated by incubating total cell lysates with agarose beads coupled with antibodies directed against either FLAG or the myc epitope. No anti-FLAG immunoreactive proteins in the size range of SpAgo1 were pulled down from strain S51 (negative control). Conversely, FLAG-SpAgo1 was immunoprecipitated from strain S155 with anti-FLAG beads but not anti-myc beads (**Figure 4.6A**). To determine if/how SpAgo1 was affected by loss of kinases that function in RNAi, a group of kinase deletion strains were generated from strain S155 by disrupting protein-kinase-encoding genes with kanamycin resistance module KanMX6 as previously described (Bimbó et al. 2005). Immunoprecipitation of FLAG-SpAgo1 from these kinase deletion strains was then confirmed (**Figure 4.6B**) before proceeding to other experiments.

Unfortunately, my attempts to determine whether phosphorylation of FLAG-tagged SpAgo1 was affected by loss of specific kinases were not successful. I first used immunoprecipitation, two-dimensional gel electrophoresis, and immunblotting of FLAG-tagged SpAgo1, but there were many technical issues with this approach (data not shown). The preliminary data suggest SpAgo1 has at least three distinct phosphorylation states. However, I was not able to reproduce the data to a satisfactory level.

As a second approach to identify phosphorylation changes in SpAgo1, anti-FLAG immunoprecipitates from parental and kinase deletion strains were separated on SDS-PAGE gels and then stained by Coomassie Brilliant Blue. Gels slices (band A in **Figure 4.7**) containing the abundant ~100 kDa protein presumed to be SpAgo1 were cut out of the gels and then sheared. Samples were

then submitted to Creative Proteomics (http://www.creative-proteomics.com, Shirley, NY 11967, USA) for liquid chromatography–tandem mass spectrometry, which confirmed SpAgo1 was enriched in band A. Unfortunately, phosphopeptides in SpAgo1 isolated from the parental strain S155 or any of the kinase deletion strains were not detected. As such, the phosphorylation states of SpAgo1 in wild-type and kinase deletions strains are not known.

A

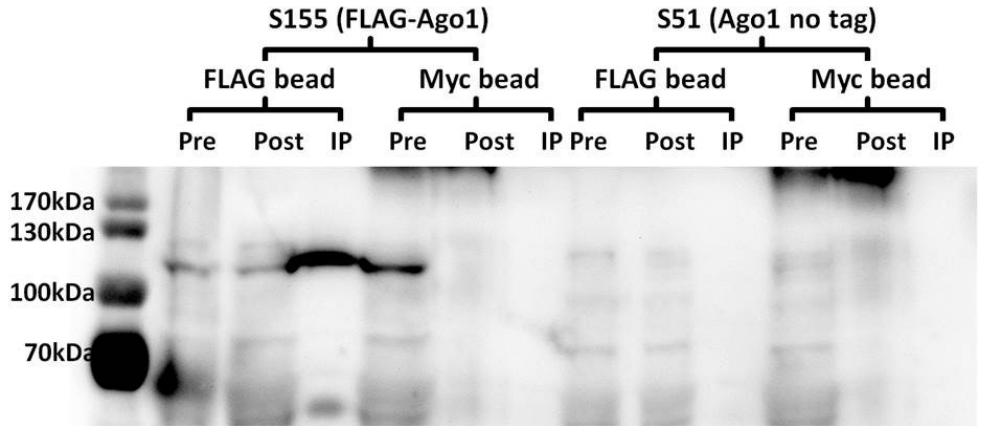

B

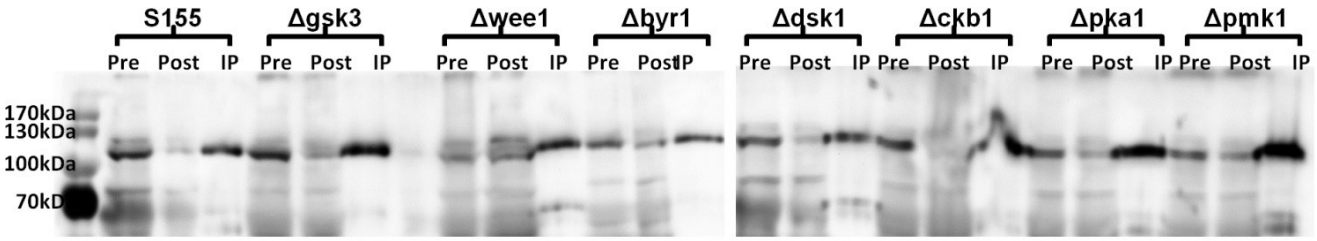

Figure 4.6 Immunoblotting of FLAG-SpAgo1 from immunoprecipitations with anti-FLAG and anti-myc coated beads.

(A) Immunoblot with anti-FLAG antibody probe of FLAG and c-Myc IPs confirmed that FLAG-SpAgo1 was expressed in S155 but not S51 strain.

(B) Immunoblot analyses of SpAgo1 from kinase deletion strains derived from strain S155.

4.2.6. Three kinases are required for PABP release from transcripts bound with RITS complex

In anti-FLAG pull-downs from three kinase deletion strains (Δ*gsk3*, Δ*byr1*, and Δ*dsk1*) containing an integrated FLAG-tagged SpAgo1 cassette, I noticed a protein band (~80 kDa) that was absent in the parental strain S155 and other kinase deletion strains (**Figure 4.7**). This may indicate that certain kinases affect interactions between SpAgo1 and other proteins. Mass spectrometry analysis of the gel slices containing this band identified peptides from poly(A) binding protein (PABP), Hsp90, SpAgo1, and a 51.7 kDa uncharacterized RNA binding protein in samples from Δ*gsk3*, Δ*byr1*, and Δ*dsk1* (**Table 4.7**). In contrast, only SpAgo1 peptides were detected in gel slices cut from the same position in lanes containing immunoprecipitates from the parental strain S155. No peptides were detected in gel slices at the same size range in the S51 strain (which expresses untagged endogenous SpAgo1). The presence of Hsp90 and SpAgo1 peptides in Δ*gsk3*, Δ*byr1*, and Δ*dsk1* strains most likely reflect degradation products since both proteins were abundant in the ~100 kDa band. Therefore, PABP, which has a predicted molecular mass of 71.5 kDa, is most likely the novel protein that co-immunoprecipitates with SpAgo1 from Δ*gsk3*, Δ*byr1*, and Δ*dsk1* strains.

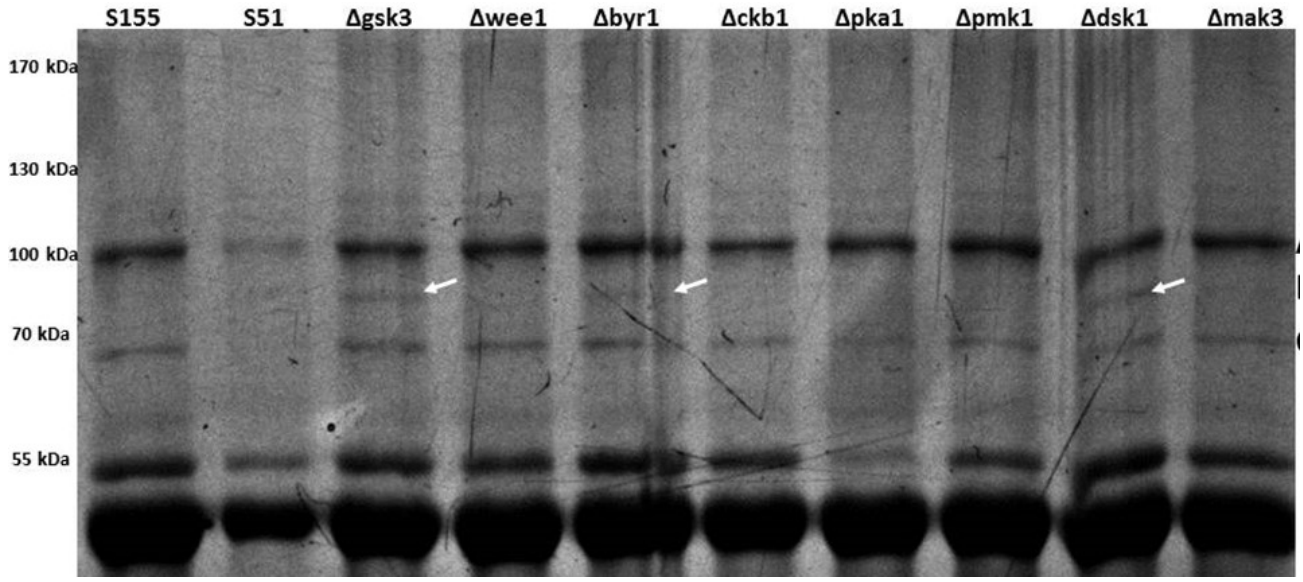

Figure 4.7 Coomassie Brilliant Blue staining of FLAG immunoprecipitates from kinase deletion and control strains. FLAG immunoprecipitates were eluted from the anti-FLAG beads, separated on SDS-PAGE gels, and then stained with Coomassie Brilliant Blue G-250. Protein bands enriched in three of the kinase deletion strains are marked by white arrows.

Table 4.6 Mass Spectrometry identified that PABP co-immunoprecipitates with SpAgo1 in three kinase deletion strains

Strains	Accession	Description	Score	Coverage %	Unique Peptides	MW [kDa]
S155						
	O74957	*ago1*, Protein Argonaute [AGO1_SCHPO]	9.39	3.60	3	94.4
Δ*gsk3*						
	O74957	*ago1*, Protein Argonaute [AGO1_SCHPO]	59.36	26.03	17	71.5
	P41887	*swo1*, Heat shock protein 90 [HSP90_SCHPO]	13.06	7.10	4	80.5
	O60176	SPBC23E6.01c, Uncharacterized RNA-binding protein [YG41_SCHPO]	4.32	4.19	2	51.7
	P31209	***pab1*, Polyadenylate-binding protein**, cytoplasmic and nuclear [PABP_SCHPO]	8.84	8.88	3	71.5
Δ*byr1*						
	O60176	SPBC23E6.01c, Uncharacterized RNA-binding protein [YG41_SCHPO]	14.91	10.99	4	51.7
	P31209	***pab1*, Polyadenylate-binding protein**, cytoplasmic and nuclear [PABP_SCHPO]	12.31	7.50	5	71.5
	P41887	*swo1*, Heat shock protein 90 [HSP90_SCHPO]	10.85	6.53	4	80.5
	O74957	*ago1*, Protein Argonaute [AGO1_SCHPO]	3.87	2.28	2	94.4
Δ*dsk1*						
	P31209	***pab1*, Polyadenylate-binding protein**, cytoplasmic and nuclear [PABP_SCHPO]	91.39	36.75	19	71.5
	O60176	SPBC23E6.01c, Uncharacterized RNA-binding protein [YG41_SCHPO]	8.03	10.78	3	51.7
	P41887	*swo1*, Heat shock protein 90 [HSP90_SCHPO]	7.47	5.54	3	80.5

Since PABP binds to RNAs, I investigated whether the retention of PABP could lead to more RNA transcripts, especially pericentromeric RNAs, associated with SpAgo1. Total RNA co-immunoprecipitated with FLAG-SpAgo1 was eluted from the beads, treated with DNase, and reverse transcribed into cDNA which was then used as templates to measure the relative abundance of pericentromeric and actin transcripts by qRT-PCR as described above.

The least amount of actin and pericentromeric RNA was observed in the immunoprecipitates from strain S51 (**Figure 4.8**). This was to be expected since the strain expresses only endogenous non-tagged SpAgo1 which should not be pulled down with anti-FLAG. In strain S155, the anti-FLAG immunoprecipitates contained slightly more actin mRNA and 10-100 fold more pericentromeric RNA (**Figure 4.8**). This was not unexpected either since SpAgo1 is known to bind to pericentromeric RNAs. The small amount of actin mRNA is likely due to non-specific interaction with SpAgo1, which after all is an RNA-binding protein. Among the immunoprecipitates from the six kinase deletion strains, all showed increased levels of pericentromeric and actin transcripts associated with anti-FLAG beads. However, Δ*gsk3*, Δ*byr1*, and Δ*dsk1*, in which PABP was retained with SpAgo1, showed significantly more RNA binding than kinase deletion strains Δ*wee1*, Δ*pka1*, and Δ*ckb1* in which PABP was not detected in the anti-FLAG immunoprecipitations (**Figure 4.8**).

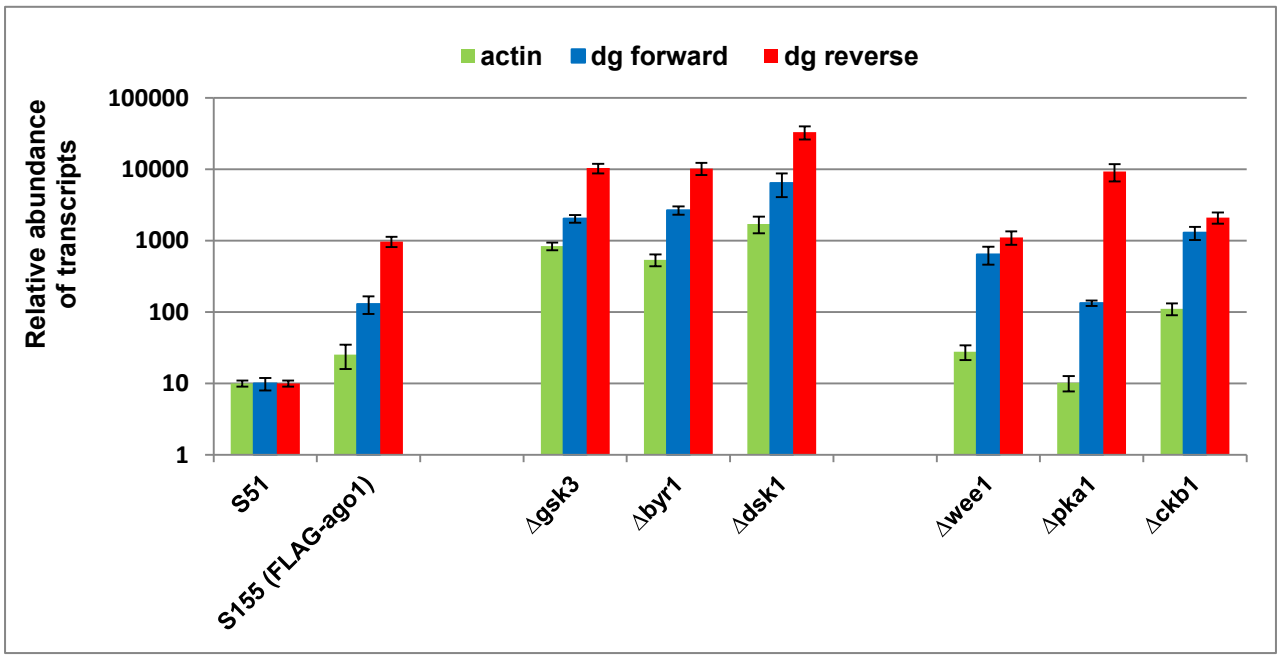

Figure 4.8 Loss of *gsk3*, *byr1*, or *dsk1* results in increased association of SpAgo1 with RNA. FLAG-SpAgo1 was immunoprecipitated from yeast strains and the associated RNAs were eluted from the anti-FLAG beads. Pericentromeric dg forward and reverse RNA transcripts and actin mRNA in the positive control S155 (3xFLAG-SpAgo1) and its kinase deletion derivatives were quantitated and normalized according to the negative control S51 strain (endogenous SpAgo1). PABP co-immunoprecipitated with FLAG-SpAgo1 from Δ*gsk3*, Δ*byr1*, and Δ*dsk1* strains. This was not observed when Δ*wee1*, Δ*pka1*, and Δ*ckb1* were used. The y axis indicates relative abundance of pericentromeric transcripts in log10 scale, the error bar represents standard error of the mean (SEM).

4.2.7. Pka1 is essential for the biogenesis or stability of the RITS component Chp1.

In addition to SpAgo1, the RITS complex in *S. pombe* is composed of the chromodomain protein Chp1 which binds methylated histone H3, and the adaptor protein Tas3 which links SpAgo1 to Chp1 (Verdel et al. 2004; Petrie et al. 2005). Given the importance of the RITS complex in transcriptional gene-silencing, I investigated whether the de-repression of pericentromeric transcription in the kinase deletion strains was due to changes in this complex. At the time of analyses, antibodies were only available for Chp1 (to our knowledge at least). Therefore, I probed FLAG-SpAgo1 immunoprecipitates from selected kinase deletion strains and their parental strain S155 with an antibody against Chp1.

Chp1 was co-immunoprecipitated with FLAG-SpAgo1 in all of the kinase deletion strains examined except Δ*pka1* (**Figure 4.9A**). Data in Figure 4.9B show that the efficiency of FLAG-SpAgo1 pulldowns were comparable between strains. These data suggest that the Pka1 kinase may be required for Chp1 interaction with SpAgo1 via Tas3, or involved in the biogenesis or stability of Chp1. Subsequently, immunoblotting of total cell lysates using an antibody against Chp1 revealed that Δ*pka1* contains significantly less Chp1 compared to the parental strain and other kinase deletion strains (**Figure 4.9A**). This indicates that Pka1 is required for the biogenesis and/or stability of Chp1 rather than its interaction with other RITS components. However, further research is needed to elucidate how this kinase regulates Chp1 stability.

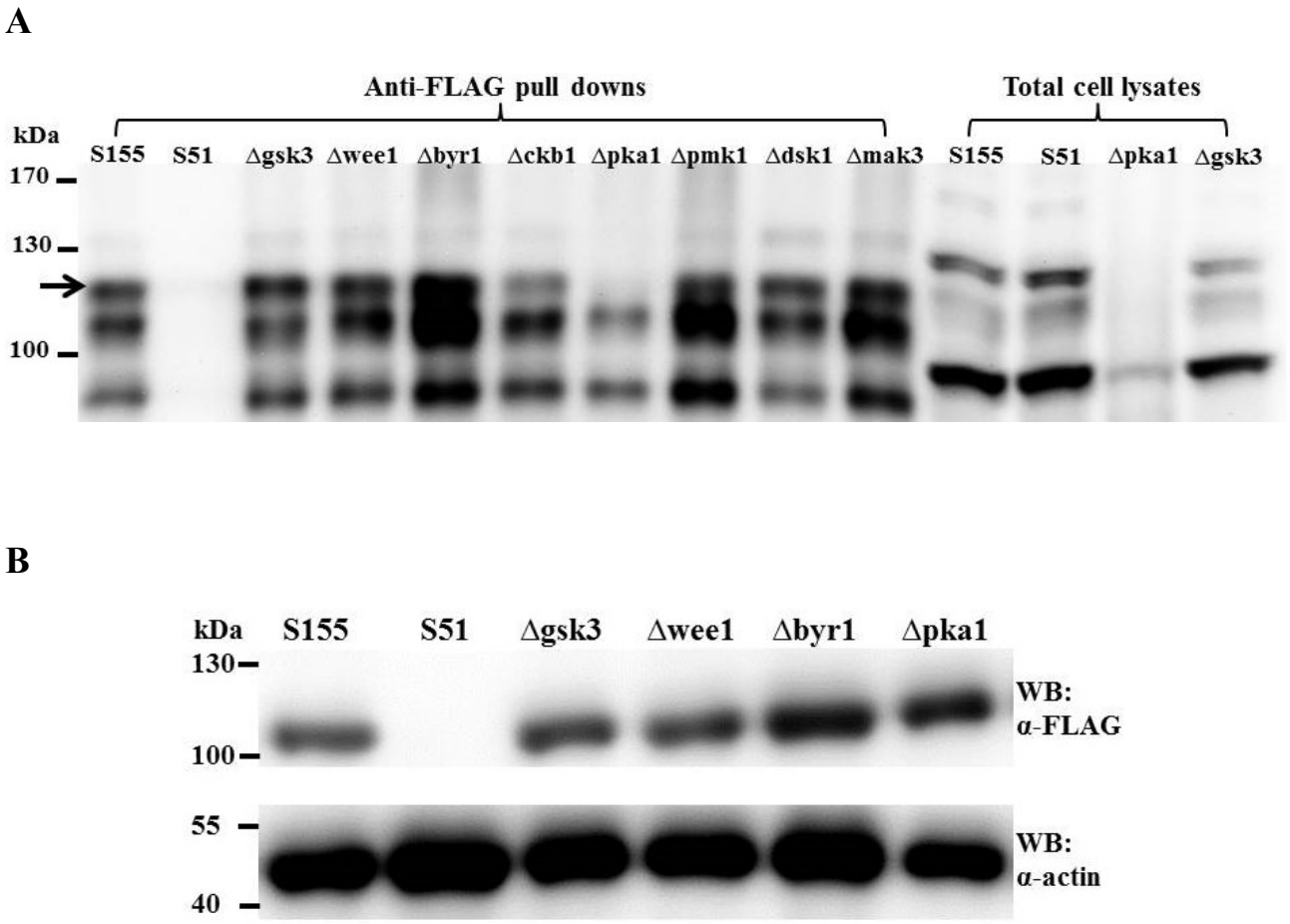

Figure 4.9 Anti-FLAG immunoprecipitations and total cell lysates probed with anti-Chp1.
(A) Anti-FLAG immunoprecipitates or total cell lysates were probed with anti-Chp1 to examine the potential co-immunoprecipitation of Chp1 with FLAG-SpAgo1. The observed band size of Chp1 is at 109 kDa (marked by the black arrow), and an additional band is at 102 kDa (possible degradation product). Antibody datasheet is at http://www.abcam.com/chp1-antibody-chip-grade-ab18191.html
(B) The immunoprecipitated proteins were also probed with antibodies against FLAG and actin (loading control).

4.3. Summary

In this chapter, I identified a number of protein kinases that are required for RNAi-mediated pericentromeric silencing in *S. pombe*. Subsequent complementation assays showed these kinases are *bona fide* regulators of heterochromatin assembly at centromeres. However, their expression levels need to be precisely regulated to properly exert functions. Conversely, none of the phosphatase deletions strains used in my study showed any defects in RNAi-mediated pericentromeric silencing.

Use of predictive algorithms suggests that the phosphorylation status of SpAgo1 at multiple sites is affected by multiple protein kinases and phosphatases. Four kinases (Gsk3, Byr1, Ckb1, and Pka1) that were identified as being important for RNAi in *S. pombe* were among the predicted kinases. However, my attempts to further determine if any of these kinases catalyze specific phosphorylation events in SpAgo1 were non-informative mainly due to technical issues/limitations.

A number of the kinases that regulate RNAi may regulate association of PABP with SpAgo1. Moreover, the kinase Pka1 was found to be essential for the biogenesis or stability of Chp1, a critical component of the RITS complex. This suggests that some of the kinases that are required for RNAi-mediated heterochromatin silencing act by regulating SpAgo1 interactions with other proteins.

Chapter 5

Discussion

5.1. Overview

RNAi is a "master regulator" of gene expression in eukaryotes that is crucial for a variety of important biological processes. However, the current understanding of regulatory mechanisms that control RNAi is limited compared to the large body of knowledge regarding biogenesis of small RNAs and essential RNAi components, the mechanism of RNAi, and pharmaceutical applications (Friedman et al. 2009; Bartel 2009). In my studies, mechanisms that regulate the structure and function of core RNAi components were characterized using the budding yeast *S. cerevisiae* and the fission yeast *S. pombe* as experimental organisms.

My research showed that introduction of ScaDcr1 and ScaAgo1 (or hAgo2), but not human RISC components (hAgo2, hDcr, and TRBP2), established a functional RNAi system in RNAi-deficient *S. cerevisiae*. One explanation is that hDcr, which recognizes the 2 nt overhangs of dsRNA molecules, was unable to recognize and/or cleave the dsRNA substrates used in my studies that have long (>150 nt) ssRNA tails. In contrast, adjacent homodimers of the non-canonical ScaDcr1 cooperatively cleave dsRNA substrates from the interior. Therefore, ScaDcr1 catalyzed cleavage is not restricted by the end structure of dsRNAs. My studies further revealed that hDcr forms a stable complex with hAgo2 but not with ScaAgo1. Moreover, this interaction was stimulated by the induction of the dsRNA silencing constructs and but independent of the dicer cofactor TRBP2. This suggests that the process of dsRNA precursors and/or interaction between hDcr and dsRNA induces complex formation with hAgo2. In contrast, ScaDcr1 does not form stable complexes with either ScaAgo1 or hAgo2 in *S. cerevisiae* though RNAi-mediated reporter gene silencing was restored. I hypothesized that ScaDcr1 slowly releases processed dsRNAs to minimize their exposure to other nucleases before transferring to Argonaute proteins. The above findings suggest that RNAi

machineries in distinct phyla of eukaryotes are conserved in function but divergent in mechanisms. My studies also showed that RNAi-mediated reporter gene silencing is dependent on the ATPase activity of Hsp90, most likely to facilitate conformational changes in Argonaute to accommodate dsRNA. Therefore, the regulation of RNAi pathways by Hsp90 is an evolutionarily conserved process in eukaryotes from budding yeast to mammals.

Sequence alignments of hAgo2 and SpAgo1 with respect to known phosphorylated amino acid residues on the former suggest that the majority of these sites are positionally conserved. The comprehensive screening of kinase deletion strains identified a group of kinases that are required for RNAi-mediated pericentromeric silencing. While my studies did not produce conclusive evidence that SpAgo1 is a *bona fide* phosphoprotein, several kinases were showed to be required for the biogenesis of Chp1 or for RNA binding specificity of *S. pombe* Ago1.

In summary, regulatory mechanisms that control RNAi activity were investigated in two experimental organisms. My results indicate that RNAi, as a master regulator of gene expression, is subject to intricate and extensive regulation on its core components, especially Argonaute proteins.

5.2. Why is human RISC unable to reconstitute RNAi in *S. cerevisiae*?

Unlike introduction of ScaDcr1 and ScaAgo1 (or hAgo2) restored RNAi pathway in the RNAi-deficient experimental organism *S. cerevisiae*, my studies showed that the transformation of hDcr and hAgo2, with or without hDcr cofactor TRBP2, was unable to reconstitute RNAi in *S. cerevisiae*. This finding contradicts with another report that hAgo2, hDcr and TRBP2 can functionally reconstitute RNAi in *S. cerevisiae* (Suk et al. 2011). The apparent discrepancy between my data and those of Suk et al may be explained by the difference in the silencing constructs

employed. In my experiments, *GFP* or *URA3* silencing constructs that produce dsRNA transcripts with long (>150 nt) terminal ssRNA overhangs (**Figure 3.1A-C**) were used. In contrast, the silencing construct against *GFP* employed by Suk and colleagues produced single-stranded antisense transcripts that formed dsRNA substrates by annealing to *GFP* mRNA (**Figure 3.1D**). It is quite likely that this hybridization process itself between antisense *GFP* and *GFP* mRNA reduced *GFP* abundance by blocking translation of the mRNA. Therefore, it is not clear whether the reduction of *GFP* fluorescence observed by Suk and colleagues was in fact the result of *bona fide* RNAi-mediated silencing or antisense-based silencing.

At least two possibilities could explain why human RISC is unable to restore RNAi in *S. cerevisiae*: 1. hDcr cannot recognize and/or cleave the transcripts of the silencing constructs; 2. hDcr cleaved small RNA duplexes cannot be transferred to hAgo2. Previous studies and my own research support the first hypothesis more than the second. First, it has been reported that human RISC assembles spontaneously *in vitro*, and the complex can process dsRNA, perform guide-strand selection, and hAgo2 loading (MacRae et al. 2008). However, it is unknown whether human RISC is able to conduct these activities independent of other cofactors or chaperones *in vivo*. As we know Hsp90 is required for small RNA loading onto Argonaute (Miyoshi et al. 2010; Iwasaki et al. 2010). Second, my studies showed that hAgo2 and ScaDcr1 effectively restored RNAi-mediated gene silencing in *S. cerevisiae*, which indicates that the function of hAgo2 in RNAi is largely preserved when expressed in *S. cerevisiae*.

The differences between canonical (*e.g*. hDcr) and non-canonical (*e.g*. ScaDcr1) Dicer proteins with respect to domain architectures and RNA cleavage mechanisms could account for the inability of hDcr to recognize and cleave the dsRNA substrates in *S. cerevisiae*. The PAZ domain of hDcr

recognizes the 2 nt of 3' overhang of Drosha-processed dsRNAs in the cytoplasm, and the distance between the PAZ and RNase III domains as a molecular ruler to determine the length of cleaved dsRNA substrates (Zhang et al. 2004; MacRea et al. 2006; Park et al. 2011). Therefore, canonical Dicers are better suited for cleavage of miRNAs and *trans*-acting siRNAs with short and defined terminal structures (Vaucheret 2006). Conversely, multiple homodimers of ScaDcr1 cooperatively bind on dsRNA substrates, and the distance between the catalytic centres of adjacent homodimers determines the length of the dsRNA cleavage products (Weinberg et al. 2011). Therefore, non-canonical fungal Dicers, which cleavage from the interior and then work outward, are more suitable to process dsRNA substrates with protected termini or long single-stranded extensions, as long as the dsRNA region can accommodate multiple homerdimer binding. Moreover, a recent study of Dicer in another budding yeast species *C. albicans* (CaDcr1) indicates that the terminus-independent cleavage activity of this enzyme may allow it to function in ribosomal RNA processing and RNA splicing (Bernstein et al. 2012).

The transcripts of the silencing constructs employed in my studies have long ssRNA segments (>50 nt) extending from dsRNA region. Therefore, these dsRNA substrates can be processed by ScaDcr1 from the interior, but not by hDcr which recognize 2 nt terminal overhangs (**Figure 5.1**). The intrinsic differences of dsRNA substrates recognition by canonical and non-canonical Dicer proteins have significant implications for RNAi systems in mammalians and fungi.

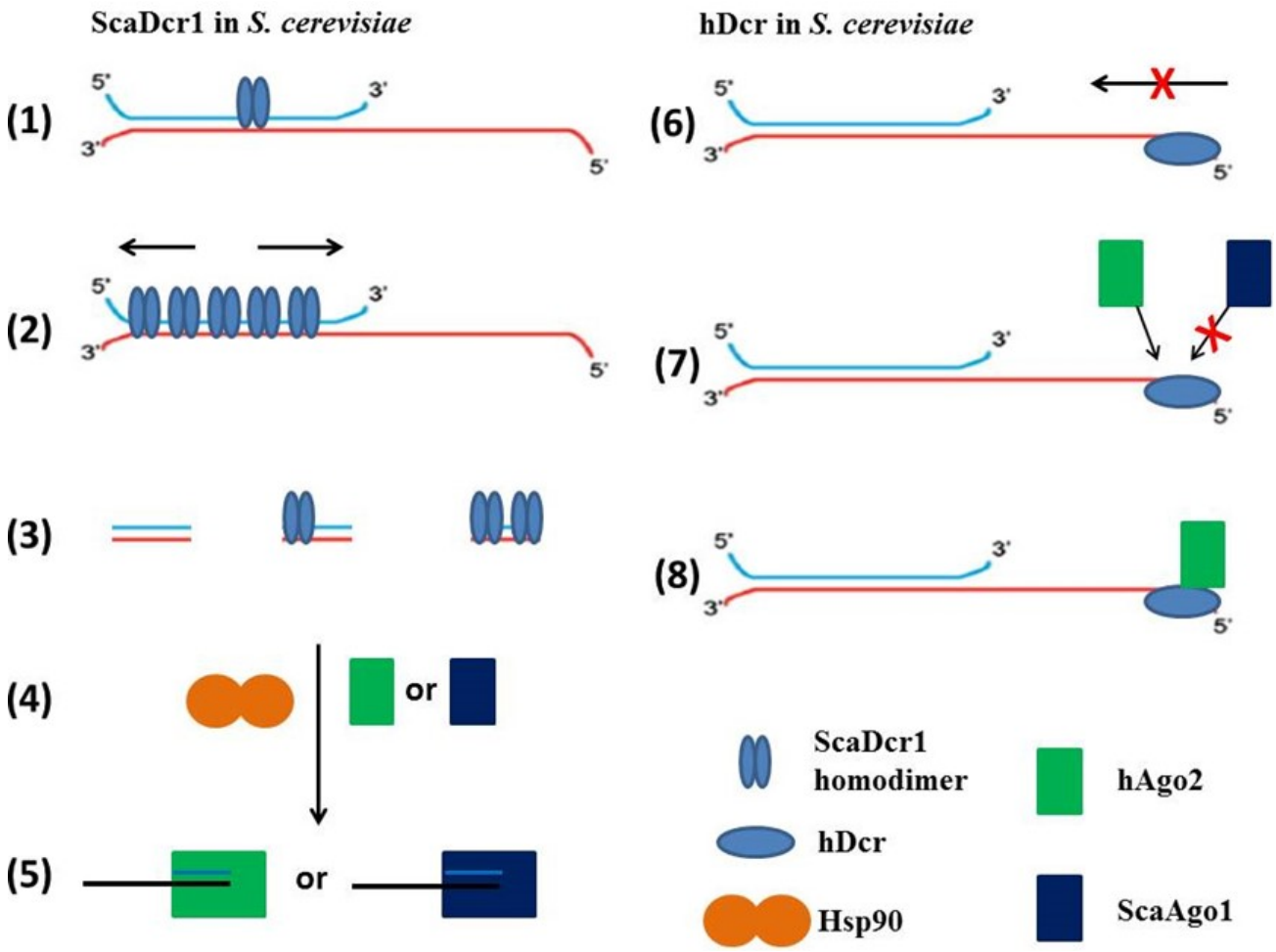

Figure 5.1 Models of *S. castellii* and human RNAi systems in *S. cerevisiae*.

ScaDcr1 in *S. cerevisiae*: (1) Homodimer of ScaDcr1 binds from the interior of dsRNA substrates with long ssRNA overhangs. This binding may or may not be dependent on specific sequences or structures.

(2) Initial binding of ScaDcr1 may guide and facilitate subsequent binding. The slow-release model allows the binding of homodimers to spread at both directions before RNA cleavage.

(3) Small RNA could either directly cut-and-released in the nucleus, or retained by one or two ScaDcr1 homodimers to facilitate loading onto Argonaute.

(4) The ATPase activity of Hsp90 facilitates structural rearrangements of ScaAgo1 or hAgo2 to accommodate small RNA loading. It is possible that other proteins are required for small RNA transfer from ScaDcr1 to Argonaute proteins.

(5) Small RNA bound ScaAgo1 or hAgo2 undergo strand separation and silence mRNA targets with complementary sequence.

hDcr in *S. cerevisiae*: (6) hDcr interacts with the long ssRNA overhang of dsRNA substrates. However, it is unable to trigger dsRNA cleavage.

(7) hAgo2 but not ScaAgo1 can be recruited in close proximity to hDcr. This process is independent of hDcr co-factor TRBP2.

(8) Human RISC cannot activate RNA cleavage, and thus is unable to trigger target gene silencing.

5.3. RNAi pathways are conserved in function and divergent in mechanisms in eukaryotes

My studies showed that hDcr formed a stable complex with hAgo2 but not with ScaAgo1 in *S. cerevisiae.* Moreover, this interaction was stimulated by the induction of dsRNA substrates, but it is independent of the expression of hDcr cofactor TRBP2. It is unknown how the induction of dsRNA substrates promotes hDcr to interact with hAgo2. The above finding suggests: 1. hDcr directly or indirectly interact with but cannot cleave dsRNA substrates, which brings hAgo2 into proximity; 2. TRBP2 is not required for hDcr-hAgo2 interaction but can function as a bridge to strengthen the link and facilitate the transfer of dsRNA between them; 3. hDcr interacts with hAgo2 but not ScaAgo1 suggesting the interaction between core RNAi components is species specific. A former student from our laboratory showed that the PIWI-box, a subregion of the PIWI domain in hAgo2, binds directly to the RNase III domain of hDcr (Tahbaz et al. 2004). However, important questions remain for what occurs in budding yeast. For example, does hDcr directly associate with the dsRNA substrates, or indirectly via another protein factor? If the interaction is direct, where does hDcr bind on dsRNA substrates with long ssRNA termini? If the binding is indirect, what protein factor(s) is required?

Stable interaction between ScaDcr1 and ScaAgo1 (or hAgo2) was not detected, even though RNAi-induced gene silencing was observed (**Figure 5.1**). Two hypotheses could explain this unexpected result: 1. ScaDcr1 transiently or weakly interacts with ScaAgo1 (or hAgo2) to swiftly transfer RNA duplexes to these proteins. This interaction is below the detection threshold of immunoprecipitation and thus the negative result; 2. ScaDcr1 simply cleaves and releases the dsRNA substrates, which are then recognized by and incorporated into ScaAgo1 or hAgo2. However, this cut-and-release model is hard to explain in light of the fact that the reconstituted RNAi system is highly efficient. Under non-inducing conditions, the "leaky" transcription of the strongSC-*GFP* silencing construct was able to silence *GFP* expression to basal levels in *S. cerevisiae*. Therefore, it

is more likely that ScaDcr1-cleaved RNA duplexes are actively transferred to Argonaute proteins via transient and/or indirect interactions. Therefore, I proposed a slow-release model for ScaDcr1 that enables cooperative binding of homodimers adjacent to the initially binding before its disassociation from the dsRNA template. Slow release of the RNA duplexes may protect dsRNA substrates from nucleolytic cleavage, and may even facilitate small RNA loading onto Argonaute similar to what was reported for canonical Dicers (Lee et al. 2004; Wang et al. 2009a). To conclude, RNAi systems in distinct phyla of eukaryotes are conserved in silencing gene expression but differ mechanistically.

5.4. Non-canonical Dicers in fungi may function independently of co-factor(s)

Although the introduction of ScaDcr1 and ScaAgo1 (or hAgo2) was sufficient to reconstitute RNAi in *S. cerevisiae*, I questioned whether any endogenous factor(s) may also be required. Since *S. cerevisiae* and *S. castellii* are closely related, ScaDcr1 may be able to function in concert with endogenous factor(s) that are crucial for RNAi. Most known Dicer co-factors contain multiple dsRBD. (*e.g.* TRBP2 and PACT in mammals (Duarte et al. 2000; Daher et al. 2001); R2D2 and Loq1 in *Drosophila* (Meister et al. 2004; Leuschner et al. 2005)).

Unexpectedly, the deletion strains of genes encoding dsRBPs (*RNT1*, *LRP1*, *MRPL3*, and *TIF11*) revealed that none of these proteins were required for reporter gene silencing. It is worth mentioning that I did not screen all the genes encoding dsRBPs in *S. cerevisiaeiae*. Therefore, it cannot be ruled out that ScaDcr1 has one or more cofactors that are crucial for its function in RNAi. It is also possible that ScaDcr1 exerts its function in dsRNA cleavage independent of any cofactors. Indeed, a homodimer of ScaDcr1 has four dsRBDs, which is equivalent to the number of dsRBDs in hDcr1 and TRBP2 together. Accordingly, the homodimer of ScaDcr1 may bind dsRNA substrates strong

enough all by itself. Furthermore, Rnt1, the only other known RNase III ribonuclease in *S. cerevisiae*, has one dsRBD (Elela et al. 1996). Rnt1 is involved in rDNA transcription, rRNA processing, and U2 snRNA 3' end formation, but is unable to cleave dsRNA substrates (Elela et al. 1996; Catala et al. 2008). This may indicate that the number of dsRBDs in non-canonical Dicers in fungi is crucial for its function in RNAi.

5.5. Regulation of RNAi by Hsp90 is an evolutionarily conserved process in eukaryotes

My studies provided experimental evidence that reconstituted RNAi pathways in *S. cerevisiae* are dependent on the ATPase activity of Hsp90. However, which component in the RNAi systems is the client protein of Hsp90 has not been elucidated.

A growing body of evidence suggests that structural rearrangements must occur in Argonaute proteins to accommodate the loading of RNA duplexes and in *Drosophila* at least, the Hsp90 chaperone machinery is required for this process (Iwasaki et al. 2010, 2015; Miyoshi et al. 2010; Izumi et al. 2013). Since Hsp90 and Argonaute proteins are both highly conserved across eukaryotic phyla, I hypothesized that Hsp90 regulates RNAi by mediating a conformational change of ScaAgo1 or hAgo2 in *S. cerevisiae* to facilitate dsRNA loading.

Although it cannot be ruled out that Hsp90 regulates ScaDcr1 in *S. cerevisiae*, this seems unlikely in light of previous studies. First, inhibition of Hsp90 ATPase activity does not affect Dicer binding to or processing of dsRNA substrates in *Drosophila* cells (Miyoshi et al. 2010). Conversely, Argonaute association with Dicer processed-RNA duplexes is dramatically impaired by Hsp90 inhibitors (Iwasaki et al. 2010; Miyoshi et al. 2010). Second, the rapid and reversible conformational rearrangements, which are hallmarks of Hsp90 client proteins, have been observed in Argonautes but

not in Dicer proteins (Wang et al. 2008; Johnston et al. 2010).

Bcr–Abl, a well characterized Hsp90 client, is a cytoplasmic tyrosine kinase that induces cell proliferation in the absence of cytokines (Taipale et al. 2012). This kinase is structurally dynamic and requires Hsp90 for stability before its activation. Similarly, human Argonaute proteins are thought to be less stable and more conformationally dynamic when they are not bound to small RNA. Conversely, they become protease-resistant upon miRNA binding (Elkyam et al. 2012). I propose that Hsp90 stabilizes unloaded ScaAgo1 (and hAgo2) as well as facilitates conformational rearrangements required for RNA duplex loading in budding yeast similar to what occurs in mammals and other higher eukaryotes.

5.6. Is SpAgo1 a phosphoprotein?

The majority of phosphorylation sites on hAgo2 are conserved among a wide range of Argonaute proteins from different phyla in eukaryotes including fission yeast *S. pombe*. At least four out of the seven reported phospho-amino acid residues in hAgo2 are conserved in SpAgo1. Specifically, S288, Y371, Y513, and S779 in SpAgo1 correspond to T307, Y393, Y529, and S798 respectively in hAgo2 (**Figure 1.6B**). Moreover, two recent publications showed that the crystal structures of Argonaute proteins from human and distantly related budding yeast *K. polysporus* are very similar. Both proteins adopt a bi-lobed shape with an internal cleft for dsRNA binding, and each domain binds to dsRNA in a conserved manner (Elkayam et al. 2012; Nakanishi et al. 2012; Schirle and MacRae 2012). Therefore, it is likely that the amino acid residues in SpAgo1 correspond to hAgo2 phosphorylation sites play important role in RNAi pathways.

Tyrosine Y529 of hAgo2 forms a RNA binding pocket with K533, N545, and K566 (Schirle and

MacRae 2012). A phosphomimetic mutant in which a glutamic acid substituted for tyrosine 529 (Y529E) exhibits reduced small RNA binding and target gene silencing (Rüdel et al. 2011). One explanation is that Y529 phosphorylation produces a negative charge that repels negatively charged small RNA duplexes. Bioinformatics algorithms predict that Y529 may be a substrate for Src or JAK2 kinases and SHP1 phosphatase. However, as yet, there is no experimental evidence to support these predictions. An unresolved issue about Argonaute phosphorylation is the localization of Y529, which lies deep in the RNA binding pocket and is presumably not readily accessible to kinases. This residue is conserved in every examined Argonaute protein which suggest it plays an important role in Argonaute function. It is possible and quite likely that Argonaute proteins undergo structural rearrangements to temporarily expose Y529 to kinases. The analogous residue in SpAgo1 is Y513,which, if phosphorylated, would be expected to inhibit RNAi.

Phosphorylation of Y393 in hAgo2 reduces the binding of hDcr and inhibits miRNA maturation. Epidermal growth factor receptor (EGFR) phosphorylates this residue in response to hypoxic stress (Shen et al. 2013), and protein tyrosine phosphatase 1B (PTP1B) catalyzes the dephosphorylation (Yang et al. 2014). However, EGFR has no homolog in yeast *S. pombe*, and the deletion of the tyrosine phosphatases Pyp1 and Pyp2 had no detectable effect on pericentromeric silencing. Therefore, it is uncertain whether phosphorylation on Y371 in SpAgo1 plays any role in RNAi activity in fission yeast.

Another graduate student in our laboratory reported that substitution of serine 798 for aspartic acid (S798D) blocks hAgo2 targeting to P-bodies and stress granules (Lopez-Orozco et al. 2015). However, RNAi–mediated gene silencing was only modestly affected, indicating that hAgo2 localization to P-bodies and stress granules is separable from its role in RNAi (Lopez-Orozco et al.

2015). RNAi-mediated gene silencing in *S. pombe* appears to be confined mainly to the nucleus and it is unclear if *bona fide* RNAi occurs in the cytoplasm. Although a pool of SpAgo1 localizes to P-body-like structures in the cytoplasm of fission yeast (Carmichael et al, 2006), the significance of this is not clear. As such, I could not conclude whether phosphorylation of S779 in SpAgo1 has a similar effect on Argonaute localization and/or function.

It is worth mentioning that all hAgo2 phosphorylation events that have been studied in detail, result in reduced RNAi activity. Phosphorylation of Y529 prevents small RNA loading, phosphorylation of Y393 inhibits hDcr binding and miRNA maturation, and phosphorylation of S798 blocks hAgo2 localization to P-bodies and stress granules. Therefore, deletion of the culprit kinase genes would be expected to lead to more robust RNAi activity. A genome-wide screen of kinases that regulate hAgo2 function revealed kinases that negatively affect RNAi as well as others that stimulate RNAi (J. Lopez-Orozco, in preparation). Conversely, my studies identified 13 kinase genes that are required for pericentromeric silencing, a process that is dependent on RNAi activity. Therefore, it is unlikely that any of the kinases identified in my studies catalyze a phosphorylation that plays a similar role in *S. pombe* as phosphorylation of Y393, Y529, and S798 in hAgo2. My screen did not identify any kinases that significantly inhibit RNAi. This could be due to the fact that levels of pericentromeric transcripts are normally very low and therefore, further reduction of pericentromeric transcripts may not be clearly revealed.

5.7. Kinases regulate pericentromeric silencing in RNAi-dependent and RNAi-independent mechanisms

None of the phosphatase genes assayed in my screen had any effect on RNAi, unlike a parallel

screen in mammalian cells (J. Lopez-Orozco, in preparation). Possible explanations include: 1. My screen was limited to the availability of commercially non-essential phosphatase deletion strains; 2. If multiple phosphatases catalyze a single dephosphorylation on an RNAi core component, the phenotype of a single phosphatase gene deletion could be masked.

The kinases identified in my screen could regulate pericentromeric silencing in two major ways: 1. By catalyzing phosphorylation of core RNAi components (Ago1, Dcr1, and Rdp1) or their essential binding partners (*e.g.* Tas3 and Chp1 for Ago1, Hrr1 and Cid12 for Rdp1); 2. By phosphorylation of non-RNAi protein factors that are essential for pericentromeric silencing.

Wee1 is the only tyrosine kinase identified in my studies that is required for pericentromeric silencing in *S. pombe*. Phylogenetic analysis revealed that there are many fewer protein tyrosine kinases in fission yeast compared to mammals (Hunter and Cooper 1985; Hunter 1995; Hanks et al. 1995). I hypothesized that Wee1 may regulate pericentromeric silencing by at least two different mechanisms: 1. Wee1 and Cdc25 phosphatase play antagonistic roles in regulating Cdc2, which lies at the heart of the eukaryotic cell cycle (Raleigh et al. 2000; Elder et al. 2001). In this scenario, Wee1 regulates pericentromeric silencing, a cell cycle dependent process, via Cdc2 and other cell cycle proteins; 2. Wee1 regulates pericentromeric silencing via Hsp90 and a subgroup of client proteins that may include SpAgo1 (Mollapour et al. 2010).

Byr1 and Pmk1 are two mitogen-activated protein (MAP) kinases. MAP kinases regulate a diverse array of cell functions including gene expression, mitosis, proliferation, differentiation, and apoptosis (Pearson et al. 2001; Ligterink and Hirt 2001). Adams et al reported that hAgo2 expression is regulated by EGFR and MAP kinase signalling (Adams et al. 2009). Moreover, phosphorylation of serine 387 on hAgo2 is blocked by a p38 MAP kinase inhibitor (Zeng et al. 2008). Although SpAgo1

does not appear to have a corresponding “serine 387”, it cannot be ruled out at this point that SpAgo1 is phosphorylated by MAPK-mediated pathways.

Finally, I found that Pka1, a cAMP-dependent protein kinase, is required for biosynthesis and/or stability of the essential RITS components Chp1. This chromodomain-containing protein interacts with Ago1 through Tas3 as a bridge (Sadaie et al. 2004; Martienssen et al. 2005; Schalch et al. 2011). Potentially, Pka1-mediated phosphorylation of Chp1 protects the protein from degradation via the proteasome. Whether Pka1 phosphorylation plays any other roles in RNAi remains to be determined. Further studies on Pka1 and other kinases identified in my screen could help us better understand regulation of RNAi pathways across eukaryotic phyla.

5.8. RNA binding specificity of *S. pombe* Ago1is dependent on multipke kinases

Deletion strains of three kinase genes, *gsk3*, *bry1*, and *dsk1*, led to strong association of PABP with SpAgo1, an effect that was not observed in other kinase deletion or parental strains. Furthermore, there were significantly more pericentromeric transcripts and actin mRNAs bound to SpAgo1 in *gsk3*, *bry1*, and *dsk1* deletion strains. This suggests that SpAgo1 non-selectively binds RNAs in the absence of certain kinases. In order to have selective RNA silencing, Argonaute proteins need to be able to discern between Dicer processed dsRNAs and other RNA transcripts.

Gsk3 is the most studied kinase in this group. It is a ubiquitous kinase with over 100 known substrates (Beurel et al. 2011; 2015). Moreover, it has been reported that Gsk3 phosphorylates Drosha at Serine 300 and 302 in human cells, a reaction that is necessary for the localization of Drosha to the nucleus (Tang et al. 2010; 2011). However, both SpDcr1 and SpAgo1 lack the canonical Gsk3 phosphorylation motif Ser-Pro-Ser-Leu-Glu-Arg-Ser (SPSLERS) that is present in

human Drosha (Tang et al. 2011). Of note, deletion of *gsk3* led to the largest increase in pericentromeric transcripts among the kinase mutants screened. Therefore, it is clear that the phosphorylation catalyzed by Gsk3 is crucial for pericentromeric silencing.

5.9. Future directions

To further investigate why hDcr was unable to support RNAi in *S. cerevisiae*, multiple dsRNA substrates with different terminal structures should be employed to test the hypothesis that hDcr cannot recognize and/or cleave dsRNA substrates used in my studies. The finding that ScaDcr1 can work with hAgo2 to support RNAi means that *S. cerevisiae* can be employed to further examine the structure, function, and post-translational modifications on hAgo2. A series phosphomimetic and non-phosphomimetic mutant of hAgo2 can be generated and to test the influence of specific phosphorylation on hAgo2 function.

Co-immunoprecipitation of transformed ScaAgo1 or hAgo2 with endogenous Hsp90 in *S. cerevisiae* could provide unequivocal experimental evidence that Hsp90 regulation on RNAi via Argonaute proteins is evolutionary conserved. Furthermore, *S. cerevisiae* could also be utilized as a model system to investigate what Hsp90 co-chaperones are required for modulating structural rearrangements of Argonaute proteins. This will lead to a better understanding of how Hsp90 machinery regulates RNAi pathways in mammalian cells.

There are also several unanswered questions for the non-canonical RNAi pathways discovered in some budding yeast species. For example, how do these Dicers discern between target dsRNA substrates and other transcripts containing dsRNA regions? Does the binding of the first Dicer homodimer depend on specific sequence or on certain structural elements? How does the initial

binding affect subsequent adjacent binding of other homodimers? Is there a minimum number of homodimers needed to activate cooperative cleavage? The study of non-canonical Dicers in fungi may shed light onto how RNAi evolved from an anti-viral mechanism to an omnipresent regulator of gene expression.

Another unanswered question is whether SpAgo1 is a phosphoprotein? If so, what kinases and phosphatases catalyze the reaction? Two dimensional gel electrophoresis and mass spectrometry need to be optimized to comparably study SpAgo1 phosphorylation in wild-type and kinase/phosphatase deletion strains. Furthermore, phosphomimetic and non-phosphomimetic mutants of putative phospho-serine, -threonine, and -tyrosine residues on SpAgo1 can be utilized to examine if the phosphorylation sites are required for RNAi activity. Live-cell imaging of SpAgo1 phosphomutants could also provide information on whether phosphorylation modulates subcellular localization or interaction with RITS essential components Chp1 and Tas3.

REFERENCES:

Abou-Elela, S., and Ares, M. . 1998. Depletion of yeast RNase III blocks correct U2 3' end formation and results in polyadenylated but functional U2 snRNA. EMBO J. **17**(13): 3738-3746

Adams, B., Claffey, K., and White, B. 2009. Argonaute-2 expression is regulated by EGFR/MAPK signaling and correlates with a transformed phenotype in breast cancer cells. Endocrinology **150**(1): 14-23.

Adams, B.D., Claffey, K.P., and White, B.A. 2009. Argonaute-2 expression is regulated by epidermal growth factor receptor and mitogen-activated protein kinase signaling and correlates with a transformed phenotype in breast cancer cells. Endocrinology **150**(1): 14-23.

Ali, M.M., Roe, S.M., Vaughan, C.K., Meyer, P., Panaretou, B., Piper, P.W., Prodromou, C., and Pearl, L.H. 2006. Crystal structure of an Hsp90–nucleotide–p23/Sba1 closed chaperone complex. Nature **440**(7087): 1013-1017.

Aligue, R., Akhavan-Niak, H., and Russell, P. 1994. A role for Hsp90 in cell cycle control: Wee1 tyrosine kinase activity requires interaction with Hsp90. EMBO J. **13**(24): 6099-6106. PMID:7813446.

Allen, E., Xie, Z., Gustafson, A.M., and Carrington, J.C. 2005. microRNA-directed phasing during trans-acting siRNA biogenesis in plants. Cell **121**(2): 207-221.

Ambros, V. 2003. MicroRNA pathways in flies and worms: growth, death, fat, stress, and timing. Cell **113**(6): 673-676.

Anderson, P., and Kedersha, N. 2006. RNA granules. J. Cell Biol. **172**(6): 803-808。

Andrei, M.A., Ingelfinger, D., Heintzmann, R., Achsel, T., Rivera-Pomar, R., and Luhrmann, R. 2005. A role for eIF4E and eIF4E-transporter in targeting mRNPs to mammalian processing bodies. RNA **11**(5): 717-727.

Ard, R., Tong, P., and Allshire, R.C. 2014. Long non-coding RNA-mediated transcriptional interference of a permease gene confers drug tolerance in fission yeast. Nature Communications **27**(5): 5576.

Asangani, I., Rasheed, S., Nikolova, D., Leupold, J., Colburn, N., Post, S., and Allgayer, H. 2008. MicroRNA-21 (miR-21) post-transcriptionally downregulates tumor suppressor Pdcd4 and stimulates invasion, intravasation and metastasis in colorectal cancer. Oncogene **27**(15): 2128-2136.

Babiarz, J.E., Ruby, J.G., Wang, Y., Bartel, D.P., and Blelloch, R. 2008. Mouse ES cells express endogenous shRNAs, siRNAs, and other Microprocessor-independent, Dicer-dependent small RNAs. Genes Dev. **22**(20): 2773-2785.

Bahler, J., Steever, A.B., Wheatley, S., Wang, Y., Pringle, J.R., Gould, K.L., and McCollum, D. 1998. Role of polo kinase and Mid1p in determining the site of cell division in fission yeast. J. Cell Biol. **143**(6): 1603-1616.

Bartel, D.P. 2004. MicroRNAs: genomics, biogenesis, mechanism, and function. Cell **116**(2): 281-297.

Baum, J., Papenfuss, A.T., Mair, G.R., Janse, C.J., Vlachou, D., Waters, A.P., Cowman, A.F., Crabb, B.S., and de Koning-Ward, T.F. 2009. Molecular genetics and comparative genomics reveal RNAi is not functional in malaria parasites. Nucleic Acids Res. **37**(11): 3788-3798.

Baumberger, N., Tsai, C., Lie, M., Havecker, E., and Baulcombe, D.C. 2007. The Polerovirus silencing suppressor P0 targets ARGONAUTE proteins for degradation. Current Biology **17**(18): 1609-1614.

Behm-Ansmant, I., Rehwinkel, J., Doerks, T., Stark, A., Bork, P., and Izaurralde, E. 2006. mRNA degradation by miRNAs and GW182 requires both CCR4:NOT deadenylase and DCP1:DCP2 decapping complexes. Genes Dev. **20**(14): 1885-1898.

Bernstein, D.A., Vyas, V.K., Weinberg, D.E., Drinnenberg, I.A., Bartel, D.P., and Fink, G.R. 2012. Candida albicans Dicer (CaDcr1) is required for efficient ribosomal and spliceosomal RNA maturation. Proc. Natl. Acad. Sci. U. S. A. **109**(2): 523-528.

Beurel, E., Grieco, S.F., and Jope, R.S. 2015. Glycogen synthase kinase-3 (GSK3): regulation, actions, and diseases. Pharmacol. Ther. **148**: 114-131.

Beurel, E., Song, L., and Jope, R.S. 2011. Inhibition of glycogen synthase kinase-3 is necessary for the rapid antidepressant effect of ketamine in mice. Mol. Psychiatry **16**(11): 1068-1070.

Bimbo, A., Jia, Y., Poh, S.L., Karuturi, R.K., den Elzen, N., Peng, X., Zheng, L., O'Connell, M., Liu, E.T., Balasubramanian, M.K., and Liu, J. 2005. Systematic deletion analysis of fission yeast protein kinases. Eukaryot. Cell. **4**(4): 799-813.

Blachere, N.E., Udono, H., Janetzki, S., Li, Z., Heike, M., and Srivastava, P.K. 1993. Heat shock protein vaccines against cancer. Journal of Immunotherapy **14**(4): 352-356.

Blom, N., Sicheritz‐Pontén, T., Gupta, R., Gammeltoft, S., and Brunak, S. 2004. Prediction of post‐translational glycosylation and phosphorylation of proteins from the amino acid sequence. Proteomics **4**(6): 1633-1649.

Boland, A., Tritschler, F., Heimstadt, S., Izaurralde, E., and Weichenrieder, O. 2010. Crystal structure and ligand binding of the MID domain of a eukaryotic Argonaute protein. EMBO Rep. **11**(7): 522-527.

Borkovich, K.A., Farrelly, F.W., Finkelstein, D.B., Taulien, J., and Lindquist, S. 1989. Hsp82 is an Essential Protein that is Required in Higher Concentrations for Growth of Cells at Higher Temperatures. Mol. Cell. Biol. **9**(9): 3919-3930.

Breinig, F., Sendzik, T., Eisfeld, K., and Schmitt, M.J. 2006. Dissecting toxin immunity in virus-infected killer yeast uncovers an intrinsic strategy of self-protection. Proc. Natl. Acad. Sci. U. S. A. **103**(10): 3810-3815.

Bühler, M., Verdel, A., and Moazed, D. 2006. Tethering RITS to a nascent transcript initiates RNAi-and heterochromatin-dependent gene silencing. Cell **125**(5): 873-886.

Cai, Y., Yu, X., Hu, S., and Yu, J. 2009. A brief review on the mechanisms of miRNA regulation. Genomics, Proteomics & Bioinformatics **7**(4): 147-154.

Camblong, J., Beyrouthy, N., Guffanti, E., Schlaepfer, G., Steinmetz, L.M., and Stutz, F. 2009. Trans-acting antisense RNAs mediate transcriptional gene cosuppression in S. cerevisiae. Genes Dev. **23**(13): 1534-1545.

Carmell, M.A., Girard, A., van de Kant, Henk JG, Bourc'his, D., Bestor, T.H., de Rooij, D.G., and Hannon, G.J. 2007. MIWI2 is essential for spermatogenesis and repression of transposons in the mouse male germline. Developmental Cell **12**(4): 503-514.

Carmichael, J.B., Stoica, C., Parker, H., McCaffery, J.M., Simmonds, A.J., and Hobman, T.C. 2006. RNA interference effector proteins localize to mobile cytoplasmic puncta in Schizosaccharomyces pombe. Traffic **7**(8): 1032-1044.

Carmichael, J.B., Provost, P., Ekwall, K., and Hobman, T.C. 2004. ago1 and dcr1, two core components of the RNA interference pathway, functionally diverge from rdp1 in regulating cell cycle events in Schizosaccharomyces pombe. Mol. Biol. Cell **15**(3): 1425-1435.

Carthew, R.W., and Sontheimer, E.J. 2009. Origins and mechanisms of miRNAs and siRNAs. Cell **136**(4): 642-655.

Catala, M., Tremblay, M., Samson, E., Conconi, A., and Abou Elela, S. 2008. Deletion of Rnt1p alters the proportion of open versus closed rRNA gene repeats in yeast. Mol. Cell. Biol. **28**(2): 619-629.

Celenza, J.L., and Carlson, M. 1989. Mutational analysis of the Saccharomyces cerevisiae SNF1 protein kinase and evidence for functional interaction with the SNF4 protein. Mol. Cell. Biol. **9**(11): 5034-5044.

Cenik, E.S., Fukunaga, R., Lu, G., Dutcher, R., Wang, Y., Hall, T.M.T., and Zamore, P.D. 2011. Phosphate and R2D2 restrict the substrate specificity of Dicer-2, an ATP-driven ribonuclease. Mol. Cell **42**(2): 172-184.

Cerutti, L., Mian, N., and Bateman, A. 2000. Domains in gene silencing and cell differentiation proteins: the novel PAZ domain and redefinition of the Piwi domain. Trends Biochem. Sci. **25**(10): 481-482.

Chadli, A., Bouhouche, I., Sullivan, W., Stensgard, B., McMahon, N., Catelli, M.G., and Toft, D.O. 2000. Dimerization and N-terminal domain proximity underlie the function of the molecular chaperone heat shock protein 90. Proc. Natl. Acad. Sci. U. S. A. **97**(23): 12524-12529.

Chapman, E.J., and Carrington, J.C. 2007. Specialization and evolution of endogenous small RNA pathways. Nature Reviews Genetics **8**(11): 884-896.

Cheloufi, S., Dos Santos, C.O., Chong, M.M., and Hannon, G.J. 2010. A dicer-independent miRNA biogenesis pathway that requires Ago catalysis. Nature **465**(7298): 584-589.

Chen, E.S., Zhang, K., Nicolas, E., Cam, H.P., Zofall, M., and Grewal, S.I. 2008. Cell cycle control of centromeric repeat transcription and heterochromatin assembly. Nature **451**(7179): 734-737.

Cheung, A.L., Nishina, K.A., Trotonda, M.P., and Tamber, S. 2008. The SarA protein family of Staphylococcus aureus. Int. J. Biochem. Cell Biol. **40**(3): 355-361.

Chiu, Y.L., and Rana, T.M. 2003. siRNA function in RNAi: a chemical modification analysis. RNA **9**(9): 1034-1048.

Chong, M.M., Zhang, G., Cheloufi, S., Neubert, T.A., Hannon, G.J., and Littman, D.R. 2010. Canonical and alternate functions of the microRNA biogenesis machinery. Genes Dev. **24**(17): 1951-1960.

Crevel, G., Bennett, D., and Cotterill, S. 2008. The human TPR protein TTC4 is a putative Hsp90 co-chaperone which interacts with CDC6 and shows alterations in transformed cells. PloS one **3**(3): 1737.

Daher, A., Longuet, M., Dorin, D., Bois, F., Segeral, E., Bannwarth, S., Battisti, P.L., Purcell, D.F., Benarous, R., Vaquero, C., Meurs, E.F., and Gatignol, A. 2001. Two dimerization domains in the trans-activation response RNA-binding protein (TRBP) individually reverse the protein kinase R inhibition of HIV-1 long terminal repeat expression. J. Biol. Chem. **276**(36): 33899-33905.

De Fougerolles, A., Vornlocher, H., Maraganore, J., and Lieberman, J. 2007. Interfering with disease: a progress report on siRNA-based therapeutics. Nature reviews Drug discovery **6**(6): 443-453.

Deng, W., and Lin, H. 2002. Miwi, a murine homolog of piwi, encodes a cytoplasmic protein essential for spermatogenesis. Developmental cell **2**(6): 819-830.

Denli, A.M., Tops, B.B., Plasterk, R.H., Ketting, R.F., and Hannon, G.J. 2004. Processing of primary microRNAs by the Microprocessor complex. Nature **432**(7014): 231-235.

Ding, L., and Han, M. 2007. GW182 family proteins are crucial for microRNA-mediated gene silencing. Trends Cell Biol. **17**(8): 411-416.

Dinger, M.E., Pang, K.C., Mercer, T.R., and Mattick, J.S. 2008. Differentiating protein-coding and noncoding RNA: challenges and ambiguities. PLoS Comput Biol **4**(11): e1000176.

Doyle, M., Jantsch, M.F. 2002. New and old roles of the double-stranded RNA-binding domain. J. Struct. Biol 140(1–3):147–53

Drinnenberg, I.A., Fink, G.R., and Bartel, D.P. 2011. Compatibility with killer explains the rise of RNAi-deficient fungi. Science **333**(6049): 1592.

Drinnenberg, I.A., Weinberg, D.E., Xie, K.T., Mower, J.P., Wolfe, K.H., Fink, G.R., and Bartel, D.P. 2009. RNAi in budding yeast. Science **326**(5952): 544-550.

Duarte, M., Graham, K., Daher, A., Battisti, P., Bannwarth, S., Segeral, E., Jeang, K., and Gatignol, A. 2000. Characterization of TRBP1 and TRBP2. J. Biomed. Sci. **7**(6): 494-506.

Ekwall, K. 2004. The RITS complex—a direct link between small RNA and heterochromatin. Mol. Cell **13**(3): 304-305.

Elder, R.T., Yu, M., Chen, M., Zhu, X., Yanagida, M., and Zhao, Y. 2001. HIV-1 Vpr induces cell cycle G2 arrest in fission yeast (Schizosaccharomyces pombe) through a pathway involving regulatory and catalytic subunits of PP2A and acting on both Wee1 and Cdc25. Virology **287**(2): 359-370.

Elela, S.A., Igel, H., and Ares, M. 1996. RNase III cleaves eukaryotic preribosomal RNA at a U3 snoRNP-dependent site. Cell **85**(1): 115-124.

Ender, C., and Meister, G. 2010. Argonaute proteins at a glance. J. Cell. Sci. **123**(Pt 11): 1819-1823.

Erkine, A.M., Szent‐Gyorgyi, C., Simmons, S.F., and Gross, D.S. 1995. The upstream sequences of the HSP82 and HSC82 genes of Saccharomyces cerevisiae: regulatory elements and nucleosome positioning motifs. Yeast **11**(6): 573-580.

Ernst, R., Klemm, R., Schmitt, L., and Kuchler, K. 2005. Yeast ATP‐Binding Cassette Transporters: Cellular Cleaning Pumps. Meth. Enzymol. **400**: 460-484.

Eulalio, A., Tritschler, F., and Izaurralde, E. 2009. The GW182 protein family in animal cells: new insights into domains required for miRNA-mediated gene silencing. RNA **15**(8): 1433-1442.

Eulalio, A., Rehwinkel, J., Stricker, M., Huntzinger, E., Yang, S.F., Doerks, T., Dorner, S., Bork, P., Boutros, M., and Izaurralde, E. 2007. Target-specific requirements for enhancers of decapping in miRNA-mediated gene silencing. Genes Dev. **21**(20): 2558-2570.

Fabian, M.R., Mathonnet, G., Sundermeier, T., Mathys, H., Zipprich, J.T., Svitkin, Y.V., Rivas, F., Jinek, M., Wohlschlegel, J., and Doudna, J.A. 2009. Mammalian miRNA RISC recruits CAF1 and PABP to affect PABP-dependent deadenylation. Mol. Cell **35**(6): 868-880.

Fabian, M.R., Sonenberg, N., and Filipowicz, W. 2010. Regulation of mRNA translation and stability by microRNAs. Annu. Rev. Biochem. **79**: 351-379.

Fagard, M., Boutet, S., Morel, J.B., Bellini, C., and Vaucheret, H. 2000. AGO1, QDE-2, and RDE-1 are related proteins required for post-transcriptional gene silencing in plants, quelling in fungi, and RNA interference in animals. Proc. Natl. Acad. Sci. U. S. A. **97**(21): 11650-11654.

Fagegaltier, D., Bouge, A.L., Berry, B., Poisot, E., Sismeiro, O., Coppee, J.Y., Theodore, L., Voinnet, O., and Antoniewski, C. 2009. The endogenous siRNA pathway is involved in heterochromatin formation in Drosophila. Proc. Natl. Acad. Sci. U. S. A. **106**(50): 21258-21263.

Farazi, T.A., Juranek, S.A., and Tuschl, T. 2008. The growing catalog of small RNAs and their association with distinct Argonaute/Piwi family members. Development **135**(7): 1201-1214.

Findley, S.D., Tamanaha, M., Clegg, N.J., and Ruohola-Baker, H. 2003. Maelstrom, a Drosophila spindle-class gene, encodes a protein that colocalizes with Vasa and RDE1/AGO1 homolog, Aubergine, in nuage. Development **130**(5): 859-871.

Fire, A., Xu, S., Montgomery, M.K., Kostas, S.A., Driver, S.E., and Mello, C.C. 1998. Potent and specific genetic interference by double-stranded RNA in Caenorhabditis elegans. Nature **391**(6669): 806-811.

Fischer, S.E., Montgomery, T.A., Zhang, C., Fahlgren, N., Breen, P.C., Hwang, A., Sullivan, C.M., Carrington, J.C., and Ruvkun, G. 2011. The ERI-6/7 helicase acts at the first stage of an siRNA amplification pathway that targets recent gene duplications. PLoS Genet **7**(11): e1002369.

Flynt, A.S., Greimann, J.C., Chung, W., Lima, C.D., and Lai, E.C. 2010. MicroRNA biogenesis via splicing and exosome-mediated trimming in Drosophila. Mol. Cell **38**(6): 900-907.

Förstemann, K., Horwich, M.D., Wee, L., Tomari, Y., and Zamore, P.D. 2007. Drosophila microRNAs are sorted into functionally distinct argonaute complexes after production by dicer-1. Cell **130**(2): 287-297.

Freeman, B.C., Felts, S.J., Toft, D.O., and Yamamoto, K.R. 2000. The p23 molecular chaperones act at a late step in intracellular receptor action to differentially affect ligand efficacies. Genes Dev. **14**(4): 422-434. PMID:10691735.

Friedman, J.M., Liang, G., Liu, C.C., Wolff, E.M., Tsai, Y.C., Ye, W., Zhou, X., and Jones, P.A. 2009. The putative tumor suppressor microRNA-101 modulates the cancer epigenome by repressing the polycomb group protein EZH2. Cancer Res. **69**(6): 2623-2629.

Gatignol, A., Buckler-White, A., Berkhout, B., and Jeang, K.T. 1991. Characterization of a human TAR RNA-binding protein that activates the HIV-1 LTR. Science **251**(5001): 1597-1600.

Ghildiyal, M., Seitz, H., Horwich, M.D., Li, C., Du, T., Lee, S., Xu, J., Kittler, E.L., Zapp, M.L., Weng, Z., and Zamore, P.D. 2008. Endogenous siRNAs derived from transposons and mRNAs in Drosophila somatic cells. Science **320**(5879): 1077-1081.

Gibbings, D., Mostowy, S., and Voinnet, O. 2013. Autophagy selectively regulates miRNA homeostasis. Autophagy **9**(5): 781-783.

Gietz, R.D., Schiestl, R.H., Willems, A.R., and Woods, R.A. 1995. Studies on the transformation of intact yeast cells by the LiAc/SS‐DNA/PEG procedure. Yeast **11**(4): 355-360.

Golden, D.E., Gerbasi, V.R., and Sontheimer, E.J. 2008. An inside job for siRNAs. Mol. Cell **31**(3): 309-312.

Gregory, R.I., Chendrimada, T.P., Cooch, N., and Shiekhattar, R. 2005. Human RISC couples microRNA biogenesis and posttranscriptional gene silencing. Cell **123**(4): 631-640.

Grewal, S.I., and Jia, S. 2007. Heterochromatin revisited. Nature Reviews Genetics **8**(1): 35-46.

Gunawardane, L.S., Saito, K., Nishida, K.M., Miyoshi, K., Kawamura, Y., Nagami, T., Siomi, H., and Siomi, M.C. 2007. A slicer-mediated mechanism for repeat-associated siRNA 5' end formation in Drosophila. Science **315**(5818): 1587-1590.

Ha, M., and Kim, V.N. 2014. Regulation of microRNA biogenesis. Nature reviews Molecular cell biology **15**(8): 509-524.

Halder, J., Kamat, A.A., Landen, C.N.,Jr, Han, L.Y., Lutgendorf, S.K., Lin, Y.G., Merritt, W.M., Jennings, N.B., Chavez-Reyes, A., Coleman, R.L., Gershenson, D.M., Schmandt, R., Cole, S.W., Lopez-Berestein, G., and Sood, A.K. 2006. Focal adhesion kinase targeting using in vivo short interfering RNA delivery in neutral liposomes for ovarian carcinoma therapy. Clin. Cancer Res. **12**(16): 4916-4924.

Hammond, S.M., Bernstein, E., Beach, D., and Hannon, G.J. 2000. An RNA-directed nuclease mediates post-transcriptional gene silencing in Drosophila cells. Nature **404**(6775): 293-296.

Hanks, S.K., and Hunter, T. 1995. Protein kinases 6. The eukaryotic protein kinase superfamily: kinase (catalytic) domain structure and classification. FASEB J. **9**(8): 576-596.

Hannon, G.J. 2002. RNA interference. Nature **418**(6894): 244-251.

Hansen, L.K., Houchins, J., and O'Leary, J.J. 1991. Differential regulation of HSC70, HSP70, HSP90α, and HSP90β mRNA expression by mitogen activation and heat shock in human lymphocytes. Exp. Cell Res. **192**(2): 587-596.

Harrison, B.R., Yazgan, O., and Krebs, J.E. 2009. Life without RNAi: noncoding RNAs and their functions in *Saccharomyces cerevisiae*. Biochemistry and Cell Biology **87**(5): 767-779.

Heald, R., McLoughlin, M., and McKeon, F. 1993. Human wee1 maintains mitotic timing by protecting the nucleus from cytoplasmically activated Cdc2 kinase. Cell **74**(3): 463-474.

Henderson, I.R., and Jacobsen, S.E. 2007. Epigenetic inheritance in plants. Nature **447**(7143): 418-424.

Henderson, I.R., Zhang, X., Lu, C., Johnson, L., Meyers, B.C., Green, P.J., and Jacobsen, S.E. 2006. Dissecting Arabidopsis thaliana DICER function in small RNA processing, gene silencing and DNA methylation patterning. Nat. Genet. **38**(6): 721-725.

Heo, I., and Kim, V.N. 2009. Regulating the regulators: posttranslational modifications of RNA silencing factors. Cell **139**(1): 28-31.

Horman, S.R., Janas, M.M., Litterst, C., Wang, B., MacRae, I.J., Sever, M.J., Morrissey, D.V., Graves, P., Luo, B., and Umesalma, S. 2013. Akt-mediated phosphorylation of argonaute 2 downregulates cleavage and upregulates translational repression of MicroRNA targets. Mol. Cell **50**(3): 356-367.

Houseley, J., and Tollervey, D. 2008. The nuclear RNA surveillance machinery: the link between ncRNAs and genome structure in budding yeast? Biochimica et Biophysica Acta (BBA)-Gene Regulatory Mechanisms **1779**(4): 239-246.

Hoyle, N.P., Castelli, L.M., Campbell, S.G., Holmes, L.E., and Ashe, M.P. 2007. Stress-dependent relocalization of translationally primed mRNPs to cytoplasmic granules that are kinetically and spatially distinct from P-bodies. J. Cell Biol. **179**(1): 65-74.

Hunter, T. 1995. Protein kinases and phosphatases: the yin and yang of protein phosphorylation and signaling. Cell **80**(2): 225-236.

Hunter, T., and Cooper, J.A. 1985. Protein-tyrosine kinases. Annu. Rev. Biochem. **54**(1): 897-930.

Huntzinger, E., and Izaurralde, E. 2011. Gene silencing by microRNAs: contributions of translational repression and mRNA decay. Nature Reviews Genetics **12**(2): 99-110.

Hutvagner, G., and Simard, M.J. 2008. Argonaute proteins: key players in RNA silencing. Nature reviews Molecular cell biology **9**(1): 22-32.

Hutvagner, G., and Zamore, P.D. 2002. A microRNA in a multiple-turnover RNAi enzyme complex. Science **297**(5589): 2056-2060.

Hutvagner, G., McLachlan, J., Pasquinelli, A.E., Balint, E., Tuschl, T., and Zamore, P.D. 2001. A cellular function for the RNA-interference enzyme Dicer in the maturation of the let-7 small temporal RNA. Science **293**(5531): 834-838.

Ikeda, K., Satoh, M., Pauley, K.M., Fritzler, M.J., Reeves, W.H., and Chan, E.K. 2006. Detection of the argonaute protein Ago2 and microRNAs in the RNA induced silencing complex (RISC) using a monoclonal antibody. J. Immunol. Methods **317**(1): 38-44.

Ito, H., Fukuda, Y., Murata, K., and Kimura, A. 1983. Transformation of intact yeast cells treated with alkali cations. J. Bacteriol. **153**(1): 163-168.

Iwasaki, S., Kobayashi, M., Yoda, M., Sakaguchi, Y., Katsuma, S., Suzuki, T., and Tomari, Y. 2010. Hsc70/Hsp90 chaperone machinery mediates ATP-dependent RISC loading of small RNA duplexes. Mol. Cell **39**(2): 292-299.

Jakymiw, A., Lian, S., Eystathioy, T., Li, S., Satoh, M., Hamel, J.C., Fritzler, M.J., and Chan, E.K. 2005. Disruption of GW bodies impairs mammalian RNA interference. Nat. Cell Biol. **7**(12): 1267-1274.

Janbon, G., Maeng, S., Yang, D., Ko, Y., Jung, K., Moyrand, F., Floyd, A., Heitman, J., and Bahn, Y. 2010. Characterizing the role of RNA silencing components in Cryptococcus neoformans. Fungal Genetics and Biology **47**(12): 1070-1080.

Jee, D., and Lai, E.C. 2014. Alteration of miRNA activity via context-specific modifications of Argonaute proteins. Trends Cell Biol. **24**(9): 546-553.

Jiang, F., Ye, X., Liu, X., Fincher, L., McKearin, D., and Liu, Q. 2005. Dicer-1 and R3D1-L catalyze microRNA maturation in Drosophila. Genes Dev. **19**(14): 1674-1679.

Johnston, M., Geoffroy, M.C., Sobala, A., Hay, R., and Hutvagner, G. 2010. HSP90 protein stabilizes unloaded argonaute complexes and microscopic P-bodies in human cells. Mol. Biol. Cell **21**(9): 1462-1469.

Josa-Prado, F., Henley, J.M., and Wilkinson, K.A. 2015. SUMOylation of Argonaute-2 regulates RNA interference activity. Biochem. Biophys. Res. Commun. **464**(4): 1066-1071.

Kahvejian, A., Svitkin, Y.V., Sukarieh, R., M'Boutchou, M.N., and Sonenberg, N. 2005. Mammalian poly(A)-binding protein is a eukaryotic translation initiation factor, which acts via multiple mechanisms. Genes Dev. **19**(1): 104-113.

Kamal, A., Thao, L., Sensintaffar, J., Zhang, L., Boehm, M.F., Fritz, L.C., and Burrows, F.J. 2003. A high-affinity conformation of Hsp90 confers tumour selectivity on Hsp90 inhibitors. Nature **425**(6956): 407-410.

Kanasty, R.L., Whitehead, K.A., Vegas, A.J., and Anderson, D.G. 2012. Action and reaction: the biological response to siRNA and its delivery vehicles. Molecular Therapy **20**(3): 513-524.

Karginov, F.V., and Hannon, G.J. 2013. Remodeling of Ago2-mRNA interactions upon cellular stress reflects miRNA complementarity and correlates with altered translation rates. Genes Dev. **27**(14): 1624-1632.

Kasschau, K.D., Fahlgren, N., Chapman, E.J., Sullivan, C.M., Cumbie, J.S., Givan, S.A., and Carrington, J.C. 2007. Genome-wide profiling and analysis of Arabidopsis siRNAs. PLoS Biol **5**(3): e57.

Kedersha, N., and Anderson, P. 2002. Stress granules: sites of mRNA triage that regulate mRNA stability and translatability. Biochem. Soc. Trans. **30**(Pt 6): 963-969.

Khraiwesh, B., Arif, M.A., Seumel, G.I., Ossowski, S., Weigel, D., Reski, R., and Frank, W. 2010. Transcriptional control of gene expression by microRNAs. Cell **140**(1): 111-122.

Khvorova, A., Reynolds, A., and Jayasena, S.D. 2003. Functional siRNAs and miRNAs exhibit strand bias. Cell **115**(2): 209-216.

Kim, V.N., Han, J., and Siomi, M.C. 2009. Biogenesis of small RNAs in animals. Nature reviews Molecular cell biology **10**(2): 126-139.

Kirino, Y., Vourekas, A., Sayed, N., de Lima Alves, F., Thomson, T., Lasko, P., Rappsilber, J., Jongens, T.A., and Mourelatos, Z. 2010. Arginine methylation of Aubergine mediates Tudor binding and germ plasm localization. RNA **16**(1): 70-78.

Klahre, U., Crete, P., Leuenberger, S.A., Iglesias, V.A., and Meins, F.,Jr. 2002. High molecular weight RNAs and small interfering RNAs induce systemic posttranscriptional gene silencing in plants. Proc. Natl. Acad. Sci. U. S. A. **99**(18): 11981-11986.

Knight, S.W., and Bass, B.L. 2001. A role for the RNase III enzyme DCR-1 in RNA interference and germ line development in Caenorhabditis elegans. Science **293**(5538): 2269-2271.

Kok, K.H., Ng, M.H., Ching, Y.P., and Jin, D.Y. 2007. Human TRBP and PACT directly interact with each other and associate with dicer to facilitate the production of small interfering RNA. J. Biol. Chem. **282**(24): 17649-17657.

Kuehner, J.N., and Brow, D.A. 2008. Regulation of a eukaryotic gene by GTP-dependent start site selection and transcription attenuation. Mol. Cell **31**(2): 201-211.

Kwapisz, M., Wery, M., Despres, D., Ghavi-Helm, Y., Soutourina, J., Thuriaux, P., and Lacroute, F. 2008. Mutations of RNA polymerase II activate key genes of the nucleoside triphosphate biosynthetic pathways. EMBO J. **27**(18): 2411-2421.

Laemmli, U. 1970. Most commonly used discontinuous buffer system for SDS electrophoresis. Nature **227**: 680-685.

Lamontagne, B., Larose, S., Boulanger, J., and Elela, S.A. 2001. The RNase III family: a conserved structure and expanding functions in eukaryotic dsRNA metabolism. Yeast **45**(191): 154-158.

Landthaler, M., Gaidatzis, D., Rothballer, A., Chen, P.Y., Soll, S.J., Dinic, L., Ojo, T., Hafner, M., Zavolan, M., and Tuschl, T. 2008. Molecular characterization of human Argonaute-containing ribonucleoprotein complexes and their bound target mRNAs. RNA **14**(12): 2580-2596 .

Lau, P., Potter, C.S., Carragher, B., and MacRae, I.J. 2009. Structure of the human Dicer-TRBP complex by electron microscopy. Structure **17**(10): 1326-1332.

Lau, P., Guiley, K.Z., De, N., Potter, C.S., Carragher, B., and MacRae, I.J. 2012. The molecular architecture of human Dicer. Nature structural & molecular biology **19**(4): 436-440.

Lee, Y., Ahn, C., Han, J., Choi, H., Kim, J., Yim, J., Lee, J., Provost, P., Rådmark, O., and Kim, S. 2003. The nuclear RNase III Drosha initiates microRNA processing. Nature **425**(6956): 415-419.

Lee, Y.S., Nakahara, K., Pham, J.W., Kim, K., He, Z., Sontheimer, E.J., and Carthew, R.W. 2004. Distinct roles for Drosophila Dicer-1 and Dicer-2 in the siRNA/miRNA silencing pathways. Cell **117**(1): 69-81.

Lee, R.C., and Ambros, V. 2001. An extensive class of small RNAs in Caenorhabditis elegans. Science **294**(5543): 862-864.

Leung, A.K. 2014. Poly(ADP-ribose): an organizer of cellular architecture. J. Cell Biol. **205**(5): 613-619.

Leung, A.K., Calabrese, J.M., and Sharp, P.A. 2006. Quantitative analysis of Argonaute protein reveals microRNA-dependent localization to stress granules. Proc. Natl. Acad. Sci. U. S. A. **103**(48): 18125-18130.

Leuschner, P.J., Obernosterer, G., and Martinez, J. 2005. MicroRNAs: Loquacious speaks out. Current biology **15**(15): 603-605.

Leuschner, P.J., Ameres, S.L., Kueng, S., and Martinez, J. 2006. Cleavage of the siRNA passenger strand during RISC assembly in human cells. EMBO Rep. **7**(3): 314-320.

Li, Z., and Rana, T.M. 2014. Therapeutic targeting of microRNAs: current status and future challenges. Nature reviews Drug discovery **13**(8): 622-638.

Lingel, A., Simon, B., Izaurralde, E., and Sattler, M. 2003. Structure and nucleic-acid binding of the Drosophila Argonaute 2 PAZ domain. Nature **426**(6965): 465-469.

Lippman, Z., and Martienssen, R. 2004. The role of RNA interference in heterochromatic silencing. Nature **431**(7006): 364-370.

Liu, J., Valencia-Sanchez, M.A., Hannon, G.J., and Parker, R. 2005. MicroRNA-dependent localization of targeted mRNAs to mammalian P-bodies. Nat. Cell Biol. **7**(7): 719-723.

Liu, J., Rivas, F.V., Wohlschlegel, J., Yates, J.R., Parker, R., and Hannon, G.J. 2005. A role for the P-body component GW182 in microRNA function. Nat. Cell Biol. **7**(12): 1261-1266.

Liu, J., Carmell, M.A., Rivas, F.V., Marsden, C.G., Thomson, J.M., Song, J.J., Hammond, S.M., Joshua-Tor, L., and Hannon, G.J. 2004. Argonaute2 is the catalytic engine of mammalian RNAi. Science **305**(5689): 1437-1441.

Liu, Q., Rand, T.A., Kalidas, S., Du, F., Kim, H.E., Smith, D.P., and Wang, X. 2003. R2D2, a bridge between the initiation and effector steps of the Drosophila RNAi pathway. Science **301**(5641): 1921-1925.

Liu, X., Jiang, F., Kalidas, S., Smith, D., and Liu, Q. 2006. Dicer-2 and R2D2 coordinately bind siRNA to promote assembly of the siRISC complexes. RNA **12**(8): 1514-1520.

Livak, K.J., and Schmittgen, T.D. 2001. Analysis of relative gene expression data using real-time quantitative PCR and the 2− ΔΔCT method. Methods **25**(4): 402-408.

Lo, W.S., Duggan, L., Emre, N.C., Belotserkovskya, R., Lane, W.S., Shiekhattar, R., and Berger, S.L. 2001. Snf1--a histone kinase that works in concert with the histone acetyltransferase Gcn5 to regulate transcription. Science **293**(5532): 1142-1146.

Loison, G., Losson, R., and Lacroute, F. 1980. Constitutive mutants for orotidine 5 phosphate decarboxylase and dihydroorotic acid dehydrogenase in Saccharomyces cerevisiae. Curr. Genet. **2**(1): 39-44.

Loison, G., Losson, R., and Lacroute, F. 1980. Constitutive mutants for orotidine 5 phosphate decarboxylase and dihydroorotic acid dehydrogenase in Saccharomyces cerevisiae. Curr. Genet. **2**(1): 39-44.

Lopez-Orozco, J., Pare, J.M., Holme, A.L., Chaulk, S.G., Fahlman, R.P., and Hobman, T.C. 2015. Functional analyses of phosphorylation events in human Argonaute 2. RNA **21**(12): 2030-2038.

Lund, A.H., and van Lohuizen, M. 2004. Epigenetics and cancer. Genes Dev. **18**(19): 2315-2335.

Lye, L., Owens, K., Shi, H., Murta, S.M., Vieira, A.C., Turco, S.J., Tschudi, C., Ullu, E., and Beverley, S.M. 2010. Retention and loss of RNA interference pathways in trypanosomatid protozoans. PLoS Pathog **6**(10): e1001161.

Ma, J., Ye, K., and Patel, D.J. 2004. Structural basis for overhang-specific small interfering RNA recognition by the PAZ domain. Nature **429**(6989): 318-322.

MacRae, I.J., Ma, E., Zhou, M., Robinson, C.V., and Doudna, J.A. 2008. In vitro reconstitution of the human RISC-loading complex. Proc. Natl. Acad. Sci. U. S. A. **105**(2): 512-517.

Macrae, I.J., Zhou, K., Li, F., Repic, A., Brooks, A.N., Cande, W.Z., Adams, P.D., and Doudna, J.A. 2006. Structural basis for double-stranded RNA processing by Dicer. Science **311**(5758): 195-198.

Mahalingam, D., Swords, R., Carew, J., Nawrocki, S., Bhalla, K., and Giles, F. 2009. Targeting HSP90 for cancer therapy. Br. J. Cancer **100**(10): 1523-1529.

Maloney, A., and Workman, P. 2002. HSP90 as a new therapeutic target for cancer therapy: the story unfolds. Expert opinion on biological therapy **2**(1): 3-24.

Mamnun, Y.M., Schüller, C., and Kuchler, K. 2004. Expression regulation of the yeast PDR5 ATP-binding cassette (ABC) transporter suggests a role in cellular detoxification during the exponential growth phase. FEBS Lett. **559**(1): 111-117.

Mann, M., and Jensen, O.N. 2003. Proteomic analysis of post-translational modifications. Nat. Biotechnol. **21**(3): 255-261.

Martens, J.A., Laprade, L., and Winston, F. 2004. Intergenic transcription is required to repress the Saccharomyces cerevisiae SER3 gene. Nature **429**(6991): 571-574.

Martienssen, R.A., Zaratiegui, M., and Goto, D.B. 2005. RNA interference and heterochromatin in the fission yeast Schizosaccharomyces pombe. TRENDS in Genetics **21**(8): 450-456.

Martinez, N.J., and Gregory, R.I. 2013. Argonaute2 expression is post-transcriptionally coupled to microRNA abundance. RNA **19**(5): 605-612.

Matranga, C., Tomari, Y., Shin, C., Bartel, D.P., and Zamore, P.D. 2005. Passenger-strand cleavage facilitates assembly of siRNA into Ago2-containing RNAi enzyme complexes. Cell **123**(4): 607-620.

Matzke, M.A., and Birchler, J.A. 2005. RNAi-mediated pathways in the nucleus. Nature Reviews Genetics **6**(1): 24-35.

McLaughlin, S.H., Sobott, F., Yao, Z., Zhang, W., Nielsen, P.R., Grossmann, J.G., Laue, E.D., Robinson, C.V., and Jackson, S.E. 2006. The co-chaperone p23 arrests the Hsp90 ATPase cycle to trap client proteins. J. Mol. Biol. **356**(3): 746-758.

McManus, M.T., and Sharp, P.A. 2002. Gene silencing in mammals by small interfering RNAs. Nature reviews genetics **3**(10): 737-747.

Meister, G., and Tuschl, T. 2004. Mechanisms of gene silencing by double-stranded RNA. Nature **431**(7006): 343-349.

Meister, G., Landthaler, M., Patkaniowska, A., Dorsett, Y., Teng, G., and Tuschl, T. 2004. Human Argonaute2 mediates RNA cleavage targeted by miRNAs and siRNAs. Mol. Cell **15**(2): 185-197.

Meister, G., Landthaler, M., Dorsett, Y., and Tuschl, T. 2004. Sequence-specific inhibition of microRNA- and siRNA-induced RNA silencing. RNA **10**(3): 544-550.

Mello, C.C., and Conte, D. 2004. Revealing the world of RNA interference. Nature **431**(7006): 338-342.

Meng, F., Henson, R., Wehbe–Janek, H., Ghoshal, K., Jacob, S.T., and Patel, T. 2007. MicroRNA-21 regulates expression of the PTEN tumor suppressor gene in human hepatocellular cancer. Gastroenterology **133**(2): 647-658.

Mercer, T.R., Dinger, M.E., and Mattick, J.S. 2009. Long non-coding RNAs: insights into functions. Nature Reviews Genetics **10**(3): 155-159.

Meyer, P., Prodromou, C., Liao, C., Hu, B., Mark Roe, S., Vaughan, C.K., Vlasic, I., Panaretou, B., Piper, P.W., and Pearl, L.H. 2004. Structural basis for recruitment of the ATPase activator Aha1 to the Hsp90 chaperone machinery. EMBO J. **23**(3): 511-519.

Miyoshi, T., Takeuchi, A., Siomi, H., and Siomi, M.C. 2010. A direct role for Hsp90 in pre-RISC formation in Drosophila. Nature structural & molecular biology **17**(8): 1024-1026.

Miyoshi, K., Okada, T.N., Siomi, H., and Siomi, M.C. 2009. Characterization of the miRNA-RISC loading complex and miRNA-RISC formed in the Drosophila miRNA pathway. RNA **15**(7): 1282-1291.

Miyoshi, K., Tsukumo, H., Nagami, T., Siomi, H., and Siomi, M.C. 2005. Slicer function of Drosophila Argonautes and its involvement in RISC formation. Genes Dev. **19**(23): 2837-2848.

Moazed, D. 2009. Small RNAs in transcriptional gene silencing and genome defence. Nature **457**(7228): 413-420.

Mollapour, M., and Neckers, L. 2012. Post-translational modifications of Hsp90 and their contributions to chaperone regulation. Biochimica et Biophysica Acta (BBA)-Molecular Cell Research **1823**(3): 648-655.

Mollapour, M., Tsutsumi, S., and Neckers, L. 2010. Hsp90 phosphorylation, Wee1 and the cell cycle. Cell Cycle **9**(12): 2310-2316.

Mollapour, M., Tsutsumi, S., Donnelly, A.C., Beebe, K., Tokita, M.J., Lee, M., Lee, S., Morra, G., Bourboulia, D., and Scroggins, B.T. 2010. Swe1 Wee1-dependent tyrosine phosphorylation of Hsp90 regulates distinct facets of chaperone function. Mol. Cell **37**(3): 333-343.

Morrissey, D.V., Lockridge, J.A., Shaw, L., Blanchard, K., Jensen, K., Breen, W., Hartsough, K., Machemer, L., Radka, S., and Jadhav, V. 2005. Potent and persistent in vivo anti-HBV activity of chemically modified siRNAs. Nat. Biotechnol. **23**(8): 1002-1007.

Moser, J.J., Eystathioy, T., Chan, E.K., and Fritzler, M.J. 2007. Markers of mRNA stabilization and degradation, and RNAi within astrocytoma GW bodies. J. Neurosci. Res. **85**(16): 3619-3631.

Motamedi, M.R., Verdel, A., Colmenares, S.U., Gerber, S.A., Gygi, S.P., and Moazed, D. 2004. Two RNAi complexes, RITS and RDRC, physically interact and localize to noncoding centromeric RNAs. Cell **119**(6): 789-802.

Nakanishi, K., Weinberg, D.E., Bartel, D.P., and Patel, D.J. 2012. Structure of yeast Argonaute with guide RNA. Nature **486**(7403): 368-374.

Nakazawa, Y., Hiraguri, A., Moriyama, H., and Fukuhara, T. 2007. The dsRNA-binding protein DRB4 interacts with the Dicer-like protein DCL4 in vivo and functions in the trans-acting siRNA pathway. Plant Mol. Biol. **63**(6): 777-785.

NIU, X., PENG, Z., DUAN, W., Wang, H., and Wang, P. 2006. Inhibition of HPV 16 E6 oncogene expression by RNA interference in vitro and in vivo. International Journal of Gynecological Cancer **16**(2): 743-751.

Okamura, K., Chung, W., Ruby, J.G., Guo, H., Bartel, D.P., and Lai, E.C. 2008. The Drosophila hairpin RNA pathway generates endogenous short interfering RNAs. Nature **453**(7196): 803-806.

Okamura, K., Ishizuka, A., Siomi, H., and Siomi, M.C. 2004. Distinct roles for Argonaute proteins in small RNA-directed RNA cleavage pathways. Genes Dev. **18**(14): 1655-1666.

Pak, J., and Fire, A. 2007. Distinct populations of primary and secondary effectors during RNAi in C. elegans. Science **315**(5809): 241-244.

Pare, J.M., López-Orozco, J., and Hobman, T.C. 2011. MicroRNA-binding is required for recruitment of human Argonaute 2 to stress granules and P-bodies. Biochem. Biophys. Res. Commun. **414**(1): 259-264.

Pare, J.M., Tahbaz, N., Lopez-Orozco, J., LaPointe, P., Lasko, P., and Hobman, T.C. 2009. Hsp90 regulates the function of argonaute 2 and its recruitment to stress granules and P-bodies. Mol. Biol. Cell **20**(14): 3273-3284.

Park, J., Heo, I., Tian, Y., Simanshu, D.K., Chang, H., Jee, D., Patel, D.J., and Kim, V.N. 2011. Dicer recognizes the 5 [prime] end of RNA for efficient and accurate processing. Nature **475**(7355): 201-205.

Parker, J.S., Roe, S.M., and Barford, D. 2005. Structural insights into mRNA recognition from a PIWI domain–siRNA guide complex. Nature **434**(7033): 663-666.

Parker, J.S., Roe, S.M., and Barford, D. 2004. Crystal structure of a PIWI protein suggests mechanisms for siRNA recognition and slicer activity. EMBO J. **23**(24): 4727-4737 .

Paroo, Z., Ye, X., Chen, S., and Liu, Q. 2009. Phosphorylation of the human microRNA-generating complex mediates MAPK/Erk signaling. Cell 139(1):112–22

Pearson, G., Robinson, F., Beers Gibson, T., Xu, B., Karandikar, M., Berman, K., and Cobb, M.H. 2001. Mitogen-activated protein (MAP) kinase pathways: regulation and physiological functions 1. Endocr. Rev. **22**(2): 153-183.

Petit, A.P., Wohlbold, L., Bawankar, P., Huntzinger, E., Schmidt, S., Izaurralde, E., and Weichenrieder, O. 2012. The structural basis for the interaction between the CAF1 nuclease and the NOT1 scaffold of the human CCR4-NOT deadenylase complex. Nucleic Acids Res. **40**(21): 11058-11072.

Petrie, V.J., Wuitschick, J.D., Givens, C.D., Kosinski, A.M., and Partridge, J.F. 2005. RNA interference (RNAi)-dependent and RNAi-independent association of the Chp1 chromodomain protein with distinct heterochromatic loci in fission yeast. Mol. Cell. Biol. **25**(6): 2331-2346.

Pfeffer, S., Sewer, A., Lagos-Quintana, M., Sheridan, R., Sander, C., Grässer, F.A., van Dyk, L.F., Ho, C.K., Shuman, S., and Chien, M. 2005. Identification of microRNAs of the herpesvirus family. Nature methods **2**(4): 269-276.

Piao, X., Zhang, X., Wu, L., and Belasco, J.G. 2010. CCR4-NOT deadenylates mRNA associated with RNA-induced silencing complexes in human cells. Mol. Cell. Biol. **30**(6): 1486-1494.

Piper, P.W., Millson, S.H., Mollapour, M., Panaretou, B., Siligardi, G., Pearl, L.H., and Prodromou, C. 2003. Sensitivity to Hsp90 ‐ targeting drugs can arise with mutation to the Hsp90 chaperone, cochaperones and plasma membrane ATP binding cassette transporters of yeast. European Journal of Biochemistry **270**(23): 4689-4695.

Preall, J.B., and Sontheimer, E.J. 2005. RNAi: RISC gets loaded. Cell **123**(4): 543-545.

Prodromou, C., and Pearl, L.H. 2003. Structure and functional relationships of Hsp90. Current cancer drug targets **3**(5): 301-323.

Provost, P., Dishart, D., Doucet, J., Frendewey, D., Samuelsson, B., and Radmark, O. 2002. Ribonuclease activity and RNA binding of recombinant human Dicer. EMBO J. **21**(21): 5864-5874.

Qi, H.H., Ongusaha, P.P., Myllyharju, J., Cheng, D., Pakkanen, O., Shi, Y., Lee, S.W., Peng, J., and Shi, Y. 2008. Prolyl 4-hydroxylation regulates Argonaute 2 stability. Nature **455**(7211): 421-424.

Qin, W., Shi, Y., Zhao, B., Yao, C., Jin, L., Ma, J., and Jin, Y. 2010. miR-24 regulates apoptosis by targeting the open reading frame (ORF) region of FAF1 in cancer cells. PLoS One **5**(2): e9429.

Raleigh, J.M., and O'Connell, M.J. 2000. The G(2) DNA damage checkpoint targets both Wee1 and Cdc25. J. Cell. Sci. **113 (Pt 10)**(Pt 10): 1727-1736.

Rea, S., Eisenhaber, F., O'Carroll, D., Strahl, B.D., Sun, Z., Schmid, M., Opravil, S., Mechtler, K., Ponting, C.P., and Allis, C.D. 2000. Regulation of chromatin structure by site-specific histone H3 methyltransferases. Nature **406**(6796): 593-599.

Rehwinkel, J., Behm-Ansmant, I., Gatfield, D., and Izaurralde, E. 2005. A crucial role for GW182 and the DCP1:DCP2 decapping complex in miRNA-mediated gene silencing. RNA **11**(11): 1640-1647.

Reinhart, B.J., Slack, F.J., Basson, M., Pasquinelli, A.E., Bettinger, J.C., Rougvie, A.E., Horvitz, H.R., and Ruvkun, G. 2000. The 21-nucleotide let-7 RNA regulates developmental timing in Caenorhabditis elegans. Nature **403**(6772): 901-906.

Rivas, F.V., Tolia, N.H., Song, J., Aragon, J.P., Liu, J., Hannon, G.J., and Joshua-Tor, L. 2005. Purified Argonaute2 and an siRNA form recombinant human RISC. Nature structural & molecular biology **12**(4): 340-349.

Roiniotis, J., Masendycz, P., Ho, S., and Scholz, G.M. 2005. Domain-mediated dimerization of the Hsp90 cochaperones Harc and Cdc37. Biochemistry (N. Y.) **44**(17): 6662-6669.

Rudel, S., and Meister, G. 2008. Phosphorylation of Argonaute proteins: regulating gene regulators. Biochem. J. **413**(3): e7-9.

Rudel, S., Wang, Y., Lenobel, R., Korner, R., Hsiao, H.H., Urlaub, H., Patel, D., and Meister, G. 2011. Phosphorylation of human Argonaute proteins affects small RNA binding. Nucleic Acids Res. **39**(6): 2330-2343.

Rybak, A., Fuchs, H., Hadian, K., Smirnova, L., Wulczyn, E.A., Michel, G., Nitsch, R., Krappmann, D., and Wulczyn, F.G. 2009. The let-7 target gene mouse lin-41 is a stem cell specific E3 ubiquitin ligase for the miRNA pathway protein Ago2. Nat. Cell Biol. **11**(12): 1411-1420.

Sadaie, M., Iida, T., Urano, T., and Nakayama, J. 2004. A chromodomain protein, Chp1, is required for the establishment of heterochromatin in fission yeast. EMBO J. **23**(19): 3825-3835.

Schalch, T., Job, G., Shanker, S., Partridge, J.F., and Joshua-Tor, L. 2011. The Chp1–Tas3 core is a multifunctional platform critical for gene silencing by RITS. Nature structural & molecular biology **18**(12): 1351-1357.

Schirle, N.T., and MacRae, I.J. 2012. The crystal structure of human Argonaute2. Science **336**(6084): 1037-1040.

Schirle, N.T., Sheu-Gruttadauria, J., and MacRae, I.J. 2014. Structural basis for microRNA targeting. Science **346**(6209): 608-613.

Schmitt, M.J., and Breinig, F. 2006. Yeast viral killer toxins: lethality and self-protection. Nature Reviews Microbiology **4**(3): 212-221.

Schneider, M.D., Najand, N., Chaker, S., Pare, J.M., Haskins, J., Hughes, S.C., Hobman, T.C., Locke, J., and Simmonds, A.J. 2006. Gawky is a component of cytoplasmic mRNA processing bodies required for early Drosophila development. J. Cell Biol. **174**(3): 349-358.

Shabalina, S.A., and Koonin, E.V. 2008. Origins and evolution of eukaryotic RNA interference. Trends in ecology & evolution **23**(10): 578-587.

Shapiro, A.L., Viñuela, E., and Maizel, J.V. 1967. Molecular weight estimation of polypeptide chains by electrophoresis in SDS-polyacrylamide gels. Biochem. Biophys. Res. Commun. **28**(5): 815-820.

Shen, J., Xia, W., Khotskaya, Y.B., Huo, L., Nakanishi, K., Lim, S., Du, Y., Wang, Y., Chang, W., and Chen, C. 2013. EGFR modulates microRNA maturation in response to hypoxia through phosphorylation of AGO2. Nature **497**(7449): 383-387.

Sijen, T., Steiner, F.A., Thijssen, K.L., and Plasterk, R.H. 2007. Secondary siRNAs result from unprimed RNA synthesis and form a distinct class. Science **315**(5809): 244-247.

Siligardi, G., Panaretou, B., Meyer, P., Singh, S., Woolfson, D.N., Piper, P.W., Pearl, L.H., and Prodromou, C. 2002. Regulation of Hsp90 ATPase activity by the co-chaperone Cdc37p/p50cdc37. J. Biol. Chem. **277**(23): 20151-20159.

Siomi, M.C., Sato, K., Pezic, D., and Aravin, A.A. 2011. PIWI-interacting small RNAs: the vanguard of genome defence. Nature reviews Molecular cell biology **12**(4): 246-258.

Smibert, P., Yang, J., Azzam, G., Liu, J., and Lai, E.C. 2013. Homeostatic control of Argonaute stability by microRNA availability. Nature structural & molecular biology **20**(7): 789-795.

Song, E., Lee, S., Wang, J., Ince, N., Ouyang, N., Min, J., Chen, J., Shankar, P., and Lieberman, J. 2003. RNA interference targeting Fas protects mice from fulminant hepatitis. Nat. Med. **9**(3): 347-351.

Song, J., Liu, J., Tolia, N.H., Schneiderman, J., Smith, S.K., Martienssen, R.A., Hannon, G.J., and Joshua-Tor, L. 2003. The crystal structure of the Argonaute2 PAZ domain reveals an RNA binding motif in RNAi effector complexes. Nature Structural & Molecular Biology **10**(12): 1026-1032.

Song, J.J., Smith, S.K., Hannon, G.J., and Joshua-Tor, L. 2004. Crystal structure of Argonaute and its implications for RISC slicer activity. Science **305**(5689): 1434-1437.

Sontheimer, E.J., and Carthew, R.W. 2005. Silence from within: endogenous siRNAs and miRNAs. Cell **122**(1): 9-12.

Staab, J.F., White, T.C., and Marr, K.A. 2011. Hairpin dsRNA does not trigger RNA interference in Candida albicans cells. Yeast **28**(1): 1-8.

Stoecklin, G., Mayo, T., and Anderson, P. 2006. ARE-mRNA degradation requires the 5'-3' decay pathway. EMBO Rep. **7**(1): 72-77.

Stohr, N., Lederer, M., Reinke, C., Meyer, S., Hatzfeld, M., Singer, R.H., and Huttelmaier, S. 2006. ZBP1 regulates mRNA stability during cellular stress. J. Cell Biol. **175**(4): 527-534 doi:jcb.200608071 [pii]. PMID:17101699.

Suk, K., Choi, J., Suzuki, Y., Ozturk, S.B., Mellor, J.C., Wong, K.H., MacKay, J.L., Gregory, R.I., and Roth, F.P. 2011. Reconstitution of human RNA interference in budding yeast. Nucleic Acids Res. **39**(7): e43.

Sullivan, W., Stensgard, B., Caucutt, G., Bartha, B., McMahon, N., Alnemri, E.S., Litwack, G., and Toft, D. 1997. Nucleotides and two functional states of hsp90. J. Biol. Chem. **272**(12): 8007-8012.

Svitkin, Y.V., Imataka, H., Khaleghpour, K., Kahvejian, A., Liebig, H., and Sonenberg, N. 2001. Poly (A)-binding protein interaction with eIF4G stimulates picornavirus IRES-dependent translation. RNA **7**(12): 1743-1752.

Tabara, H., Yigit, E., Siomi, H., and Mello, C.C. 2002. The dsRNA binding protein RDE-4 interacts with RDE-1, DCR-1, and a DExH-box helicase to direct RNAi in C. elegans. Cell **109**(7): 861-871.

Tahbaz, N., Carmichael, J.B., and Hobman, T.C. 2001. GERp95 belongs to a family of signal-transducing proteins and requires Hsp90 activity for stability and Golgi localization. J. Biol. Chem. **276**(46): 43294-43299.

Tahbaz, N., Kolb, F.A., Zhang, H., Jaronczyk, K., Filipowicz, W., and Hobman, T.C. 2004. Characterization of the interactions between mammalian PAZ PIWI domain proteins and Dicer. EMBO Rep. **5**(2): 189-194.

Taipale, M., Jarosz, D.F., and Lindquist, S. 2010. HSP90 at the hub of protein homeostasis: emerging mechanistic insights. Nature reviews Molecular cell biology **11**(7): 515-528.

Tang, F., Barbacioru, C., Wang, Y., Nordman, E., Lee, C., Xu, N., Wang, X., Bodeau, J., Tuch, B.B., and Siddiqui, A. 2009. mRNA-Seq whole-transcriptome analysis of a single cell. Nature methods **6**(5): 377-382.

Tang, X., Li, M., Tucker, L., and Ramratnam, B. 2011. Glycogen synthase kinase 3 beta (GSK3β) phosphorylates the RNAase III enzyme Drosha at S300 and S302. PloS one **6**(6): e20391.

Tang, G., Reinhart, B.J., Bartel, D.P., and Zamore, P.D. 2003. A biochemical framework for RNA silencing in plants. Genes Dev. **17**(1): 49-63.

Tolia, N.H., and Joshua-Tor, L. 2007. Slicer and the argonautes. Nature chemical biology **3**(1): 36-43.

Tomari, Y., and Zamore, P.D. 2005. Perspective: machines for RNAi. Genes Dev. **19**(5): 517-529.

Tritschler, F., Huntzinger, E., and Izaurralde, E. 2010. Role of GW182 proteins and PABPC1 in the miRNA pathway: a sense of deja vu. Nature reviews Molecular cell biology **11**(5): 379-384.

Tsutsumi, A., Kawamata, T., Izumi, N., Seitz, H., and Tomari, Y. 2011. Recognition of the pre-miRNA structure by Drosophila Dicer-1. Nature structural & molecular biology **18**(10): 1153-1158.

Vagin, V.V., Sigova, A., Li, C., Seitz, H., Gvozdev, V., and Zamore, P.D. 2006. A distinct small RNA pathway silences selfish genetic elements in the germline. Science **313**(5785): 320-324.

Vaucheret, H. 2006. Post-transcriptional small RNA pathways in plants: mechanisms and regulations. Genes Dev. **20**(7): 759-771.

Vaucheret, H., Beclin, C., and Fagard, M. 2001. Post-transcriptional gene silencing in plants. J. Cell. Sci. **114**(Pt 17): 3083-3091.

Vazquez, F., Vaucheret, H., Rajagopalan, R., Lepers, C., Gasciolli, V., Mallory, A.C., Hilbert, J., Bartel, D.P., and Crété, P. 2004. Endogenous trans-acting siRNAs regulate the accumulation of Arabidopsis mRNAs. Mol. Cell **16**(1): 69-79.

Verdel, A., Jia, S., Gerber, S., Sugiyama, T., Gygi, S., Grewal, S.I., and Moazed, D. 2004. RNAi-mediated targeting of heterochromatin by the RITS complex. Science **303**(5658): 672-676.

Volpe, T., Schramke, V., Hamilton, G.L., White, S.A., Teng, G., Martienssen, R.A., and Allshire, R.C. 2003. RNA interference is required for normal centromere function infission yeast. Chromosome Research **11**(2): 137-146.

Volpe, T.A., Kidner, C., Hall, I.M., Teng, G., Grewal, S.I., and Martienssen, R.A. 2002. Regulation of heterochromatic silencing and histone H3 lysine-9 methylation by RNAi. Science **297**(5588): 1833-1837.

Wagner, N.J., and Heidelberger, C. 1962. Some effects of 5-fluoroorotic acid and 5-fluorouracii, on the soluble ribonucleic acid of rat liver. Biochimica et Biophysica Acta (BBA)-Specialized Section on Nucleic Acids and Related Subjects **61**(3): 373-379.

Wang, Y., Mercier, R., Hobman, T.C., and LaPointe, P. 2013. Regulation of RNA interference by Hsp90 is an evolutionarily conserved process. Biochimica et Biophysica Acta (BBA)-Molecular Cell Research **1833**(12): 2673-2681.

Wang, Y., Sheng, G., Juranek, S., Tuschl, T., and Patel, D.J. 2008. Structure of the guide-strand-containing argonaute silencing complex. Nature **456**(7219): 209-213.

Wang, Y., Juranek, S., Li, H., Sheng, G., Wardle, G.S., Tuschl, T., and Patel, D.J. 2009. Nucleation, propagation and cleavage of target RNAs in Ago silencing complexes. Nature **461**(7265): 754-761.

Weinberg, D.E., Nakanishi, K., Patel, D.J., and Bartel, D.P. 2011. The inside-out mechanism of Dicers from budding yeasts. Cell **146**(2): 262-276.

Welker, N.C., Maity, T.S., Ye, X., Aruscavage, P.J., Krauchuk, A.A., Liu, Q., and Bass, B.L. 2011. Dicer's helicase domain discriminates dsRNA termini to promote an altered reaction mode. Mol. Cell **41**(5): 589-599.

Whitehead, K.A., Langer, R., and Anderson, D.G. 2009. Knocking down barriers: advances in siRNA delivery. Nature reviews Drug discovery **8**(2): 129-138.

Wilczynska, A., Aigueperse, C., Kress, M., Dautry, F., and Weil, D. 2005. The translational regulator CPEB1 provides a link between dcp1 bodies and stress granules. J. Cell. Sci. **118**(Pt 5): 981-992.

Wu, C., So, J., Davis-Dusenbery, B.N., Qi, H.H., Bloch, D.B., Shi, Y., Lagna, G., and Hata, A. 2011. Hypoxia potentiates microRNA-mediated gene silencing through posttranslational modification of Argonaute2. Mol. Cell. Biol. **31**(23): 4760-4774.

Xie, Z., Johansen, L.K., Gustafson, A.M., Kasschau, K.D., Lellis, A.D., Zilberman, D., Jacobsen, S.E., and Carrington, J.C. 2004. Genetic and functional diversification of small RNA pathways in plants. PLoS Biol **2**(5): e104.

Xie, Z., Chen, G., Zhang, X., Li, D., Huang, J., Yang, C., Zhang, P., Qin, Y., Duan, Y., and Gong, B. 2013. Salivary microRNAs as promising biomarkers for detection of esophageal cancer. PloS one **8**(4): e57502.

Yamada, T., Fischle, W., Sugiyama, T., Allis, C.D., and Grewal, S.I. 2005. The nucleation and maintenance of heterochromatin by a histone deacetylase in fission yeast. Mol. Cell **20**(2): 173-185.

Yang, M., Haase, A.D., Huang, F., Coulis, G., Rivera, K.D., Dickinson, B.C., Chang, C.J., Pappin, D.J., Neubert, T.A., and Hannon, G.J. 2014. Dephosphorylation of tyrosine 393 in argonaute 2 by protein tyrosine phosphatase 1B regulates gene silencing in oncogenic RAS-induced senescence. Mol. Cell **55**(5): 782-790.

Yang, J.S., Maurin, T., and Lai, E.C. 2012. Functional parameters of Dicer-independent microRNA biogenesis. RNA **18**(5): 945-957.

Yigit, E., Batista, P.J., Bei, Y., Pang, K.M., Chen, C.G., Tolia, N.H., Joshua-Tor, L., Mitani, S., Simard, M.J., and Mello, C.C. 2006. Analysis of the C. elegans Argonaute family reveals that distinct Argonautes act sequentially during RNAi. Cell **127**(4): 747-757.

Young, J.C., Moarefi, I., and Hartl, F.U. 2001. Hsp90: a specialized but essential protein-folding tool. J. Cell Biol. **154**(2): 267-274.

Yu, J.Y., DeRuiter, S.L., and Turner, D.L. 2002. RNA interference by expression of short-interfering RNAs and hairpin RNAs in mammalian cells. Proc. Natl. Acad. Sci. U. S. A. **99**(9): 6047-6052.

Zamore, P.D. 2004. Plant RNAi: How aViral Silencing Suppressor Inactivates siRNA. Current Biology **14**(5): R198-R200.

Zekri, L., Kuzuoglu-Ozturk, D., and Izaurralde, E. 2013. GW182 proteins cause PABP dissociation from silenced miRNA targets in the absence of deadenylation. EMBO J. **32**(7): 1052-1065.

Zekri, L., Huntzinger, E., Heimstadt, S., and Izaurralde, E. 2009. The silencing domain of GW182 interacts with PABPC1 to promote translational repression and degradation of microRNA targets and is required for target release. Mol. Cell. Biol. **29**(23): 6220-6231.

Zeng, Y., Sankala, H., Zhang, X., and Graves, P.R. 2008. Phosphorylation of Argonaute 2 at serine-387 facilitates its localization to processing bodies. Biochem. J. **413**(3): 429-436.

Zhang, H., Kolb, F.A., Jaskiewicz, L., Westhof, E., and Filipowicz, W. 2004. Single processing center models for human Dicer and bacterial RNase III. Cell **118**(1): 57-68.

Zhang, L., Ding, L., Cheung, T.H., Dong, M., Chen, J., Sewell, A.K., Liu, X., Yates, J.R., and Han, M. 2007. Systematic identification of C. elegans miRISC proteins, miRNAs, and mRNA targets by their interactions with GW182 proteins AIN-1 and AIN-2. Mol. Cell **28**(4): 598-613.

Zilberman, D., Cao, X., and Jacobsen, S.E. 2003. ARGONAUTE4 control of locus-specific siRNA accumulation and DNA and histone methylation. Science **299**(5607): 716-719.

Zipprich, J.T., Bhattacharyya, S., Mathys, H., and Filipowicz, W. 2009. Importance of the C-terminal domain of the human GW182 protein TNRC6C for translational repression. RNA **15**(5): 781-793.

Zou, J., Chang, M., Nie, P., and Secombes, C.J. 2009. Origin and evolution of the RIG-I like RNA helicase gene family. BMC evolutionary biology **9**(1): 1-14.